

University of New Hampshire

## University of New Hampshire Scholars' Repository

---

Master's Theses and Capstones

Student Scholarship

---

Winter 2016

### An Objective Protocol for Movable Bridge Operation in High-Wind Events Based on Hybrid Analyses by European and American Design Code

Timothy Prescott Nash  
*University of New Hampshire, Durham*

Follow this and additional works at: <https://scholars.unh.edu/thesis>

---

#### Recommended Citation

Nash, Timothy Prescott, "An Objective Protocol for Movable Bridge Operation in High-Wind Events Based on Hybrid Analyses by European and American Design Code" (2016). *Master's Theses and Capstones*. 1100.

<https://scholars.unh.edu/thesis/1100>

This Thesis is brought to you for free and open access by the Student Scholarship at University of New Hampshire Scholars' Repository. It has been accepted for inclusion in Master's Theses and Capstones by an authorized administrator of University of New Hampshire Scholars' Repository. For more information, please contact [Scholarly.Communication@unh.edu](mailto:Scholarly.Communication@unh.edu).

**AN OBJECTIVE PROTOCOL FOR MOVABLE BRIDGE OPERATION IN HIGH-WIND EVENTS  
BASED ON HYBRID ANALYSES BY EUROPEAN AND AMERICAN DESIGN CODE**

BY

TIMOTHY PRESCOTT NASH

B.S. Civil Engineering, University of New Hampshire, 2015

THESIS

*Submitted to the University of New Hampshire  
in Partial Fulfillment of  
the Requirements for the Degree of*

Master of Science  
in  
Structural Engineering

December, 2016

**AN OBJECTIVE PROTOCOL FOR MOVABLE BRIDGE OPERATION  
IN HIGH-WIND EVENTS BASED ON HYBRID ANALYSES  
BY EUROPEAN AND AMERICAN DESIGN CODE**

BY

TIMOTHY PRESCOTT NASH

This thesis has been examined and approved in partial fulfillment of the requirements for the degree of Master of Science in Civil Engineering by:

Thesis/Dissertation Director, Dr. Erin Santini Bell,  
Associate Professor, Civil and Environmental  
Engineering

Dr. Ricardo Medina, Associate Professor, Civil and  
Environmental Engineering

Dr. Raymond Cook, Associate Professor, Civil and  
Environmental Engineering)

On December 8<sup>th</sup>, 2016

Original approval signatures are on file with the University of New Hampshire Graduate School.

## TABLE OF CONTENTS

ACKNOWLEDGEMENTS .....	vi
LIST OF TABLES.....	vii
LIST OF FIGURES .....	ix
ABSTRACT.....	xi

<b>CHAPTER</b>	<b>PAGE</b>
CHAPTER 1.....	1
1.1 OVERVIEW .....	1
1.2 LITERATURE AND CODE REVIEW .....	3
1.2.1 Movable Bridges .....	4
1.2.2 Related Work.....	6
CHAPTER 2.....	9
WIND LOADING BY CODE .....	9
REVIEW OF STRUCTURAL DYNAMICS .....	12
CHAPTER 3.....	18
3.1 THE MEMORIAL BRIDGE – A MOVABLE LIFT BRIDGE .....	18
3.1.1 Structural Systems and Geometry .....	20
3.2 LIVING BRIDGE PROJECT .....	21
3.3 THE NEED FOR A DECISION MAKING PROTOCOL .....	22
CHAPTER 4.....	24
4.1 AERODYNAMIC SUSCEPTABILITY .....	24
4.2 DEVELOPMENT OF WIND LOADS.....	29
4.2.1 ASCE 7-10.....	29
4.2.2 Eurocode .....	31
4.2.3 AASHTO.....	32
4.2.4 Hybrid Wind Loading.....	34
4.3 ANALYSIS IN SAP2000® .....	37
4.3.1 Predictive Formula and Objective Protocol .....	38
4.3.2 Shortcomings and Validity of Protocol.....	41
4.4 DYNAMIC ANALYSIS OF THE COUNTERWEIGHTS AND LIFT SPAN .....	45

---

CHAPTER 5.....	49
5.1 OVERVIEW .....	49
5.1.1 Wind Effects .....	49
5.1.2 Model Validation, Updating, and Integration of Sensor Data .....	51
5.1.3 Traffic Considerations .....	51
5.1.4 Progressive Section Loss and the Objective Protocol .....	53
CHAPTER 6.....	55
LIST OF REFERENCES .....	58
APPENDICES.....	61
APPENDIX A .....	62
AASHTO.....	62
Aero-Elastic Check .....	62
Sample Wind Load Calculation .....	62
Excel Calculations .....	63
EUROCODE .....	65
Sample Wind Load Calculation .....	65
Excel Calculations .....	66
ASCE 7-10 AND HYBRID LOADING .....	68
Excel Calculations .....	69
DESIGN MANUAL FOR ROADS AND BRIDGES (DMRB) .....	75
Solvency Ratio .....	75
DMRB 2.1.1.3c – Limiting Criteria.....	75
Mean Hourly Wind Speed Calculation .....	75
Excel Calculations .....	78
APPENDIX B .....	80
COUNTERWEIGHT TUNED MASS DAMPER CALCULATIONS.....	80
APPENDIX C .....	83
CUSTOM BRIDGE SECTIONS .....	83
Lift Span .....	83
South Span.....	84
South Tower .....	85
Tabulation of Critical Moment Capacities.....	85

---

SITE ANNUAL WIND DATA FROM NOAA .....	86
APPENDIX D .....	88
MODELING IN SAP2000® AND AUTOCAD .....	88
Member Capacity .....	88
Load Combination Development.....	88
STEEL CONNECTION DESINGS.....	90
Pinned and Moment Connection Calculations .....	90
Splice Connection Calculations .....	96
Welded Mounting and End Plate Connections .....	101

## ACKNOWLEDGEMENTS

*“If I have seen further, it is by standing on the shoulders of giants.” – Sir Isaac Newton*

No work is done without the considerable aid and generosity of others, and this work is not exclusionary. I owe tremendous gratitude to the people who have helped me along the way and while I certainly cannot thank them all – here are those who stand at the forefront of my appreciation...

My family, for the love and support they so constantly supply.

My friends, for their undying humor and steadfastness.

À monsieur Scott Battey, pour ses encouragements constants et pour me rappeler toujours du pouvoir d'imagination.

Mr. Jason Bailey, for his continual support and kindness and for constantly showing me my own potential.

My professors, both past and present – Dr. Erin Bell, Dr. Ricardo Medina, Dr. Robert Henry, Dr. Raymond Cook, and Dr. Tat Fu – for their perpetual commitment to the education and betterment of both myself and the countless students they've influenced through the years.

And lastly...

My father, Eric Nash, who's original talent, formidable intellect, and genuine adoration for the arts and sciences has ever instilled in me an unquenchable desire to learn.

My mother, Margaret Nash, who's absolute selflessness, kindness, and support is an inspiration to not only to myself, but our family, friends, and the people she works with every day.

*The Living Bridge Project is a joint effort funded by the National Science Foundation (IIP 14-30260), the New Hampshire Department of Transportation, and the Federal Highway Association.*

## LIST OF TABLES

Table 1 - Bending and torsional modes for SAP2000® models .....	28
Table 2 - Bridge stability to excitation .....	29
Table 3 - Wind loads developed by Eurocode .....	32
Table 4 - AASHTO developed wind loads .....	34
Table 5 - ASCE basic wind pressure numerical coefficients as a function of temperature .....	35
Table 6 - Hybrid load cases for SAP2000® analysis (all load cases include dead load) .....	37
Table 7 - Sample tabulation of minor moment data for critical lift span members .....	38
Table 8 - Critical member capacity/demand checks at 100mph wind and 0 degrees Fahrenheit .....	41
Table 9 - Predicted moment demands for critical members at 0 degrees Fahrenheit and 100mph winds .....	42
Table 10 - Summary of critical member capacities .....	43
Table 11 - Bridge member areas and lengths .....	63
Table 12 - AASHTO total wind pressure calculations in Excel .....	63
Table 13 - Final AASHTO wind loads from Excel .....	64
Table 14 - Tabulation of wind loads developed by Eurocode .....	66
Table 15 - Reference air density for VLOOKUP in Excel .....	67
Table 16 - Excel member elevation and geometry data for ASCE analysis .....	69
Table 17 - Basic pressure profile and polynomial function in Excel .....	70
Table 18 - Example ASCE wind loads at 100mph and variable temperature .....	71
Table 19 - Eurocode minimum wind loads by temperature .....	72
Table 20 - Final hybrid wind loads after application of Eurocode minimums for 100mph wind .....	73
Table 21 - Final hybrid wind loads after application of Eurocode minimums for 50mph wind .....	74
Table 22 - DMRB susceptibility recommendation and input .....	78
Table 23 - DMRB susceptibility warnings by temperature, wind speed, and lift state .....	79
Table 24 - DMRB calculated variables .....	79
Table 25 - Input table for amplification factor calculations .....	80
Table 26 - Sample tabulation of H2 factor data for typical TMD system .....	81
Table 27 - Critical lift and south span member moment capacities .....	85
Table 28 - Loading for TDP .....	89
Table 29 - Summary of pinned and moment connection capacities .....	91
Table 30 - Available slip critical shear .....	91



---

Table 31 - Shear and tension check of coped web.....	92
Table 32 - Available bearing shear.....	92
Table 33 - Available bevel weld strength.....	93
Table 34 - Available fillet weld strength.....	93
Table 35 - Block shear check in axial and shear directions.....	94
Table 36 - Summary of contributing moment capacities.....	95
Table 37 - Splice connection capacity summary.....	97
Table 38 - Available slip critical shear.....	97
Table 39 - Block shear check in axial and shear directions.....	98
Table 40 - Shear and tension checks for web of splice connection.....	99
Table 41 - Available plate bearing.....	99
Table 42 - Splice connection moment capacity calculation.....	100
Table 43 - Fillet weld strength check for pontoon plate.....	101
Table 44 - Fillet weld strength check for end plate.....	102

## LIST OF FIGURES

Figure 1 - London Tower Bridge, United Kingdom (www.towerbridge.org, 2016) .....	4
Figure 2 - Arthur Kill Bridge, the largest vertical lift in the world (Google Maps).....	5
Figure 3 - A.G. Davenport's wind load chain .....	9
Figure 4 - Typical wind profile where wind velocity varies with altitude (Taly, 2014) .....	11
Figure 5 - Collapse of the Tacoma Narrows Bridge.....	13
Figure 6 - Memorial Bridge (Portsmouth, NH) southern tower and counterweight .....	15
Figure 7 - Amplification factor vs. frequency ratio for a typical TMD system (Connor, 2002) .....	16
Figure 8 - The Memorial Bridge as seen from Portsmouth (2016) .....	18
Figure 9 - Portsmouth, NH (aerial rendering from Google Maps) .....	19
Figure 10 - Elevation of the vertical lift span in its lifted and un-lifted states .....	20
Figure 11 – Overview UNH's Living Bridge Project.....	21
Figure 12 - Velocity magnitude of currents beneath Memorial Bridge.....	22
Figure 13 - SAP2000® models for the south span (left) and lift span (right) of the Memorial Bridge .....	25
Figure 14 - Southern boundary condition (pin-roller combination allowing thermal expansion) ..	26
Figure 15 - Basic pressure profile as established in Excel.....	30
Figure 16 - Wind directions (Figure 8.2 in Section 8 of Eurocode).....	31
Figure 17 - Wind profiles varied by temperature as a function of height .....	35
Figure 18 - Wind loading vs. height for tower column.....	36
Figure 19 – Minor moment for lift span section H-H in the lifted position at -4 degrees Fahrenheit .....	38
Figure 20 - Lift span section H-H interpolated minor moments at 40 Fahrenheit .....	39
Figure 21 – Lift span section H-H temperature interpolated minor moment data and wind speed input.....	40
Figure 22 - Max moment trends and inconsistencies .....	44
Figure 23 - Counterweight natural frequency as a function of cable length.....	46
Figure 24 – Amplification factor vs. frequency ratio for counterweight and tower system (Connor, 2002) .....	48
Figure 25 - Wind rose for Portsmouth, NH .....	50
Figure 26 - Truck blow over on the Mackinac Bridge (2013).....	52
Figure 27 – Degradation of the original Memorial Bridge truss system (Jim Cole, 2010) .....	53
Figure 28 - Eurocode c(e) factor .....	65

---

Figure 29 - Lift span area as calculated in AutoCAD .....	66
Figure 30 - Net Projected area of lift span ( $A_{net}$ ) .....	75
Figure 31 - Front face of windward truss ( $A_{windward}$ ) .....	75
Figure 32 - DMRB terrain and bridge factor.....	76
Figure 33 - DMRB fetch correction factor .....	77
Figure 34 - Memorial Bridge typical fixed-span cross section .....	78
Figure 35 - Excel sample showing natural frequencies as a function of counterweight elevation .....	80
Figure 36 - Plan view of turbine deployment platform.....	88
Figure 37 - Pinned connection detail.....	90
Figure 38 - Full moment connection detail.....	90
Figure 39 - TDP splice location diagram.....	96
Figure 40 - Splice connection detail .....	97
Figure 41 - End plate details .....	101
Figure 42 - Pontoon plate detail .....	101

**ABSTRACT**

AN OBJECTIVE PROTOCOL FOR MOVABLE BRIDGE OPERATION  
DURING HIGH-WIND EVENTS BASED ON HYBRID WIND ANALYSIS BY  
EUROPEAN AND AMERICAN DESIGN CODE

by

Timothy Prescott Nash

University of New Hampshire

December, 2016

Movable bridges play an integral role in modern transportation infrastructure. As means of passage for both vehicular and naval traffic at a single location, their reliable performance is a necessity. However, with the thousands of movable bridges in the US – which are typically located in coastal environments that are typically highly susceptible to extreme weather events – there are few objective protocols defining the environmental conditions in which they can be safely operated. In order to define such conditions, wind speed and temperature variable wind loads were developed using multiple, structural load development codes for a case study site: the Memorial Bridge in Portsmouth, NH. These loads were developed, examined, and combined to create hybrid load cases for input and analysis in SAP2000® to determine structural response levels in the bridge members. The results from SAP2000® were used to predict the demands the Memorial Bridge will experience in both its lifted and un-lifted positions in variable environmental conditions, such that the viability of a lift can be more objectively defined. These results were compiled in conjunction with bridge's aerodynamic susceptibility and an investigation of the

dynamics of the bridge's counterweight system, both of which were found to be of minimal concern in terms of bridge structural safety. Following the future integration of structural health monitoring (SHM) and weather data acquisition systems at the case study site, the protocol will be refined and expanded to more accurately predict safe lifting conditions.

## CHAPTER 1

### INTRODUCTION

#### 1.1 OVERVIEW

Structural engineering is one of the oldest professions in the world. Reaching as far back as the Ancient Egyptian Imhotep, structural engineers design the roads, bridges, and buildings that are so integral to a functional society. Indeed, the well-being of a nation can be directly linked to the quality of its infrastructure – buildings provide residence to production while roads and bridges form the arterioles to commerce. A country with access to timely public transport systems, robust water treatment facilities, and safe roads and bridges is an efficient and capable one (Aschauer, 1990). This was true for ancient civilizations, such as the Ancient Greeks and Romans, who understood the value of civil infrastructure to public health and welfare.

Despite the advantages of a healthy and extensive infrastructure, America's is ailing at best. A 2013 report by the American Society of Civil Engineers graded the US's infrastructure on the basis of "capacity, funding, future need, operation and maintenance, public safety, resilience, and innovation" (ASCE, 2013) and found the national average to be a D+ where an A is exceptional and an F is failing. One in nine bridges was found to be structurally deficient with an annual estimated \$20.5 billion, which is \$7.7 billion more than the current annual investment, needed to ameliorate this deficiency. On top of this, according to the Federal Highway Administration, nearly a third of all bridges in the US have exceeded their 50-year design life (National Economic Council and the President's Council on Economic Advisors, 2014).

A bridge type particularly susceptible to degradation and deficiency is the movable bridge. Movable bridges possess all the complexity of a typical bridge compounded by that of mechanized systems. Such systems are often required to lift entire bridge spans, as much as five-hundred

feet in length and weighing multiple millions of pounds, high enough for commercial vessels to pass beneath them. They must do this regularly and perfectly as often as every half hour for the entirety of their design life. This is no small task considering most movable bridges are located over bodies of water, making them more susceptible to corrosion, naval collision, and storms – one of the many reasons that, of the over 3000 movable bridges in the US, only about 1900 of them are operable today (Koglin, 2003). The consequences of failure are also higher for a movable bridge. An inoperable lift has the ability to stop not only vehicular traffic, but naval traffic as well. Large shipping vessels can cost as much as \$9 million a year to operate and their delay as a result of a dysfunctional lift span can have large economic ramifications. As such, the proper maintenance of movable bridges is essential. As stated by Catbas (2013) in his paper *Movable Bridge Maintenance Monitoring*, “Maintenance and performance monitoring of movable bridges is often more essential and justified than for fixed bridges given their dual service role and the potential for deterioration and other problems with the integrated systems that are essential for ensuring their operation and safety.”

While there is a clear need for the maintenance and monitoring of movable bridges, such operations can be expensive and, as previously stated, American infrastructure is currently underfunded. Traditional means and methods must therefore become more innovative; more adaptable. The President’s Council of Economic Advisors addressed this issue, stating:

*“Bridge stewards and owners need to become, inevitably, more strategic by adopting and implementing systematic processes for bridge preservation as an integral component of their overall management of bridge assets... The objective of a good bridge preservation program is to employ cost effective strategies and actions to maximize the useful life of bridges. Applying the appropriate bridge preservation treatments and activities at the appropriate time can extend bridge useful life at lower lifetime cost.” (FHWA, 2011)*

The preservative treatments described above are part of a governmental push towards systematic preventative maintenance (SPM) – an activity Congress added to the Highway Bridge Program in 2008 (National Economic Council and the President’s Council on Economic Advisors, 2014). SPM includes maintenance activities that keep a bridge, or elements of a bridge, in good health, prevent deterioration, and extend its design life. In the case of movable bridges, potential measures of this preventative nature are numerous.

At present, there are few objective criteria defining when a movable bridge should be operated. Generally, the operation of a lift is left to the discretion of the operators who are given loose guidelines for unsafe wind and environmental conditions. This presents an area for significant improvement given that most movable bridges are susceptible to strong winds, storms, and fatigue damage from repetitious lifts (Catbas, 2010). This thesis describes the development of a hybrid wind analysis, which melds aspects of multiple international design codes, used to analyze a vertical lift bridge in Portsmouth, NH. As part of a smart infrastructure project, this analysis and its results were used to develop an objective protocol for the operation of the bridge’s lift span during high-wind events. Through future data acquisition from an array of sensors located at the bridge, this protocol will be refined and modified to predict in real-time whether the conditions at the bridge are favorable to a lift, the health of the structural and mechanical systems, as well as the overall design life of the bridge and its systems.

## **1.2 LITERATURE AND CODE REVIEW**

The work conducted in this thesis was preceded by a thorough review of literature and design code. An understanding of movable bridges, their types, and their history was developed followed by an overview of similar wind-related research that has been conducted to date. International



engineering codes and the design equations therein were assessed and an analysis procedure was created from them. The results of all the above finding are surmised herein.

### **1.2.1 Movable Bridges**

Movable bridges have existed for millennia. The earliest record of a movable bridge exists in the form of a drawbridge providing passage over a moat. Queen Nitocris of Babylon is recorded to have built a retractable bridge as early as the 4<sup>th</sup> century BCE and King Xerxes did similarly with pontoons over the Hellespont in the same period (Koglin, 2003).

Since ancient times, movable bridges have evolved considerably. The development of the steam engine created new forms of vehicular and naval traffic which, in turn, prompted the development of new types of movable bridges to accommodate them (Koglin, 2003). Before the advent of the steam engine, the most common type of movable bridge was the draw or bascule type bridge – the famed London Tower Bridge shown in Figure 1 is an example of this type. The main reason for the prevalence of bascule bridges was the militaristic defense benefits they offered.



*Figure 1 - London Tower Bridge, United Kingdom (www.towerbridge.org, 2016)*

Following the invention of the steam engine, the swing bridge became popular. It remained popular through much of the 1800's and the Industrial Revolution, but it's considerable drawbacks

led to the popularization of the vertical lift. While vertical lift bridges restrict the allowable height of vessels that pass beneath them, they distribute the weight of their lift spans to each of their fixed spans, rather than one, as does the swing bridge. This distribution of weight allows vertical lift spans to extend considerable lengths. Indeed, some of the largest lift bridges in the world have spans of over 500 feet – the Arthur Kill Railroad Bridge’s lift spans a total of 558 feet, shown in Figure 2, from New York to New Jersey.



*Figure 2 - Arthur Kill Bridge, the largest vertical lift in the world (Google Maps)*

Lift bridges are not only better at spanning large distances, but also at resisting wind. Consider the bascule type bridge. Bascule’s typically consist of either a single or double leaf that lifts to stand vertically, perpendicular to the direction of the wind. In this position, a high surface area is exposed to the wind and thus a greater force is generated by it. The problem of high surface areas doesn’t exist in the same way for swing type bridges, and yet swings have issues with wind as well. When a swing bridge opens, it is generally must rotate its span to be parallel with the direction of the wind. This means that the swing span is either being pushed in the direction of

the wind or fighting to open against it. This is in direct contrast with the vertical lift bridge. Vertical lifts generally move perpendicular to the direction of the wind, rather than parallel. This means the bridge's lift span rarely has to move in opposition to the direction of wind pressure. This gives vertical lift's an advantage over their counterparts and yet, this said, lift bridges are not impregnable to wind.

Typically, lift bridges operate by means of a mechanized counterweight system. The counterweights roughly balance the mass of the lift span so minimal energy is expended in a lift. During a lift, a mechanical driver will either retract or release steel cables, typically running over a sheave or sheaves, and thus cause the span to move upwards or downwards. As the bridge is raised, it moves between guides which prevent the span from swaying longitudinally. Each of these systems is susceptible to degradation from wind. Vibration of the lift span caused by wind can result in a number of problems ranging from shock to the lift mechanism, to wearing of gears, to damaging aerodynamic interactions. Strong winds can also increase friction between the span and its guides by pushing them together. This can cause not only wear, but misalignment of the lift span – causing it to become stuck. On top of all of this, there is currently very little in the way of standardized design code recommendations to address these wind effects. Long-span and cable-stayed bridges have some recommendations and are often subject to wind-tunnel tests to ensure a lack of aerodynamic interaction but such tests are not routinely carried out for movable bridges during their design.

### **1.2.2 Related Work**

Despite centuries of development and a particular susceptibility to high winds, movable bridges and their interactions with wind have not been studied in remarkable depth. Indeed, as previously mentioned, standard design code makes few recommendations for the design of movable bridges in wind. The American Association of State Highway and Transportation Officials (AASHTO) has a LRDF movable highway bridge design guide but, for wind, it typically refers and makes minor

modifications to the articles outlined in its *LRFD Bridge Design Specifications* for normal highway bridges. In European nations, where Eurocode is one of the prevailing bridge design codes, similar provisions are made for movable bridges in wind. As described in the Eurocode National Annex on wind:

“NA.2.45 – No additional guidance is given for wind actions on other types of bridges (e.g. arch bridges, moving bridges and bridges with multiple or significantly curved decks).”  
(European Committee for Standardization, 2005)

When designing movable bridges, the means and methods of analysis are often left to the experience of the designer and built off previous, similar work. Because of this, a review of work done on wind interactions with movable bridges was performed for this research.

Dr. F. Necati Catbas, P.E. has done significant work researching movable bridges with the University of Central Florida. Florida has one of highest amounts of movable bridges of any state in America. As he describes, movable bridges require investigation because “according to FDOT engineers, the resulting rehabilitation and repairs [of a movable bridge] can cost roughly 100 times more than of a fixed bridge per square feet basis.” (Catbas, 2013). He goes on to describe the legitimacy of movable bridges as candidates for structural health monitoring (SHM) systems and, in his work, used such a system for the monitoring of a double-leafed bascule bridge in Fort Lauderdale, Florida. His aim in doing this was to learn to detect anomalies in the bridge’s performance in order to know when to perform maintenance on it. While the effects of wind were considered and monitored in this work, the specifics of how differing wind speeds and environmental conditions affected the operability of the bridge were not.

In 1991, Arie Reij of the Delft University of Technology researched this very issue. The primary purpose of his work was to define what wind speed movable bridges can safely operate at. His work, however, focused on the effects of wind on bridge lift system machinery. He determined,

based upon the average available and maximum available power for a typical lift motor for bridges in the province of Zeeland (in the Netherlands), the maximum permissible wind was about 14mps (31.3mph). This value, however, takes into account the probability of extreme high gust speeds occurring and, as Reij states, “might be increased if the reliability with which its occurrence can be predicted is increased.” (Reij, 1991). On top of this, the work did not focus directly on the effects of wind on the structure of a bridge, nor did it examine the effects of wind based on modern design codes.

The lack of research done on movable bridge interactions with wind in regards to their operation required the development of an original approach to the issue. Wind loads needed to be developed by code, but more than this, they needed to be manipulated and their derivations understood so as to apply them based on the variable environmental conditions (such as temperature and wind speed) that would influence the viability of a lift. This development began with a review of modern design code.

## CHAPTER 2

### STATE OF THE PRACTICE FOR WIND LOAD DEVELOPMENT

#### WIND LOADING BY CODE

Wind is an extremely complex, dynamic, unpredictable phenomenon. In its idealized form, the pressure induced by wind is simple to quantify. Using basic fluid mechanics, the pressure caused by a fluid flow at a static pressure and temperature and constant velocity is equal to:

$$q = \frac{1}{2}\rho V^2 \quad (1)$$

In the above equation,  $\rho$  is the fluid density and  $V$  is its velocity. This quantification, however, is unreasonable when establishing wind loads for a number of reasons. First, the velocity of wind is hardly ever constant. Wind is dynamic – it gusts, it buffets, and it changes in both speed and direction. Second, wind is variable in temperature and pressure, and thus density, and the environments it moves through are hardly ever uniform. Alan Garnett Davenport, a pioneer of wind engineering, described the complexity of wind actions and its primary influencers in a wind load chain (see Figure 3). As he shows, wind load is a function of the topography, climate, aerodynamics of the structure in question, and many other factors. In his paper *The Spectrum of Horizontal Gustiness Near the Ground in High Winds*, submitted in 1961 to the Quarterly Journal of the Royal Meteorological Society, Davenport attempted to quantify some of these factors statistically (Davenport, 1961). His work heavily influenced much of the modern wind design code, equations, and what is referred to as a three-second gust speed.

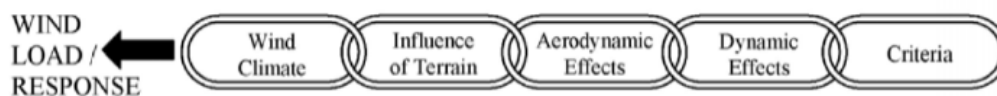


Figure 3 - A.G. Davenport's wind load chain

Most design codes simplify wind loads to a constant, quasi-statically applied pressure or force derived from a base velocity pressure and three-second gust. The base velocity pressure is established directly from Equation 1, above. Multipliers either amplify or reduce the magnitude of the final wind load based on the surrounding topography, wind direction, and the importance, location, and height of the structure in question. For simplicity's sake, codes often simplify analyses further by specifying a temperature and pressure for design. By ASCE standards for example, analysis is done at 60 degrees Fahrenheit and atmospheric pressure which results in the design Equation 2, below, where 0.00256 is a numerical coefficient established from the density of air at that temperature and pressure.

$$q_z = 0.00256K_zK_{zt}K_dV^2 \quad (2)$$

For the purposes of the analyses in this report, results from only a singular temperature value were insufficient. Lift spans are highly susceptible to thermal expansion and contraction and require analysis at multiple temperatures. Thus, the numerical coefficient described above was modified based on local temperature variations for analyses by Eurocode, ASCE, and hybrid code.

The factor  $V$  in Equation 2 is the base wind speed, established from the location of the structure. The base wind speed is formulated from a three-second gust – that is, the average “three-second gust wind speeds at standard meteorological heights of 33ft (10m) in open terrain with nominal return periods (or mean recurrence intervals) of 50 years” as defined by the ASCE Task Committee on Wind-Induced Forces. The importance of how this factor is established cannot be understated. A thorough examination of design codes will reveal that the base wind speed is typically developed using this three-second gust at 33 feet in altitude. This has profound implications on the transferability of the factor. Results from Eurocode, for example, at a base

wind speed of 100mph are founded upon the same definition of wind speed as ASCE, making them comparable.

For the site in question, the topographical effects on wind were simple to assess. Lift bridges typically span over open water, making them fully exposed. This said, lift bridges also typically reach significant heights and altitude plays a significant role in the velocity of wind. In general, the closer wind is to the ground, the slower it moves. For practical purposes, its velocity is essentially zero at ground level, increasing logarithmically as altitude is increased until about 300 feet. Here, wind speed varies minimally until about 1200 feet, where topography and surface roughness play, in essence, no role in the wind's velocity, as seen in Figure 4 below (Abrahams, 2000). Design code handles this variation in different ways. AASHTO and Eurocode, for example, simplify the wind profile to a uniform one by applying a constant, conservative load based on the height of the structure in question. ASCE applies the  $K_z$  factor seen in Equation 2 above, resulting in a stepwise basic wind pressure function applied to structures, which increases in magnitude with height.

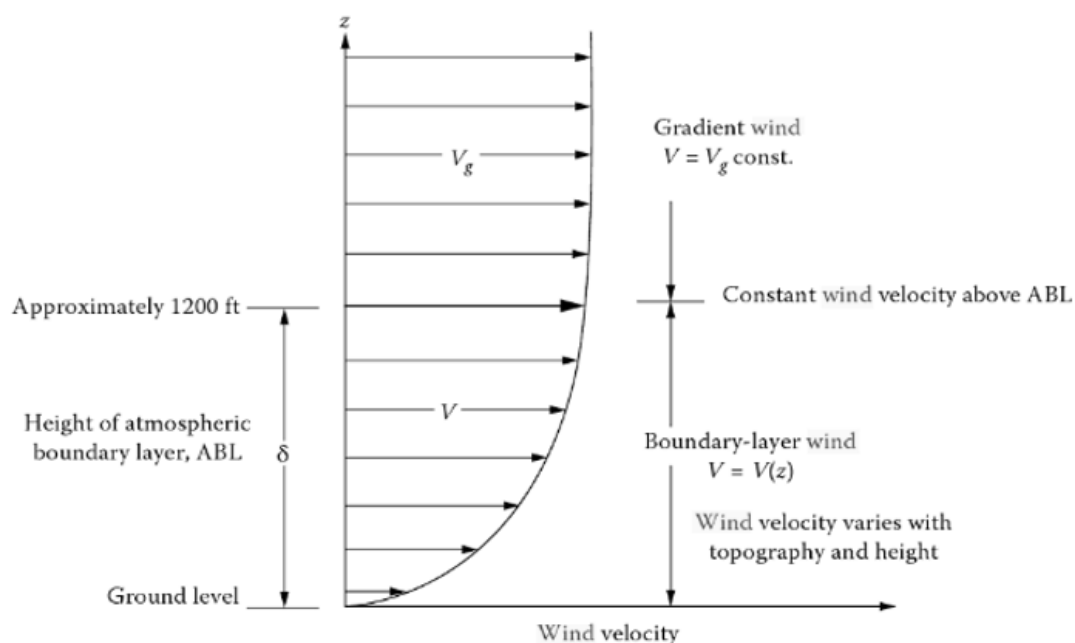


Figure 4 - Typical wind profile where wind velocity varies with altitude (Taly, 2014)



Following the development of a basic wind pressure profile, codes typically modify it based on structural geometry by use of a drag coefficient. In the case of Eurocode, this factor is simply called  $C$ , and is a function of the width and depth of a bridge deck. ASCE 7-10 specifies this factor as  $C_p$ , based upon the windward and leeward faces of a structure. For the analyses in this report however, the coefficient  $C_f$  was used in place of  $C_p$ , which was designed for use on buildings not truss systems like that of a lift bridge.  $C_f$  is a far more conservative factor based upon the solidity of ratio,  $\varepsilon$ , of the system and is defined by the equation below for a square, trussed tower configuration:

$$C_f = 4.0\varepsilon^2 - 5.9\varepsilon + 4.0 \quad (3)$$

The final factor typically applied when determining a design wind pressure is defined by ASCE as  $G$ , the gust effect factor, which is a function of the natural frequency of a structure.  $G$  is a modifier which reduces the wind load for structural systems which are considered rigid or, by ASCE standards, those having a natural frequency of less than 1Hz. For multiple reasons discussed later in this report, the gust factor required examination that began with a review of structural dynamics.

## REVIEW OF STRUCTURAL DYNAMICS

The parameters outlined in international design code, in general, exempt the applicability of quasi-statically applied wind loads when a structure is considered susceptible to dynamic interaction. The susceptibility of a structural system is based heavily on its rigidity as well as its geometry – its aspect ratio, solidity and permeability, as well as the shape of the members or components it is constructed from. Should these properties meet certain criteria, a many types of aerodynamic interaction can occur.

Slender structures have a tendency to induce a phenomena known as vortex shedding. All systems create some form of vortex shedding when exposed to fluid flow, but in the case of a slender bridge, this shedding can be potentially hazardous should it occur near the resonant frequency of the structural system. This famously occurred at the Tacoma Narrows Bridge in 1940, resulting in its imminent collapse (see Figure 5) and eventual reconstruction (Billah, 1991).

Other forms of aerodynamic excitation include galloping and flutter, amongst many others. Usually, these excitations occur at structures like suspension or cable-stayed bridges, but this is primarily a result of their flexibility. Exactly how and why a bridge interacts dynamically with wind is usually studied using wind tunnel tests and only after its susceptibility has been determined.



*Figure 5 - Collapse of the Tacoma Narrows Bridge*

The specific limits at which a structure is considered susceptible are defined by codes individually. For example, ASCE defines rigid structures as those having a natural frequency of less than 1Hz while AASHTO defines it based upon both natural period and the aspect ratio of the system. These parameters are often vague, imprecise, situationally dependent, and little guidance is provided should a system not meet them. Wind tunnel tests are often a suggestion if aerodynamic

excitation is a concern, but the specifics of calculating whether interactions might occur are often not given. Since the bridge system in this report's potential aerodynamic interaction was a concern – as is discussed in later sections – a review of codes beyond AASHTO, ASCE, and Eurocode was done to find a means of assessing the bridge's susceptibility. Such a means was found in the Design Manual for Roads and Bridges (DMRB).

The DMRB is a set of documents on the design of roads and bridges instituted in the United Kingdom and Republic of Ireland. The "Design Rules for Aerodynamic Effects on Bridges" (BD 49/01) are found in Volume 1, Section 3 of the DMRB and contain design calculations for bridges subjected to wind. By DMRB standards, bridge's susceptibility to dynamic wind interaction can be determined using the aerodynamic susceptibility parameter,  $P_b$ , as defined by the equation below:

$$P_b = \left( \frac{\rho b^2}{m} \right) \left( \frac{16V_r^2}{bL f_b^2} \right) \quad (4)$$

Where...

$\rho$  is the density of air

$b$  is the overall width of the bridge deck

$m$  is the mass per unit length of the bridge

$V_r$  is the mean hourly wind speed

$f_b$  is the natural frequency in bending

The magnitude of the susceptibility parameter indicates a bridge's inclination to aerodynamic excitation. A value of  $P_b < 0.04$ , for example, indicates the bridge is subject to insignificant aerodynamic excitation. If  $P_b > 1.00$  however, the bridge is considered very susceptible to aerodynamic excitation such that it will require CFD modeling or wind tunnel testing. For values of  $P_b$  that fall between 0.04 and 1.00, the specifications outlined in the DMRB apply in full.



*Figure 6 - Memorial Bridge (Portsmouth, NH) southern tower and counterweight*

The final dynamic consideration that had to be made in lift bridge analysis was that of potential damping and amplification caused by the counterweights. In general, vertical lift bridges move their spans by means of massive weights inside their towers (see Figure 6, above). Suspended from steel cables, these counterweights are often free to sway and could, in theory, act as amplifiers to tower motion caused by wind or as tuned mass dampers (TMDs). TMDs have been used for decades as a means of decreasing the motion of a building during an earthquake – although the concept was originally applied to inhibit the motion of ships at sea in the early 1900's (Conner, 2002). In general, they are about 1% of the total mass of a building and are tuned such that their natural frequency matches the buildings. If this is done properly, the TMD will move out of synch with the building as it sways and thus fight, or damp, its motion. This is difficult, however. As shown by Figure 7, below, the motion of a building can be significantly magnified if the frequency of the TMD is 5-10% off from that of the building.

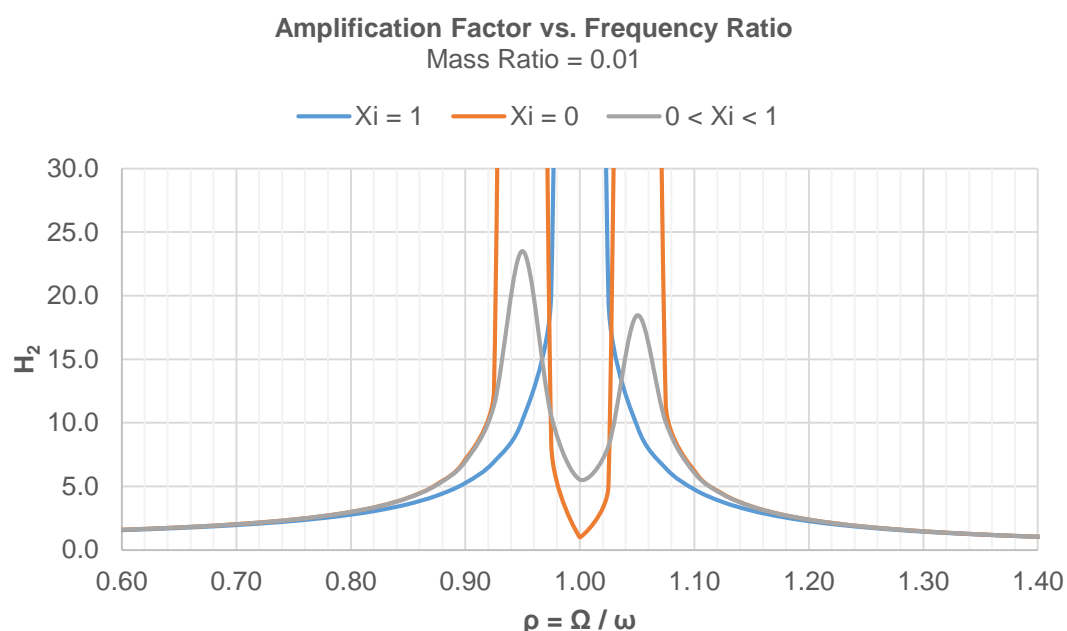


Figure 7 - Amplification factor vs. frequency ratio for a typical TMD system (Connor, 2002)

To check a counterweight's natural frequency and compare it to that of the tower which houses it can be idealized as a simple pendulum. This is not an unrealistic idealization since counterweights are usually suspended from cables which provide minimal damping. The equation for the natural period of a simple pendulum has been established for centuries and is shown below in Equation 5, where the period is independent of mass,  $g$  is the gravitational acceleration constant, and  $L$  is the length of the cable.

$$T_n = 2\pi \sqrt{\frac{L}{g}} \quad (5)$$

Where...

$L$  is the pendulum arm length

$g$  is the gravitational acceleration constant equal to  $9.81 \text{ m/s}^2$

The frequency of the counterweight can be found by taking the inverse of the natural period. To determine whether dynamic interaction occurs between the tower and weights,  $\rho$  is determined by dividing the tower natural frequency by the counterweight natural frequency. This frequency ratio is used in conjunction with the ratio of the masses of the two systems,  $\bar{m}$ , to quantify the pseudo-static amplification,  $H_2$ , described in the equation below:

$$H_2 = \frac{\sqrt{((1+\bar{m})f^2 - \rho^2)^2 + (2\xi_d \rho f(1+\bar{m}))^2}}{|D_2|} \quad (6)$$

Where...

$\bar{m}$  is the mass ratio of the counterweight to the fixed span and tower

$\xi_d$  is the damping ratio assumed to be zero

$f$  is assumed to be 1.0

$\rho$  is the ratio of natural frequencies

And...

$$|D_2| = \sqrt{\left( ((1 - \rho^2))(f^2 - \rho^2) - \bar{m}\rho^2 f^2 \right)^2 + \left( 2\xi_d \rho f(1 - \rho^2(1 + \bar{m})) \right)^2} \quad (7)$$

## CHAPTER 3

### CASE STUDY

#### 3.1 THE MEMORIAL BRIDGE – A MOVABLE LIFT BRIDGE

The Memorial Bridge (Figure 8) is a steel vertical lift bridge located in Portsmouth, NH. A port city, Portsmouth is built along the Piscataqua River – a navigable, ice-free, deep draft tidal river connecting Great Bay to the Atlantic Ocean (State of New Hampshire Division of Ports and Harbors, 2003). Home to over 20,000 residents (US Census Bureau, 2015), the city is across the river from the Portsmouth Naval shipyard and, upon passing beneath the Memorial Bridge, the location of the Market Street Terminal. With two berths capable of accommodating 300ft or 600ft vessels, the terminal handles shipments ranging from salt and scrap metal to power plant and machine components. The Piscataqua River also houses many other berths upriver from the Memorial Bridge for companies including Irving, Granite State Mineral, National Gypsum.



*Figure 8 - The Memorial Bridge as seen from Portsmouth (2016)*

Following the demolition of its predecessor – another vertical lift designed by J.A.L Waddell in 1922 – the Memorial Bridge was opened to the public in 2013 as the first and only gussetless bridge in the world (Memorial Bridge Project, 2015). This was an accomplishment its designer, Ted Zoli, pushed engineering boundaries to achieve. In its final form, the bridge possesses only 77,000 bolts, reducing the potential for error in the form of over or under-torqued bolts placed steel workers during construction – though at the expense of weight. The bridge, in sum, weights 30 percent more than the runner up in the design bid. This uniqueness makes the Memorial Bridge of particular interest to research universities and engineering firms alike. This thesis is a part of its primary research project, the Living Bridge Project, which is discussed in more depth in Section 3.2, below.

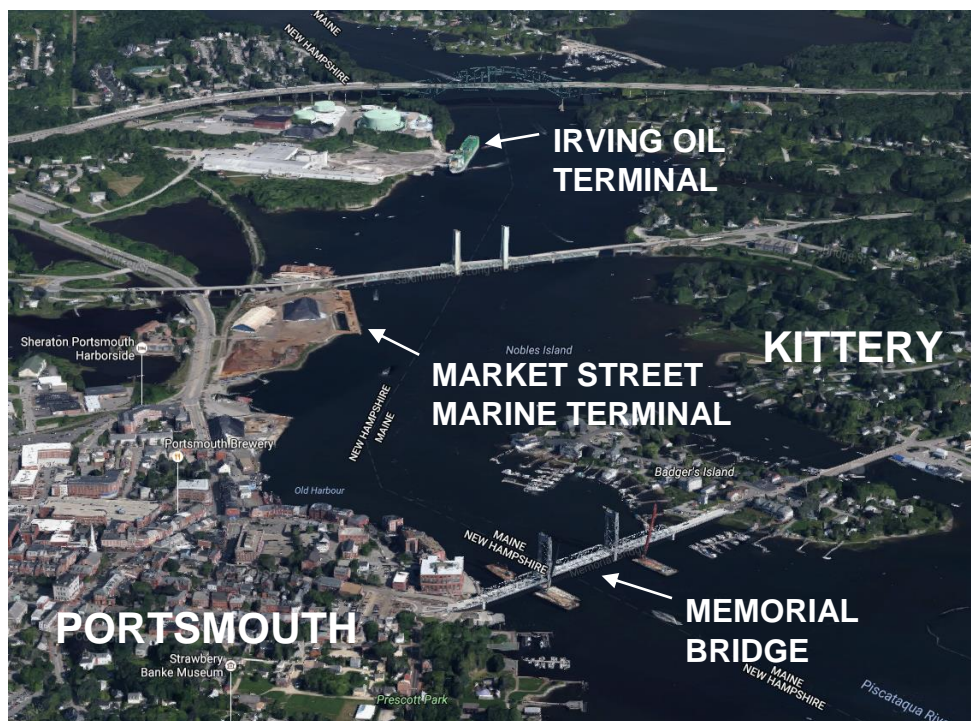


Figure 9 - Portsmouth, NH (aerial rendering from Google Maps)



### 3.1.1 Structural Systems and Geometry

The Memorial Bridge, as stated above, is a steel vertical lift bridge. It consists of a fixed south and north span of 300 feet in length, and a vertical lift span of the same. The lift span is counterbalanced by two concrete masses in each the north and south towers weighing about 1.18 million pounds each and suspended from 13.9 foot lengths of cable in the un-lifted position. With a total lift height of 154 feet from mean sea level (MSL) to bottom chord, the lift span itself weighs a total of 2,390,000 pounds.

The towers to the bridge rest on concrete piers of low-strength concrete – originally constructed for the first Memorial Bridge in 1922 (Memorial Bridge Project, 2015), which stood in the new bridge's place. The bridge is primarily composed of steel that has been covered by a metalized coating to prevent corrosion and future section loss.

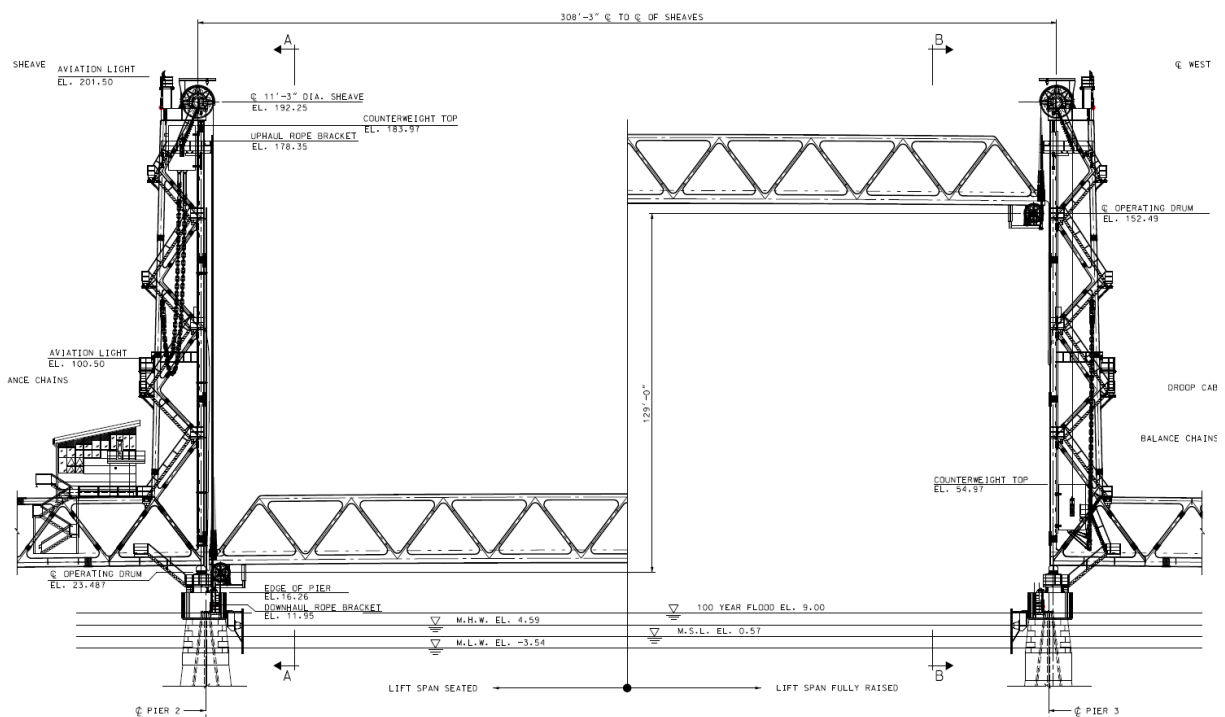


Figure 10 - Elevation of the vertical lift span in its lifted and un-lifted states

### 3.2 LIVING BRIDGE PROJECT

The Living Bridge Project is a joint effort by the University of New Hampshire, National Science Foundation (NSF), and the NH Department of Transportation (NH DOT) to transform the Memorial Bridge into a self-powered, self-diagnosing, “smart bridge”. Using an array of sensors acquiring stress, strain, and acceleration data from the bridge as well as weather, environmental, and current data from the river, the Living Bridge Project aims to extend the design life of the Memorial Bridge while investigating the design validity of this first-of-its-kind structure.

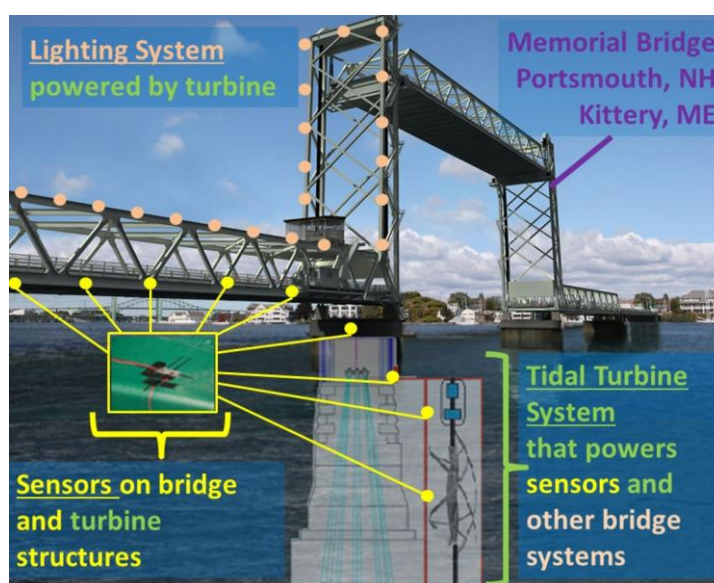


Figure 11 – Overview UNH's Living Bridge Project

In conjunction with the sensor array, the Memorial Bridge, through the Living Bridge Project, will also be home to a tidal turbine and platform. This system will be attached to the south bridge pier and, after its installation, supply power to the bridge and its sensors by means of the powerful currents which flow in the Piscataqua River (see Figure 12). While the design and calculations for the tidal deployment platform are not within the scope of this report, they are provided in Appendix D as supplemental material to be later integrated into the objective operational decision protocols for the Memorial Bridge.

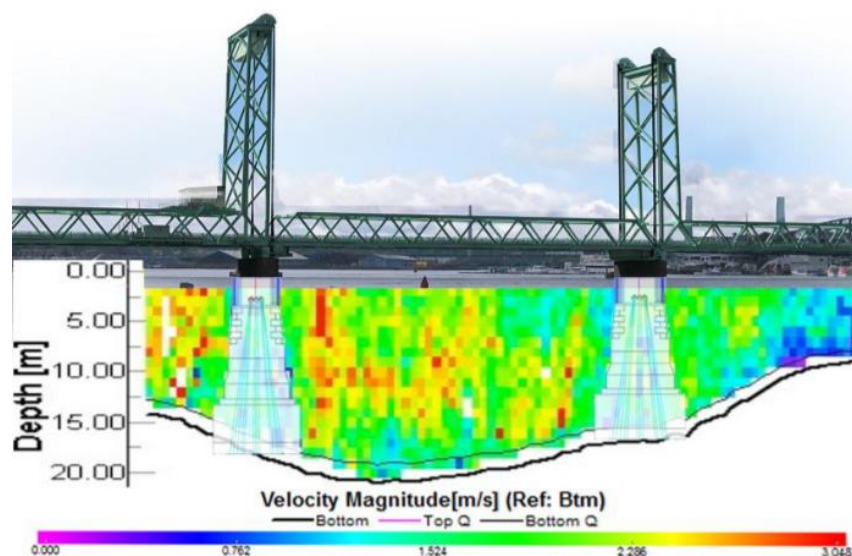


Figure 12 - Velocity magnitude of currents beneath Memorial Bridge

### 3.3 THE NEED FOR A DECISION MAKING PROTOCOL

As described previously, the decision to operate or not operate the vertical lift span of a movable bridge is generally left to the discretion of the operators. This is no less true in the case of the Memorial Bridge. Here, a specified wind speed of 50 miles per hour was set out by the lift mechanism manufacturer as the maximum operable lift speed. This speed, however, has no basis in any form of structural analysis. What is more, there is currently no objective means of determining the wind speed at the bridge location. Lift operators instead must rely on a flag on the top of a nearby building which is said to blow straight out, horizontally, at inoperable wind speeds.

On top of the ungrounded maximum lift speed, there are multiple design concerns in regards to the structure. One of the primary is the slenderness of the bridge towers. Compared to the previous towers, those on the new Memorial Bridge are significantly less wide at their base. To compound this, studies have shown existing torque in the towers, reducing member capacities.

Premature wearing of the gears of the lift system has been documented and concern over the potential for dynamic interaction between the towers and counterweights has been voiced.

The final reason for an objective basis for the lift is the location of the bridge. As shown in Figure 9, the Memorial Bridge forms a gateway to the shipping births and upper portions of the Piscataqua River. The inoperability of the lift could, in the worst case, shut down naval traffic. In the more likely case, it could get stuck in the lifted position – as did its upriver counterpart the Sarah Mildred Long Bridge – and impede vehicular traffic.

Given each of these reasons, it is clear an objective protocol for the lift of the Memorial Bridge would be of benefit. Such a protocol could loan valuable information not only about how the system behaves in variable wind conditions, but also help prevent its inoperability or failure in the long-term.

## CHAPTER 4 ANALYSIS AND RESULTS

### 4.1 AERODYNAMIC SUSCEPTABILITY

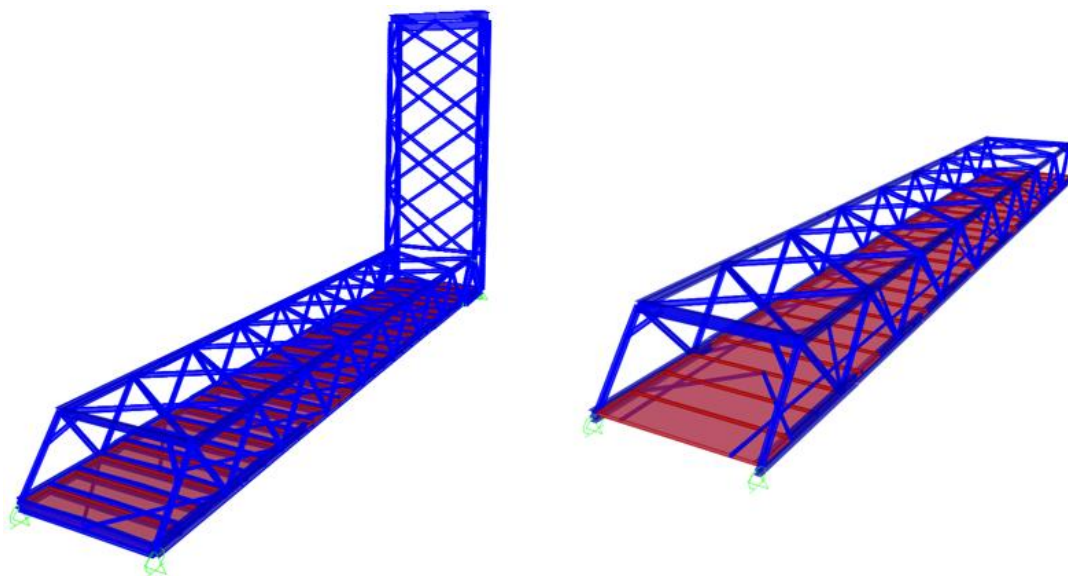
Before wind loads for the Memorial Bridge could be developed, the flexibility of its lift span and fixed spans needed to be defined. Most building and bridge codes are applicable within a certain range of natural frequencies and geometries and should a system fall outside this specified range, modifications to calculations need to be made or, at times, the code is rendered inapplicable. In the case of ASCE 7-10, a system is defined as rigid if its natural frequency is above 1 Hertz. Should a system fall under a Hertz, the gust effect factor  $G$ , which is normally taken as 0.85, must be recalculated using the equation below:

$$G_f = 0.925 \left( \frac{1 + 1.7I_z \sqrt{g_Q^2 Q^2 + g_R^2 R^2}}{1 + 1.7g_v I_z} \right) \quad (8)$$

The 1 Hertz specification is true for Eurocode as well, with the additional caveat that natural frequencies in both bending *and torsion* need to be above 1 Hertz. Notes in Eurocode also state that “for normal road and railway bridge decks of less than 40m span a dynamic response procedure is generally not needed.” (European Committee for Standardization, 2005).

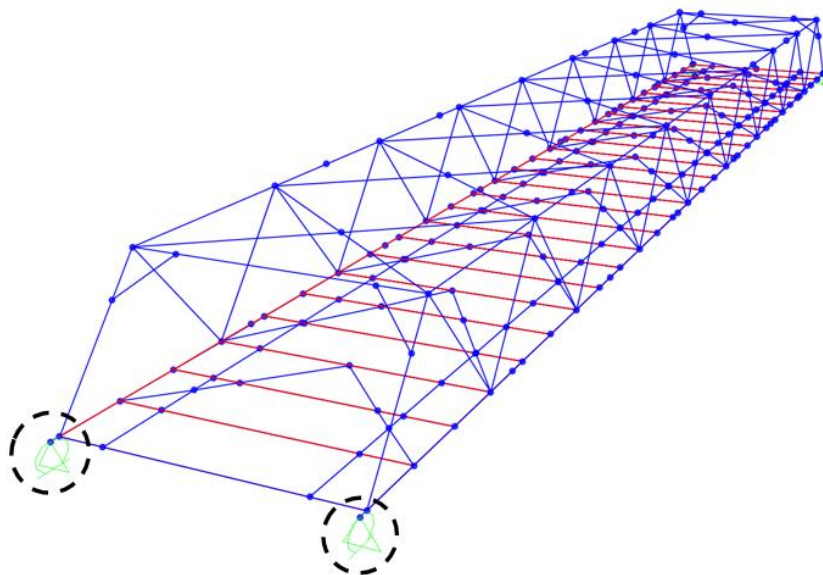
Since the spans of the Memorial Bridge are over 40m and because of concern over the natural frequency of the lift span in the up position, models of the structural systems of the Memorial Bridge were generated in SAP2000®, as shown in Figure 13 below. As-built drawing sets, provided by the designer, were used to generate separate models for the lift span of the bridge

as well as the fixed south span of the bridge (closest to Portsmouth). The south span was assumed to be symmetric with the north span given their equal lengths and tower heights. This assumption reduced the number of models that needed to be produced and, consequently, the total number of analyses that needed to be run. All connections in the bridge system were assumed to be fully-fixed, rigid connections.



*Figure 13 - SAP2000® models for the south span (left) and lift span (right) of the Memorial Bridge*

Many of the steel sections in the system required custom modeling. As described in Section 3.1, the Memorial Bridge is an innovative structure and many of the steel members used in its construction were unique. Indeed, each of the bottom and top chord members for the lift and fixed spans, as well as the fixed span tower columns, are non-standard elements which required custom modeling using SAP2000's section designer. The details for these members are given in Appendix C along with the standard W-shapes and channels used in the models.



*Figure 14 - Southern boundary condition (pin-roller combination allowing thermal expansion)*

The boundary conditions modeled in SAP2000® required careful thought and development as they greatly affect the natural frequency of the system. In the down position, the lift span is locked in place. Thermal expansion joints allow the bridge to expand and contract as temperature changes – so to reflect this, the SAP model assumed pinned conditions at one end and a pin-roller combination at the other (see Figure 14). The pin-roller combination simulated the expansion joint and allowed for longitudinal, thermal expansion and deflection, but resisted movement in the lateral direction.

In the up position, the lift span is completely suspended from cables and rests between channel guides. In theory, this allows the bridge to move, un-resisted, vertically. However, given the extreme weight of the span along with the wind loads, which are applied only laterally, it was assumed the lift span could not move vertically. The gap between the channel guides and the lift span was assumed to be negligible – enough to be filled by the lift span being pushed laterally by the force of the wind so as to induce resistance parallel to the direction of the wind. Thermal

expansion was allowed for and thus, in the lifted position, the same boundary conditions were used as the un-lifted position.

Once the system was modeled in SAP2000®, a modal analysis revealed the natural frequencies in bending and torsion for the bridge. For the lift and fixed span systems, these frequencies are shown in Table 1. As can be seen, none of the frequencies are less than 1 Hertz, however, since the 1 Hertz limit is a guideline more than a limit state for aerodynamic excitation, further checks were made to validate that the span indeed does not experience aerodynamic excitation as a result of wind forces.

While ASCE and Eurocode give a limited description of how to establish the aerodynamic susceptibility of a system, the Design Manual for Roads and Bridges (DMRB) explicitly establishes it. As described in the introductory material, the equation for aerodynamic susceptibility of a system is given by  $P_b$  in the equation below.

$$P_b = \left(\frac{\rho b^2}{m}\right) \left(\frac{16V_r^2}{bL f_b^2}\right) \quad (9)$$

Where...

$\rho$  is the density of air

$b$  is the overall width of the bridge deck

$m$  is the mass per unit length of the bridge

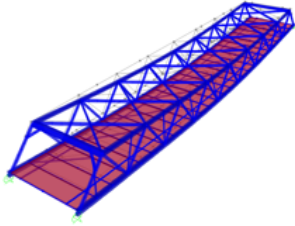

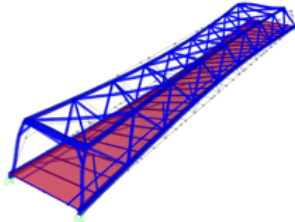
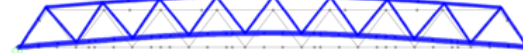
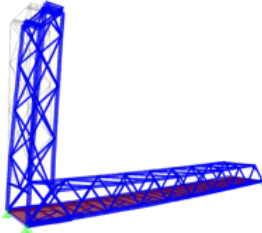
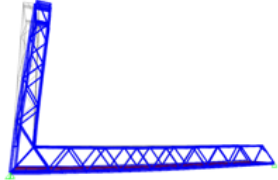
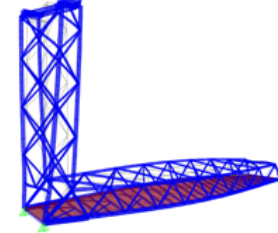
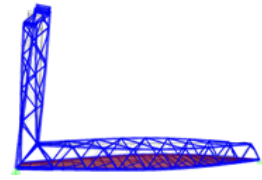
$L$  is the length of the span in question

$V_r$  is the mean hourly wind speed

$f_b$  is the natural frequency in bending



Table 1 - Bending and torsional modes for SAP2000® models

<b>LIFT SPAN</b>	<b>MODE 1</b>		 <b>F<sub>n</sub> in bending = 1.14Hz</b>
	<b>MODE 2</b>		 <b>F<sub>n</sub> in torsion = 1.48Hz</b>
<b>SOUTH SPAN</b>	<b>MODE 1</b>		 <b>F<sub>n</sub> in bending = 1.16Hz</b>
	<b>MODE 3</b>		 <b>F<sub>n</sub> in torsion = 1.67Hz</b>

The natural frequency in bending,  $f_b$ , can be established from the SAP2000® analyses run previously, with results shown in Table 1. The mean hourly wind speed is established from the equation  $V_r = S_m V_s$  and is shown in Appendix A for both the up and down positions of the lift. While analyses show that the bridge may be subject to some aerodynamic excitation (see Table 23 in Appendix A), the low solidity ratio shown in Appendix A results in no aerodynamic excitation for the bridge system, as shown in Table 2.

Table 2 - Bridge stability to excitation

Vortex Shedding	Stable
Turbulence	Stable
Galloping/flutter	Stable
Non-oscillatory divergence	Stable

## 4.2 DEVELOPMENT OF WIND LOADS

Following the establishment of the Memorial Bridge's aerodynamic stability, wind loads were developed using multiple international design codes. The calculation and tabulation of all loads was done using Microsoft Excel. Only wind loads in the direction perpendicular to the span of the bridge and at an angle normal to the water surface were considered.

### 4.2.1 ASCE 7-10

ASCE 7-10 is a United States building code created by the American Society of Civil Engineers (ASCE). Typically, it applies to buildings and similar structures but for the purposes of this report, it was used for the analysis of the Memorial Bridge by means of a drag coefficient,  $C_f$ .

Wind loads on building are usually established using the equation below, where  $G$  is a gust factor based on the rigidity of the structural system in question and  $q$  is the basic wind pressure.

$$F = qGC_p \quad (10)$$

In order to realistically capture the effects of wind on the bridge structure, however, it was necessary to use a different  $C$  factor for analyses. ASCE's *Wind Loads on Other Structures and Building Appurtenances – MWFRS* section outlines provisions for trussed tower configurations. The trussed tower section uses the force coefficient of  $C_f$  – a more conservative factor established from the solidity of the truss system in question. Given the Memorial Bridge's similarity to a truss

system, it was deemed acceptable to use this  $C_f$  factor for the development of loads, rather than the  $C_p$  factor typically used for buildings.

C <sub>f</sub> 2.52	K <sub>z</sub> by Exposure Category			Windward Pressure		
	B	C	D	q <sub>s</sub>	q <sub>z</sub>	qGC <sub>f</sub>
0	0.57	0.85	1.03	48.3	41.1	88.1
15	0.62	0.9	1.08	48.3	43.5	93.3
20	0.66	0.94	1.12	48.3	45.4	97.5
25	0.7	0.98	1.16	48.3	47.4	101.6
30	0.76	1.04	1.22	48.3	50.3	107.8
40	0.81	1.09	1.27	48.3	52.7	113.0
50	0.85	1.13	1.31	48.3	54.6	117.2
60	0.89	1.17	1.34	48.3	56.6	121.3
70	0.93	1.21	1.38	48.3	58.5	125.5
80	0.96	1.24	1.40	48.3	60.0	128.6
90	0.99	1.26	1.43	48.3	60.9	130.7
100	1.04	1.31	1.48	48.3	63.3	135.8
120	1.09	1.36	1.52	48.3	65.8	141.0
140	1.13	1.39	1.55	48.3	67.2	144.1
160	1.17	1.43	1.58	48.3	69.1	148.3
180	1.2	1.46	1.61	48.3	70.6	151.4
200	1.28	1.53	1.68	48.3	74.0	158.7

Figure 15 - Basic pressure profile as established in Excel

Following the establishment of the force coefficient, the basic wind pressure profile needed to be established, ( $G$  having been previously developed as 0.85 for a rigid structure from the SAP analysis described in Section 4.1). Using Excel, functionality was built into a spread sheet such that factors which influence the basic wind pressure profile could be manipulated and changed for variable conditions. For the development of the basic wind load by ASCE 7-10, risk Category III was used. Surrounding topography was said to be flat such that  $K_{zt} = 1.0$  for the site (see Appendix A). The Exposure Category was taken as C in the determination of  $K_z$  and the pressure profile was determined up to 200 feet in height, as shown in Figure 15, so as to cover the entirety of the tower heights. Fitting a polynomial function to the pressure profile developed allowed for the determination of pressure as a function of height.

### 4.2.2 Eurocode

Eurocode Section 8.3.2 establishes the total force of wind on a structural system in the lateral direction using the equation shown below:

$$F_W = \frac{1}{2} \rho v_b^2 C A_{ref,x} \quad (11)$$

In the above equation,  $A_{ref,x}$  is a reference area equal to the total area of members exposed to wind in the x-direction (see Figure 16). The member area is calculated in Appendix A using an AutoCAD model developed for the establishment of wind loads. The force coefficient  $C$  for Eurocode is established as the product of  $c_{f,x}$  and  $c_e$  where  $c_{f,x}$  is taken as 1.3 for typical bridge shapes and  $c_e$  is a coefficient based upon the height,  $z$ , to the center of the structural system in question (see Appendix A).

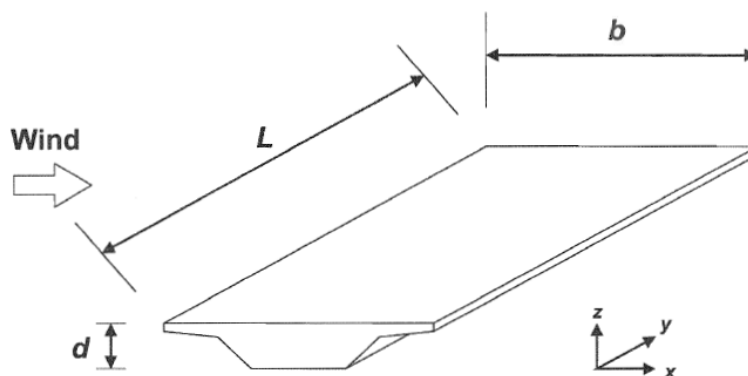


Figure 16 - Wind directions (Figure 8.2 in Section 8 of Eurocode)

The density of air,  $\rho$  in Equation 11 above, is variable by temperature. An examination of NOAA data for the bridge site reveals that, through 1996, there were annual temperature observations of over 100 degrees Fahrenheit in the summer months and multiple observations below 0 degrees Fahrenheit in the winter months. Temperatures of  $-4^{\circ}\text{F}$  ( $-20^{\circ}\text{C}$ ),  $59^{\circ}\text{F}$  ( $15^{\circ}\text{C}$ ), and  $104^{\circ}\text{F}$  ( $40^{\circ}\text{C}$ ) were therefore used in analysis to capture the full spectrum of temperature experienced at the Memorial Bridge location.

Microsoft Excel was used to calculate the uniform wind pressure distributions resulting from the above equations and assumptions. The results of the Eurocode wind load development are shown below in Table 3.

Table 3 - Wind loads developed by Eurocode

Temperature (C) -20			Temperature (C) 15			Temperature (C) 40		
<b>Lift Span (Up Position)</b>								
A_ref,x	201.1	m <sup>2</sup>	A_ref,x	201.1	m <sup>2</sup>	A_ref,x	201.1	m <sup>2</sup>
d_tot	7.91	m	d_tot	7.91	m	d_tot	7.91	m
C	5.07	-	C	5.07	-	C	5.07	-
b/d_tot	1.91	-	b/d_tot	1.91	-	b/d_tot	1.91	-
q_b	<b>784</b>	-	q_b	<b>689</b>	-	q_b	<b>633</b>	-
L_tot	326.8	m	L_tot	326.8	m	L_tot	326.8	m
F_w	<b>0.168</b>	klf	F_w	<b>0.147</b>	klf	F_w	<b>0.135</b>	klf
<b>Lift Span (Down Position)</b>								
A_ref,x	201.1	m <sup>2</sup>	A_ref,x	201.1	m <sup>2</sup>	A_ref,x	201.1	m <sup>2</sup>
d_tot	7.91	m	d_tot	7.91	m	d_tot	7.91	m
C	2.90	-	C	2.90	-	C	2.90	-
b/d_tot	1.91	-	b/d_tot	1.91	-	b/d_tot	1.91	-
L_mem,tot	326.8	m	L_mem,tot	326.8	m	L_mem,tot	326.8	m
F_w	<b>0.096</b>	klf	F_w	<b>0.084</b>	klf	F_w	<b>0.077</b>	klf
<b>South Span</b>								
A_ref,x	227.6	m <sup>2</sup>	A_ref,x	227.6	m <sup>2</sup>	A_ref,x	227.6	m <sup>2</sup>
d_tot	8.67	m	d_tot	8.67	m	d_tot	8.67	m
C	2.90	-	C	2.90	-	C	2.90	-
b/d_tot	1.74	-	b/d_tot	1.74	-	b/d_tot	1.74	-
L_mem,tot	495.3	m	L_mem,tot	495.3	m	L_mem,tot	495.3	m
F_w	<b>0.072</b>	klf	F_w	<b>0.063</b>	klf	F_w	<b>0.058</b>	klf
<b>Tower</b>								
A_ref,x	68.1	m <sup>2</sup>	A_ref,x	68.1	m <sup>2</sup>	A_ref,x	68.1	m <sup>2</sup>
d_tot	50.88	m	d_tot	50.88	m	d_tot	50.88	m
C	3.60	-	C	3.60	-	C	3.60	-
b/d_tot	0.30	-	b/d_tot	0.30	-	b/d_tot	0.30	-
L_mem,tot	130.5	m	L_mem,tot	130.5	m	L_mem,tot	130.5	m
F_w	<b>0.101</b>	klf	F_w	<b>0.089</b>	klf	F_w	<b>0.082</b>	klf

### 4.2.3 AASHTO

AASHTO's movable bridge design guide generally references the AASHTO *LRFD Bridge Design Specifications* for the establishment of wind loads, but requires that analyses be carried out for vertical lift bridges in their lifted and un-lifted positions. Using the bridge design guide, the basic equation for wind pressure is given as:

$$P_D = P_B \left( \frac{V_{DZ}^2}{10,000} \right) \quad (12)$$

Where...

$P_D$  is the design wind pressure

$P_B$  is the base wind pressure as specified by AASHTO

$V_{DZ}^2$  is the design wind speed, defined below

The basic wind speed ( $V_B$ ) in the above equation is assumed to be equal to 100mph, thus resulting in the 10,000 seen in the denominator. The design wind velocity,  $V_{DZ}$  is established from Equation 13, shown below. Designs are typically done at 60 degrees Fahrenheit and, as can be seen in the equation, it is relatively difficult to modify this temperature.

$$V_{DZ} = 2.5V_0 \left( \frac{V_{30}}{V_B} \right) \ln \left( \frac{Z}{Z_0} \right) \quad (13)$$

Where...

$V_{DZ}$  is the design wind velocity at the height,  $Z$ , of the structure

$V_{30}$  is the wind velocity at 30 feet above the design water level

$V_B$  is the base wind velocity of 100mph

$V_0$  is the friction velocity based on upwind surface characteristics

$Z_0$  is the friction length of upstream fetch, a meteorological wind characteristic

Despite the difficulty of modifying AASHTO's design equations for temperature, wind loads were developed using its specifications nonetheless for the purpose of comparison to the numbers generated by ASCE and Eurocode at the same temperature. As shown in Table 4 - AASHTO

developed wind loads, AASHTO proved to be relatively conservative because the minimum loads it requires per foot of member length as per Section 3.8.1.2. However, these loads were reduced to values comparable to those developed by ASCE and Eurocode by a provision in the movable bridge guide stating “when the movable span [of a vertical lift bridge] is normally left in the closed position, the open position shall be investigated for a load combination 60 percent of the wind pressures specified in Article 3.8 of the *AASHTO LRFT Bridge Design Specifications* applied to the structure...”

Table 4 - AASHTO developed wind loads

Uniform Wind Load (AASHTO-1) Unreduced loads			Uniform Wind Load (AASHTO-1) 60% reduction		
<b>Windward</b>			<b>Windward</b>		
<i>Lift Span</i>	<i>0.300</i>	<i>klf</i>	Lift Span	0.180	klf
<i>South Span</i>	<i>0.300</i>	<i>klf</i>	South Span	0.180	klf
<b>Leeward</b>			<b>Leeward</b>		
<i>Lift Span</i>	<i>0.150</i>	<i>klf</i>	Lift Span	0.090	klf
<i>South Span</i>	<i>0.150</i>	<i>klf</i>	South Span	0.090	klf

#### 4.2.4 Hybrid Wind Loading

Each of the wind loads developed by ASCE 7-10, Eurocode, and AASHTO had aspects desirable to the accurate representation of loading at the bridge site. Both Eurocode and ASCE’s ability to modify the density of air based on temperature was an attribute determined to be a requirement for analysis as a direct result of Figure 17, shown below. As it describes, the difference between wind loads at a temperature of -20 degrees centigrade (-4°F) and 40 degrees centigrade (104°F) is as much as 21 percent at wind speeds of 135mph.

Since AASHTO is relatively inflexible in terms of temperature varying analysis and cannot capture this effect easily, it was not used for hybrid wind load development. However, the provision in its code stating the bridge should be analyzed both the lifted and un-lifted positions was used. Because of this, it was deemed necessary to capture the effects of elevation change on wind

pressure, in conjunction with temperature variation, so as to most accurately load the lift span in both its potential positions.

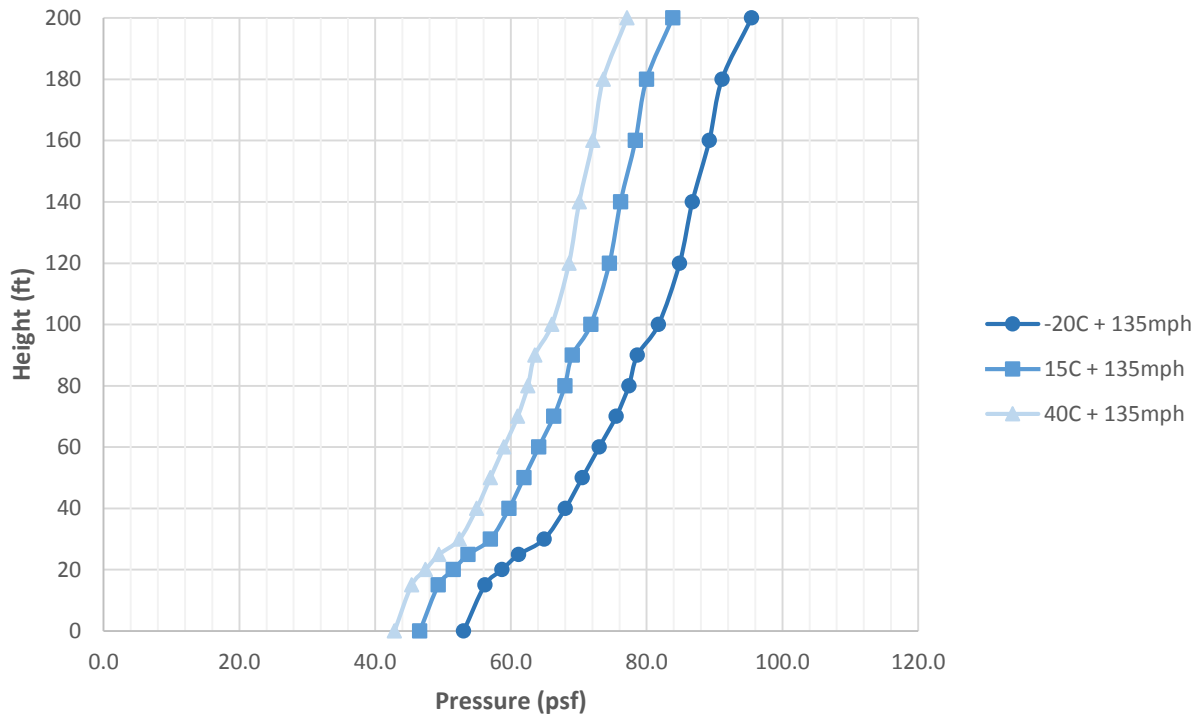


Figure 17 - Wind profiles varied by temperature as a function of height

Using the Microsoft Excel sheets previously developed at the temperatures used for Eurocode analysis, a hybrid wind load sheet was developed. Utilizing a base wind speed of 50mph and 100mph, twelve total wind load scenarios were developed (see Table 6). An AutoCAD model allowed for elevation data to be taken for each, individual member in the structural system. This, in turn, allowed for loads to be developed on a by-member basis, based on their maximum elevation to be conservative.

Table 5 - ASCE basic wind pressure numerical coefficients as a function of temperature

Temperature (°F)	Numerical Coefficient
-4	0.00291
59	0.00255
104	0.00235



After modifying numerical coefficients, a basic pressure profile could be established and a polynomial function fit to it. With this formula for pressure (in terms of elevation) for each load case, the by-member elevation data could be filtered in to establish the maximum wind load on each member in the system.

From here, the previously established Eurocode analyses could be checked against the newly established ASCE loads, taking the place of any that were smaller in magnitude to be conservative. It should be noted that this Eurocode integration is done purely on a conservative design basis and that both ASCE and Eurocode analyses were run separately so as to account for any lacking transferability between importance factors and risk categories. The resulting distribution is demonstrated below in Figure 18 for the loading of a column in the tower span where Eurocode controls in lower elevations and ASCE in higher.

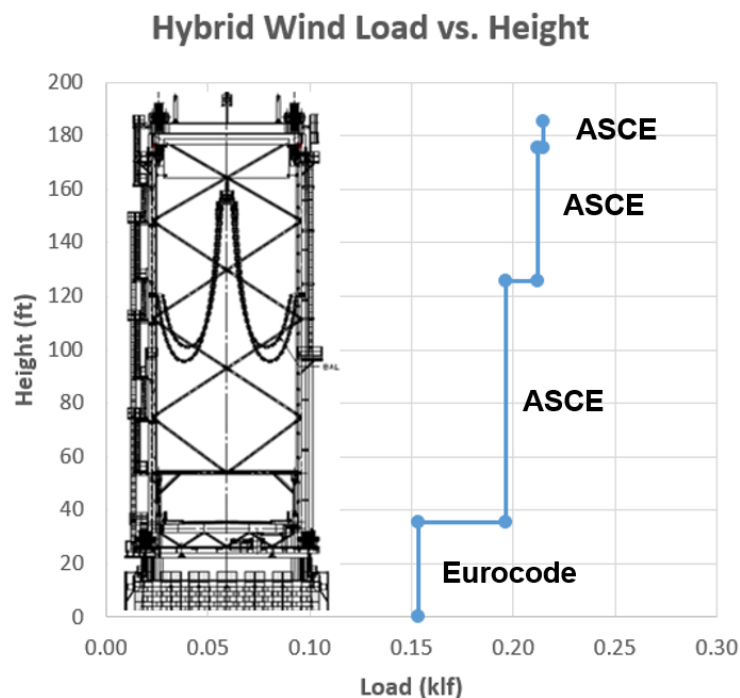


Figure 18 - Wind loading vs. height for tower column

### 4.3 ANALYSIS IN SAP2000®

The SAP2000® models used to determine the natural frequencies in bending and torsion for the aerodynamic susceptibility calculations were used for the analysis of the bridge spans under wind loading. The hybrid loads developed in Section 4.2.4 were applied to the lift span in conjunction with the dead load of the system and thermal loads corresponding to the temperatures used in the creation of the hybrid loads. A full summary of the twelve load cases used for analysis can be seen below in Table 6.

Following analysis of the lift span, the south span was analyzed. The south span analysis had to follow the lift span's so the reactions from the span in the lifted position could be transferred and applied to the tower system of the south span.

*Table 6 - Hybrid load cases for SAP2000® analysis (all load cases include dead load)*

Load Case	Lift	Temp (F)	Thermal Load (F)	Base Wind (mph)
Hybrid-1D	Down	-4	-64	100
Hybrid-2D	Down	59	-1	100
Hybrid-3D	Down	104	44	100
Hybrid-1U	Up	-4	-64	100
Hybrid-2U	Up	59	-1	100
Hybrid-3U	Up	104	44	100
Hybrid-4D	Down	-4	-64	50
Hybrid-5D	Down	59	-1	50
Hybrid-6D	Down	104	44	50
Hybrid-4U	Up	-4	-64	50
Hybrid-5U	Up	59	-1	50
Hybrid-6U	Up	104	44	50

Owing to the sheer volume of data acquired in twelve SAP analyses, critical members were selected for the tabulation of moment data only. Critical members were deemed as those seen to experience significantly higher demands than others or members deemed of interest from a design standpoint. Such members include those at the mid-span and the ends of the lift, the

bottom columns of the tower system, portal beams, and floor beams under high demands. Analysis results for these members were tabulated for use in the objective protocol described in Section 4.3.1, below, and an abridged tabulation of this nature is shown in Table 7.

Table 7 - Sample tabulation of minor moment data for critical lift span members

100 mph			50 mph		
Hyb-1D	Hyb-2D	Hyb-3D	Hyb-4D	Hyb-5D	Hyb-6D
-4	59	104	-4	59	104
↑ 401.5	→ 107.3	↓ -101.5	↑ 323.5	→ 38.1	↓ -165.0
↓ -4.7	→ -2.3	↑ 2.3	↓ -3.0	↑ 1.1	↑ 1.3
↓ -3.8	↑ -2.5	→ -3.1	↓ -2.8	↑ 1.1	↓ -1.7
↓ -28.3	→ -26.3	↑ -25.1	↓ -15.6	↑ -15.0	↑ -14.7
↓ -23.4	→ -21.7	↑ -20.6	↓ -12.2	→ -11.7	↑ -11.5
↓ -54.5	→ -46.9	↑ -42.1	↓ -23.0	→ -18.9	↑ -16.3
↓ -29.9	↑ -27.5	↑ -26.4	↑ 11.8	↓ 11.4	↓ 11.4
↑ 144.9	↓ 139.2	↓ 136.7	↓ 54.4	→ 58.7	↑ 62.6
↑ 117.7	↓ 113.5	↓ 112.0	↑ 53.1	↓ -50.0	↓ -48.0
↓ -33.2	→ -9.3	↑ 17.1	↓ -33.1	→ -8.4	↑ 17.1

#### 4.3.1 Predictive Formula and Objective Protocol

The resulting member moments from SAP2000® gave a baseline of maximum critical member demands at given temperatures and wind speeds. This baseline allowed for the interpolation of critical member demands at temperatures and wind speeds between the ones analyzed. For example, take the minor moment results for the leeward H-H top chord section of the lift span in the up position at 100mph wind speeds. At -4 degrees Fahrenheit, it's maximum demanded minor moment is -34.7 kip-ft, as shown below in Figure 19.

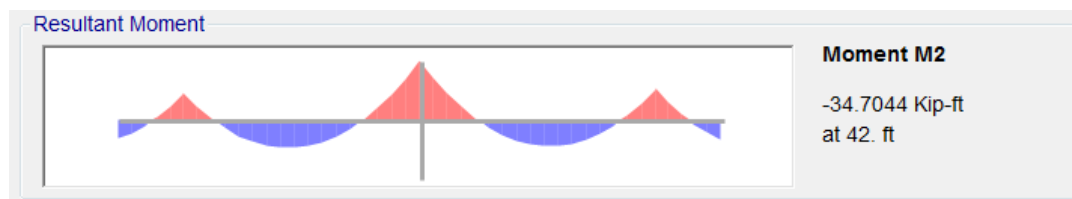


Figure 19 – Minor moment for lift span section H-H in the lifted position at -4 degrees Fahrenheit

This minor moment demand can be compared to the demand for the same section at 59 degrees Fahrenheit (-31.6kip-ft) and 104 degrees Fahrenheit (-29.7kip-ft) and an interpolation can be made to determine the demand at any temperature between the minimum and maximum. This is done in Excel by the example formula shown below:

$$=IF(\$D\$3<=59,IF(J114>I114,J114-(((59-\$D\$3)/63)*(J114-I114)),J114+((I114-J114)*((59-\$D\$3)/63))),IF(K114>J114,K114-(((104-\$D\$3)/45)*(K114-J114)),K114+((104-\$D\$3)/45)*(J114-K114)))$$

In this formula, Excel is taking an input temperature (\$D\$3) and determining whether it lies between -4 and 59 degrees Fahrenheit or 59 and 104 degrees Fahrenheit. It then uses this determination to linearly interpolate the member demand at the given temperature and 100mph wind speed.

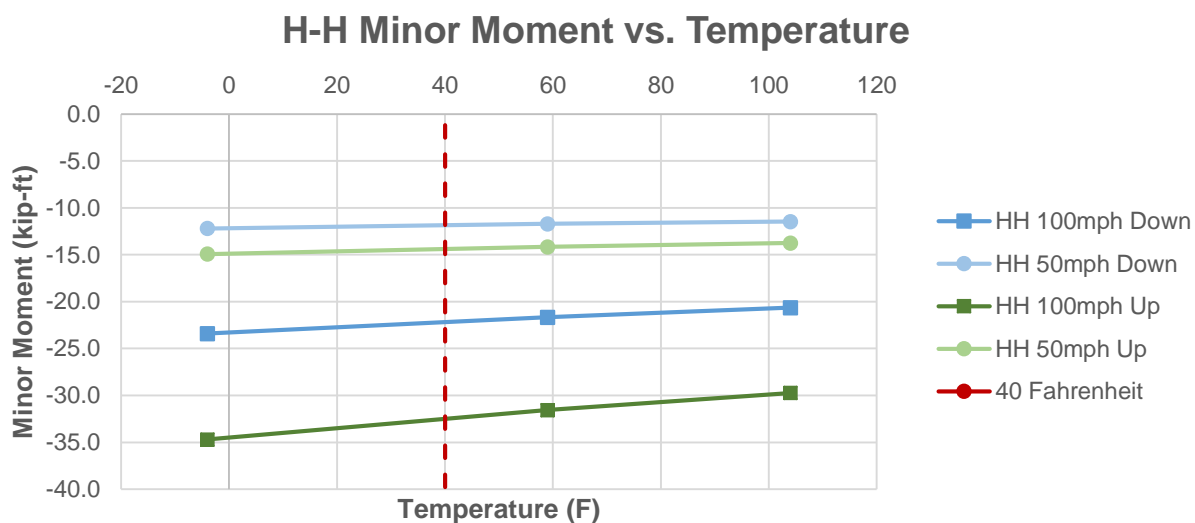


Figure 20 - Lift span section H-H interpolated minor moments at 40 Fahrenheit

Following the temperature interpolation, Excel can perform a similar interpolation to determine the moment demands at the 50mph base wind speed. An interpolation between the determined

moment demands at 50mph and 100mph allows for a prediction of moment demand at wind speeds between these values.

Figure 20, above, shows linear trends in maximum minor moments for leeward section H-H of the lift span in both the up and down position. The intersection of the dashed line with data shows the moments Excel will interpolate for an input temperature of 40 degrees Fahrenheit in each of the analyzed conditions.

The interpolated data for both wind speeds from the temperature data above is shown below where the dashed line intersects data at interpolation points for an input of 75mph wind speed. The difference between these results in the lifted and un-lifted states represents the change in minor moment predicted if a lift is made.

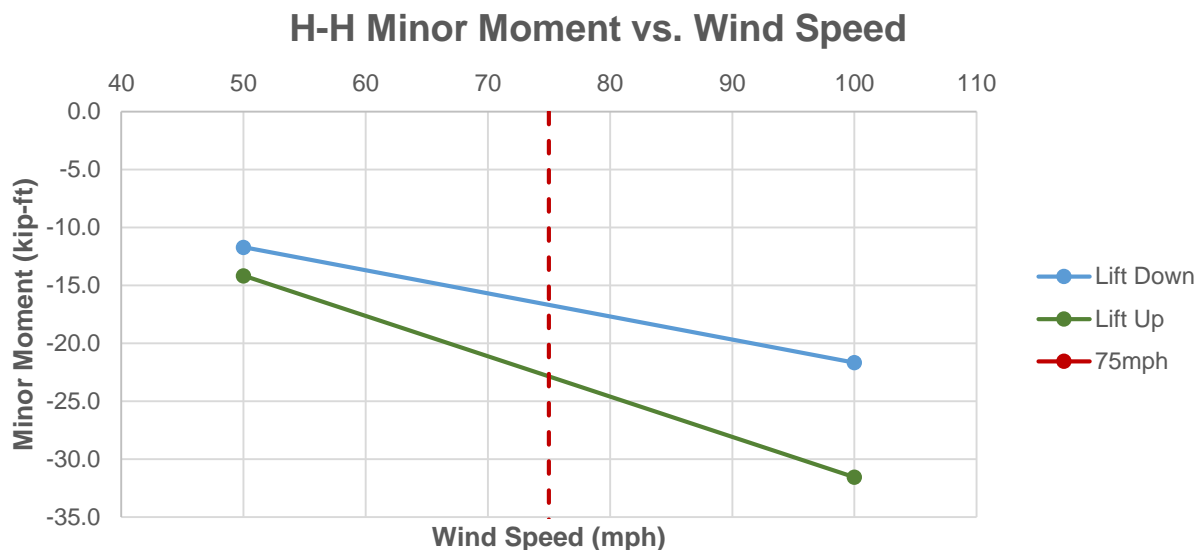


Figure 21 – Lift span section H-H temperature interpolated minor moment data and wind speed input

The interpolation above predicted a minor moment in the un-lifted state at 40 degrees Fahrenheit and 50mph winds of -17.0kip-ft and in the lifted state at the same conditions of -23.5kip-ft. Running a SAP2000® analysis at these input conditions and checking the resulting minor moments for the leeward H-H lift span section shows an actual minor moment in the un-lifted state of -16.1kip-ft

and -21.8kip-ft in the lifted. This represents a 5.4% difference between the un-lifted predictions and a 7.5% difference between the lifted predictions.

Data from SAP2000®, tabulated in Excel, can be used for the prediction of maximum moment demands for critical members in both the lift span and south span of the Memorial Bridge. By comparing the prediction results to calculated member moment capacities in the weak and strong axis directions, an objective recommendation can be made about the effect of a lift on the bridge members. This said, no cases exhibited demands in exceedance of member capacities. As shown below, critical members for the lift span and south span models have no issue handling even extreme wind loads and temperature. It follows that the objective decision protocol, regardless of input temperature and wind speed, will always suggest a safe lift.

Table 8 - Critical member capacity/demand checks at 100mph wind and 0 degrees Fahrenheit

	Model Member ID	Name	Type	Location	Major Moment (k-ft)	Minor Moment (k-ft)	Major Moment (k-ft)	Minor Moment (k-ft)
Lift Span Model	1	AA	Bottom chord	Windward	PASS	PASS	PASS	PASS
	4	II	Bottom chord	Windward	PASS	PASS	PASS	PASS
	21	II	Bottom chord	Leeward	PASS	PASS	PASS	PASS
	187	HH	Top chord	Windward	PASS	PASS	PASS	PASS
	192	HH	Top chord	Leeward	PASS	PASS	PASS	PASS
	185	BB	Top chord	Windward	PASS	PASS	PASS	PASS
	190	BB	Top chord	Leeward	PASS	PASS	PASS	PASS
	256	Portal	Portal	South	PASS	PASS	PASS	PASS
	260	Portal	Portal	North	PASS	PASS	PASS	PASS
	32	FB	Floor beam	Bottom	PASS	PASS	PASS	PASS
South Span Model	15	BC2.75	Bottom chord	Windward	PASS	PASS	PASS	PASS
	13	BC2.75	Bottom chord	Leeward	PASS	PASS	PASS	PASS
	31	TC2.75	Top chord	Windward	PASS	PASS	PASS	PASS
	29	TC2.75	Top chord	Leeward	PASS	PASS	PASS	PASS
	315	TOC	BB	Windward	PASS	PASS	PASS	PASS
	296	TOC	BB	Leeward	PASS	PASS	PASS	PASS
	307	TIC	AA	Windward	PASS	PASS	PASS	PASS
	288	TIC	AA	Leeward	PASS	PASS	PASS	PASS
	34	TC2.00	Top chord	Windward	PASS	PASS	PASS	PASS
36	TC2.00	Top chord	Leeward	PASS	PASS	PASS	PASS	

#### 4.3.2 Shortcomings and Validity of Protocol

There are numerous shortcomings and inefficiencies in the prediction formula and objective protocol described above. The first, and perhaps most obvious shortcoming, is that the protocol only makes its decision based upon member capacities for a bridge with steel members that all have flanges and webs in excess of one inch thick. The members of the Memorial Bridge are

substantial, both geometrically and in terms of strength. As such, it seems unlikely that even significant wind loads would cause demands for the members in excess of their capacities. This is, for the most part, true. In order to be fully realized, the protocol will need to account for the capacities of connections, which have a tendency to be far less than member capacities.

Table 9 - Predicted moment demands for critical members at 0 degrees Fahrenheit and 100mph winds

	Model Member ID	Name	Type	Location	LIFT IN DOWN POSITION		LIFT IN UP POSITION	
					Predicted Major Moment (k-ft)	Predicted Minor Moment (k-ft)	Predicted Major Moment (k-ft)	Predicted Minor Moment (k-ft)
<b>South Span Model</b>	15	BC2.75	Bottom chord	Windward	755.5	-8.4	768.4	-9.0
	13	BC2.75	Bottom chord	Leeward	792.4	10.4	779.5	11.1
	31	TC2.75	Top chord	Windward	267.4	-25.8	273.3	-26.5
	29	TC2.75	Top chord	Leeward	284.6	-24.6	283.0	-25.3
	315	TOC	BB	Windward	-158.6	-1674.2	-166.1	-2218.9
	296	TOC	BB	Leeward	-182.2	-1417.6	-174.6	-1962.8
	307	TIC	AA	Windward	74.7	-196.3	61.0	-193.5
	288	TIC	AA	Leeward	61.9	194.5	59.9	197.3
	34	TC2.00	Top chord	Windward	162.1	615.6	165.6	574.1
	36	TC2.00	Top chord	Leeward	173.3	-824.3	169.8	-866.1

Connection capacities aside, however, strong winds do not have a negligible impact on member demands. Table 10 below shows a summary of critical member capacities. While not insubstantial, they are comparable to predicted extreme moments in the case of the TOC column, or B-B section, of the south span tower. As shown, the minor moment experienced at 100mph wind speeds and 0 degrees Fahrenheit in the un-lifted state is 1674kip-ft for the windward B-B section and 2,219kip-ft for the lifted state. These demands are significant considering the minor moment capacity of this column is 3,555kip-ft. Even at 85 degrees, an arguably more likely temperature to experience 100mph wind speeds, the column experiences a predicted 1,761kip-ft of minor moment demand. Such large minor moment demands indicate no small impact of wind loading on the system and are worth investigation.

Table 10 - Summary of critical member capacities

	Model Member ID	Name	M_minor Capacity (k-ft)	M_major Capacity (k-ft)
Lift Span Model	1	AA	1538	5348
	4	II	2157	5851
	21	II	2157	5851
	187	HH	2504	4077
	192	HH	2504	4077
	185	BB	2049	3747
	190	BB	2049	3747
	256	Portal	2131	1444
	260	Portal	2131	1444
	32	FB	515	2861
South Span Model	15	BC2.75	4651	6807
	13	BC2.75	4651	6807
	31	TC2.75	4231	4222
	29	TC2.75	4231	4222
	315	TOC	3555	4618
	296	TOC	3555	4618
	307	TIC	1225	2774
	288	TIC	1225	2774
	34	TC2.00	3314	3921
	36	TC2.00	3314	3921

The second drawback to the prediction formula and protocol is its inability to identify trends in the location of moment data. This was the primary reason member capacities, and not connection capacities, were considered in the decision protocol. In many cases, the maximum moment experienced by a member remains in approximately the same place and changes in a predictable manner. Figure 22 shows such the trend in the moment data for the leeward H-H section of the bridge's lift span. There are many cases, however, where the location of maximum moment changes significantly and trends in moment data are not as easy to follow. This is shown in the G-G leeward section data in Figure 22.

The easiest way of overcoming this issue is to gather moment data at a specific location for each member – for example, the ends and mid-span. Such an approach would allow for accurate predictions of moment at critical locations, however, these predictions would not necessarily describe the maximum moment experienced by a member and may entirely overlook a



dangerously high demand. For this reason, and for the purposes of this report, the trends only in maximum moments were analyzed.

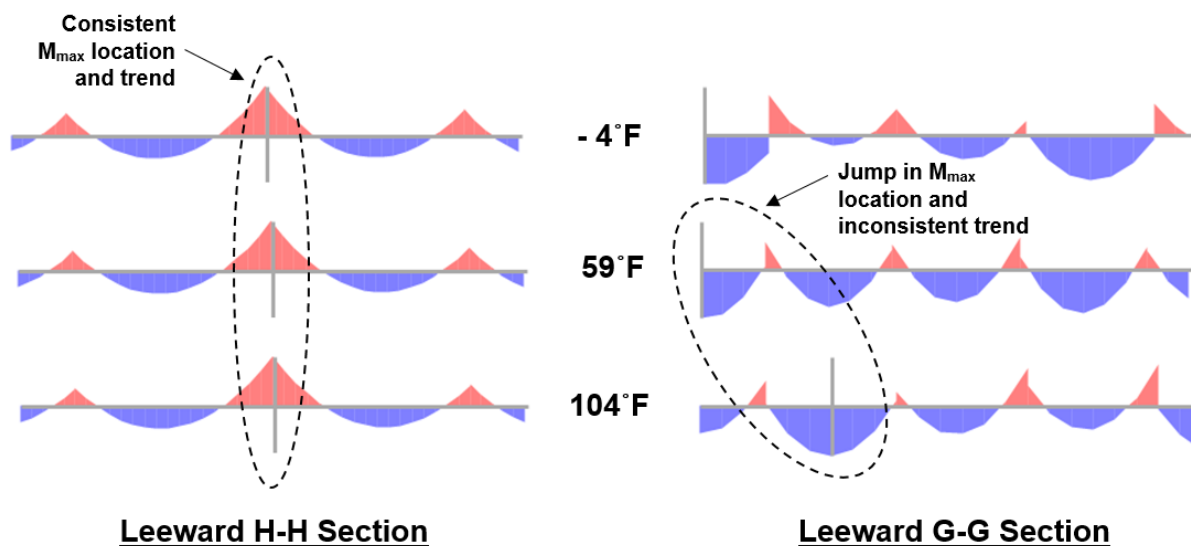


Figure 22 - Max moment trends and inconsistencies

The third issue with the prediction formula and decision protocol is that, at this moment in time, it only examines moment data for select members of the bridge system. To be completely thorough and sure of a lift decision, other forms of data would need to be gathered and analyzed. Such data would include axial, shear, torsion, and stress results. This data could be compared to the members in regards other than moment capacity and could be applied to the connections of the bridge system.

The final issue that will be discussed here is that of the input parameters. Currently, inputs are only allowed for the temperature and wind speed ranges used for SAP2000® analysis. A thorough decision protocol would include input parameters for the directionality of the wind as well as the more common wind speeds experienced at the bridge (ranging from 0mph – 100mph). This would require the redevelopment of hybrid wind loads so as to include wind from different angles of

attack as well as an analysis to determine whether such skew angles would cause misalignment of the bridge lift span during operation. This issue is discussed further in the Future Work section.

#### **4.4 DYNAMIC ANALYSIS OF THE COUNTERWEIGHTS AND LIFT SPAN**

While the results of the SAP2000® analyses showed the effects of wind on the lift of the Memorial Bridge were not a concern, the potential interaction between the counterweight of the bridge lift system and the fixed span tower remained a concern. The Memorial Bridge has two lift towers – the north tower, closest to Kittery, and the south tower, closest to Portsmouth. About 175 feet tall, the towers house counterweights which lift the bridge’s mid-span when naval traffic passes beneath it. The counterweights weigh over a million pounds each and are suspended from steel cables inside the towers.

Given the tower’s height and relative slenderness at the base, it is possible that the counterweights might interact with them either as a tuned mass damper or an amplifier to motion. As defined by Conner (2002), “A tuned mass damper (TMD) is a device consisting of a mass, spring, and a damper that is attached to a structure in order to reduce the dynamic response of the structure.” Typically, systems act as tuned mass dampers if their natural frequency matches the natural frequency of the system to which they are attached. In the case of the towers counterweights, such an interaction would be beneficial in that it would naturally reduce the vibration in the system during a lift, storm, or similar event.

In order to understand whether the counterweights act as TMDs, their natural frequencies needed to be defined. To do so, the counterweights were idealized as simple pendulum systems. This is a reasonable assumption. Since the weights are suspended from steel cables in both the lifted and un-lifted states, their behavior should, in theory mimic that of a pendulum. The natural

frequency of a pendulum has been quantifiable for centuries. It is shown in the equation below, where it can be seen to be independent of the mass of the counterweight.

$$f_{n,pendulum} = \left(2\pi \sqrt{\frac{L}{g}}\right)^{-1} \quad (14)$$

Where...

$L$  is the length of the cable

$g$  is the gravitational acceleration constant equal to 32.2 ft/s<sup>2</sup>

Using geometric data from the as-built specifications provided by the designer of the Memorial Bridge, the cable lengths for the counterweights in each the span lifted and un-lifted position could be defined. They are shown below in Figure 23, they are equal to 0.079 Hertz and 0.242 Hertz respectively, where 13.9 feet is the cable length in the span down position and 39.8 feet is the cable length in the span up position.

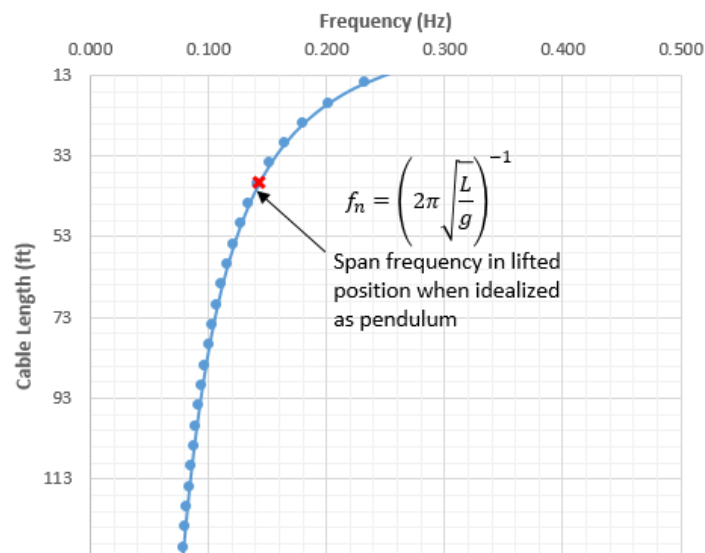


Figure 23 - Counterweight natural frequency as a function of cable length

Using this data in conjunction with the natural frequencies calculated for the determination of aerodynamic susceptibility, the frequency ratio,  $\rho$ , for the system could be determined, as shown in the equation below.

$$\rho = \frac{\Omega}{\omega} \quad (15)$$

Where...

$\Omega$  is the natural frequency of the tower system

$\omega$  is the natural frequency of the counterweight

Knowing the frequency ratio, the mass ratio for the system could be calculated and substituted into the equation for  $D_2$ , used in the calculation of the amplification factor  $H_2$  as shown below (as previously discussed in the introductory material).

$$H_2 = \frac{\sqrt{((1+\bar{m})f^2-\rho^2)^2+(2\xi_d\rho f(1+\bar{m}))^2}}{|D_2|} \quad (6)$$

Where...

$\bar{m}$  is the mass ratio of the counterweight to the fixed span and tower

$\xi_d$  is the damping ratio assumed to be zero

$f$  is assumed to be 1.0

And...

$$|D_2| = \sqrt{\left(\left((1-\rho^2)(f^2-\rho^2)-\bar{m}\rho^2f^2\right)^2 + \left(2\xi_d\rho f(1-\rho^2(1+\bar{m}))\right)^2\right)} \quad (7)$$

Plotting the amplification factor versus the frequency ratio (see Figure 24) shows that, while the amplification occurs at about +/- 35 percent of a frequency ratio of 1 (as compared to the +/- 10

percent for a typical TMD system), amplification does not occur for the counterweight system at the bridge – where the frequency ratio is equal to 4.79.

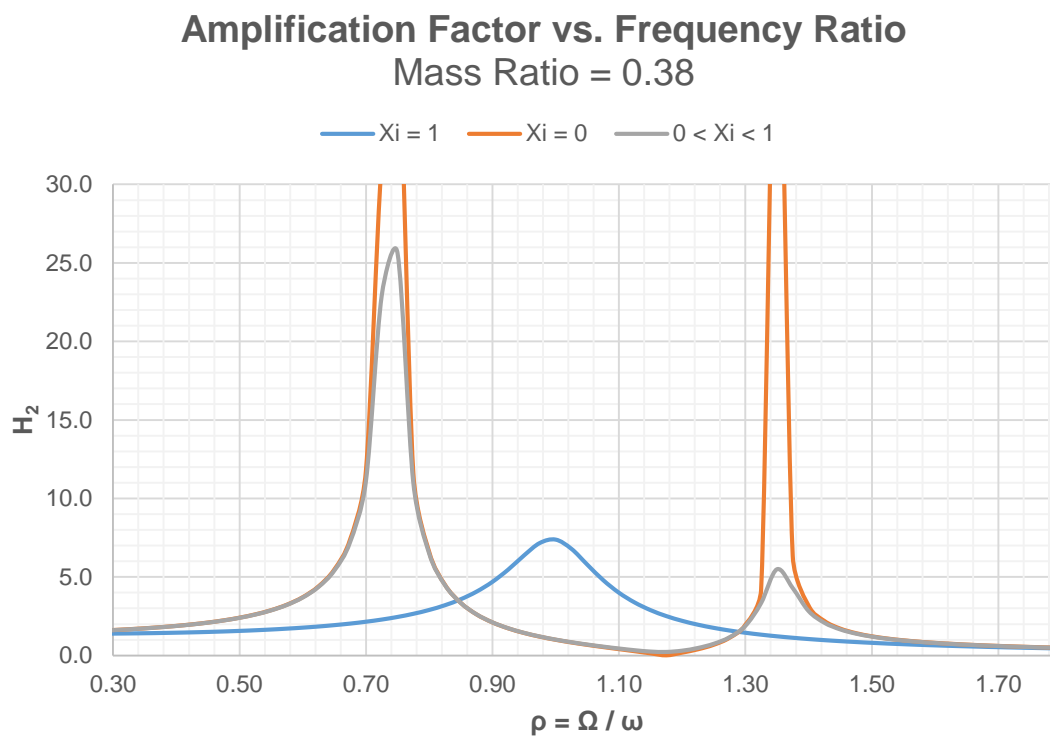


Figure 24 – Amplification factor vs. frequency ratio for counterweight and tower system (Connor, 2002)

## **CHAPTER 5**

### **APPLICATION, RECOMMENDATION, AND FUTURE WORK**

#### **5.1 OVERVIEW**

Numerous assumptions were made in the analyses performed in this research. These assumptions, while valid, leave room for significant expansion, improvement, and validation in the future. In conjunction with the improvement of analysis assumptions, the future installation of the Living Bridge Project's structural health monitors and weather sensors will yield valuable data that can be used to further refine the models developed in this work. Expansion of the load cases and scenarios created for SAP2000® analyses would help to develop more accurate results and better capture the effects of wind on the Memorial Bridge's structural systems during a lift.

##### **5.1.1 Wind Effects**

The first major assumption made in this report is that of lateral wind direction. For the development of wind loads by each Eurocode, ASCE, and AASHTO, only wind moving perpendicular to the span of the bridge and normal to the surface of the water was considered. As shown in Figure 25, this is, for the most part, a valid assumption. While the wind rose in the figure shows directionality only for September through November, this trend remains true on an annual basis (as shown in Appendix C). Since the Memorial Bridge is generally oriented span-wise in the north-to-south direction, it is thus reasonable to assume primarily lateral wind loads.

Despite the general direction of wind in Portsmouth, it still can come from other directions. It is possible that skew angles normal to the water surface and to the bridge towers could produce demands unseen in the lateral analyses. Furthermore, an unequal distribution of wind, for

example a load of high magnitude on one side of the lift span and low on the other, could result in a misalignment. This, in turn, could cause the lift to become stuck – delaying traffic.

### Wind Summary - September, October, and November

Labels of Percent Frequency on North Axis

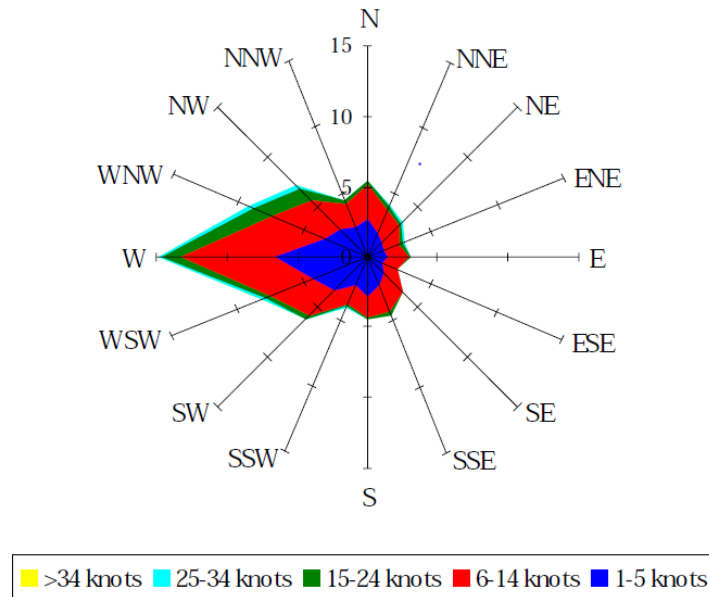


Figure 25 - Wind rose for Portsmouth, NH

It follows that, to be completely thorough, functionality should be built into the predictive formula such that the skew angle of the wind from varying directions could be input. Such a functionality would increase understanding of the bridge's behavior in a wider variety of wind loads while decreasing the likelihood of a misalignment of the lift span.

On top of the expansion of wind loading to include skew angles, further SAP2000® analyses need to be run at variable temperatures and wind speeds between those used for the baseline analyses to increase the accuracy of predicted results. At present, the predictive formula linearly interpolates between existing SAP results and an increase in such model results directly relates to an increase in the accuracy of interpolated values.

### **5.1.2 Model Validation, Updating, and Integration of Sensor Data**

As a portion of the Living Bridge Project, accelerometers and strain gauges as well as weather data sensors are to be installed at the Memorial Bridge. The data yielded from these sensors is valuable to this research in a variety of ways. First, as mentioned previously, there is currently no way to measure the actual wind speed at the Memorial Bridge. The ability to accurately read it makes the decision to lift or not lift far more objective. On top of this, the ability to read wind speeds allows trends to be recorded. Maximum and average wind speeds accurate to the site – rather than the city of Portsmouth or the Gulf of Maine – can be determined and the wind loads used for analysis updated accordingly.

The structural health monitoring sensors at the bridge allow the opportunity to validate and expand the demands predicted by the developed wind loads and SAP2000® analyses. In conjunction with this, they will allow for more accurate modeling of the bridges structural systems and (through other Living Bridge Project research) a better understanding of the rigidity of the gussetless joints and bridge system as a whole. Such an understanding will help to more accurately model and predict the dynamic behavior of the bridge and determine whether further dynamic studies should be done on the system.

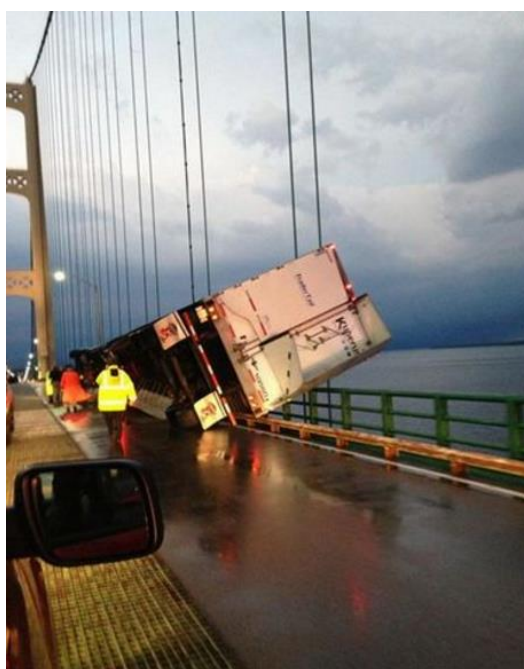
The ability to retrieve machine data from the bridge's lift systems in the future allows for a deeper look into the reasonability of the 50mph base wind speed. Building off of the work done by Reij, discussed in the introductory material, the effects of wind on the lift mechanism could be established by comparing data retrieved from weather sensors to data from the machines. This could set a more realistic bound to operable wind speeds for the Memorial Bridge.

### **5.1.3 Traffic Considerations**

In conjunction with its effect on the structural and mechanical systems of a bridge, wind plays a role in the operability of the vehicles as well. The Memorial Bridge experiences an array of traffic



forms on a day-to-day basis, ranging from pedestrian and bicycle traffic to sedan and 18-wheeler. Lightly loaded vehicles of the latter category are typically very susceptible to high wind loads. Gusts on unloaded semis and tractor trailers can cause them to shift lanes suddenly, to move laterally, or to blow over completely. Studies have shown that as much as 90% of wind-related vehicle accidents were complete blow overs. This is a problem, considering blow overs are far more destructive and disruptive in nature than lane switches or lateral movement. As shown in Figure 26, a truck on the Mackinac Bridge (a suspension bridge over the Straits of Mackinac in Michigan) was blown completely onto the guardrail of the bridge during a severe storm in 2013 where wind speeds were measured at over 65mph (Torregrossa, 2013).



*Figure 26 - Truck blow over on the Mackinac Bridge (2013)*

It follows that future work in the decision criteria for the Memorial Bridge's operation should consider wind loading on vehicles. While the 50mph base wind criteria may limit the operability of the lift span, it is possible that winds of this speed are too hazardous for vehicles to operate as well. Studies by the bridge designer, Ted Zoli, with others from HNTB Corporation and Rowan

Williams Davies and Irwin Inc. of Canada have broken ground on this very issue. Together, they proposed a simple vehicle blow over stability model which includes “complex 6 degrees of freedom aerodynamic loading on vehicles [including] the bridge aerodynamic effects.” For a case study, this model showed, for a double deck bridge, a low mass tractor-trailer blows over at wind speeds in the range of 50 - 65mph. If the same proves true for the Memorial Bridge, the 50mph wind base speed would not only limit the operability of the lift span, but traffic in general. An investigation into the shielding effects of the bridge’s truss system and aerodynamics would be required, however, to establish this.

#### ***5.1.4 Progressive Section Loss and the Objective Protocol***

The Memorial Bridge is located in a harsh marine environment. It is perpetually exposed to corrosive water and air, storms, tides, and many other destructive forces associated with locations near the ocean. The previous Memorial Bridge was put out of commission due to the excessive corrosion and eventual section loss the steel members experienced in their lifetime, as demonstrated in Figure 27.



*Figure 27 – Degradation of the original Memorial Bridge truss system (Jim Cole, 2010)*

It is not unlikely that, despite its advanced coating, the new Memorial Bridge will experience similar corrosion and section loss as the previous one within its design life. Should such a thing happen, the objective protocol and predictive formula in this work become quite useful. Estimations of section loss could be made in the field and new capacities for the bridge members or connections could be input into the protocols data. It could then make predictions based on the section loss experienced at the bridge as to whether the system can handle the operation of the lift. This, in conjunction with the structural health and weather monitoring systems of the Living Bridge Project, will make it far easier to identify problems with the structure as they occur and, potentially, stop them before they do.

## CHAPTER 6

### CONCLUSIONS

Movable bridges are, in technicality, structural systems. Such a simple description, however, understates their complexity and belittles their importance. Unlike their immovable counterparts fixed bridges, movable bridges interact with many forms of traffic. They allow vehicles and trains to pass over them while simultaneously possessing the ability to move and allow boats to pass beneath them. Their consistent operation is a necessity. Despite this necessity however, few objective protocols exist defining when a movable bridge should operate. This thesis aimed to answer this very question and define the extreme wind and temperature conditions at which the operation of the vertical lift span of the Memorial Bridge in Portsmouth, NH, can be safely carried out.

Wind loads are highly variable and entirely dependent on the characteristics of the site in question. For many structural designs, temperature is often taken to be 60 degrees Fahrenheit but this research determined there to be as much as a 20 percent difference between wind loads at extreme temperatures and for the case study site. This difference was not considered negligible and was integrated into the development of multiple load cases.

American code provided a framework with which to develop wind loads. After determining the natural frequencies of the Memorial Bridge's structural systems, a check was made to determine that the counterweight did not act to amplify the motion of the bridge's towers. Knowing such amplification did not occur and that the system could be considered rigid meant the bridge could be idealized as a trussed tower system using a standard gust factor. This led to the development of wind loads varying by height for the bridge in the up and down position at three different temperatures (-4, 59, and 104 degrees Fahrenheit) and two different wind speeds (50mph and

100mph). Eurocode formed a conservative basis to check each of the developed loads and ASCE's design guide for wind loads on petrochemical facilities showed shielding could be considered non-existent for the system. This, in turn, resulted in twelve hybrid wind load cases which could be input into SAP2000® for analysis.

The results from SAP2000® analyses provided a framework from which generalized trends in system demands for critical members of the Memorial Bridge could be drawn. Since the analyses were run at variable wind speeds and temperatures, linear predictions were able to be made about the expected demands for members in specified environmental conditions. Such predictions are made with accuracy directly related to the amount of SAP data on-hand as well as magnitude of the demands. Very small member demands prove difficult to predict while larger ones can be determined with a high degree of accuracy.

Overall, none of the wind loads developed in this research proved to be large enough for the structural system of the Memorial Bridge to be compromised. The result of this conclusion is that no environmental conditions, based on the assumptions made, will yield a no-lift decision. This said, there are numerous potential conditions which could yield a no-lift decision should this work be expanded in the future. Such conditions are as follows. First, wind at different angles of attack other than lateral and perpendicular to the water (as was considered for this report) could result in a misalignment of the bridge or vibration in the lift span that could cause a no-lift. Second, sensor data acquired in the future from the Living Bridge Project will yield insight into the actual conditions and demands experienced by the bridge its machinery and thus help to more accurately describe the conditions the bridge cannot handle in reality. Third, future section loss caused by the bridge's harsh environmental conditions in conjunction with changes to these conditions as a result of climate change could result in no-lift states due to loss in member or connection capacity. Fourth and finally, extreme wind speeds that cause the blow over of lightly

loaded trucks could limit the passage of vehicular traffic, specifically trucking traffic, for the Memorial Bridge in its un-lifted state.

In summation, this work breaks the ground for a series of future expansions which will help operators to better understand the precise conditions in which a lift should not be made at the Memorial Bridge. While, at present, it would seem the bridge is amply able to handle even significant wind loads, future analyses and data could prove to show conditions in which a lift should not be made. For now, however, the maximum operable wind speed of 50mph, as specified by the lift mechanism manufacturer, remains the speed at which the lift span should not be operated.

## LIST OF REFERENCES

Abrahams, M.J., Chen, W. (Ed.), Duan, L. (Ed.) (2000). *Bridge Engineering Handbook*. Boca Raton, Florida: CRC Press, LLC.

American Association of State Highway and Transportation Officials (2010). *AASHTO LRFD Bridge Design Specifications* (5<sup>th</sup> Edition). Washington DC, US: AASHTO.

American Association of State Highway and Transportation Officials (2012). *AASHTO LRFD Movable Highway Bridge Design Specifications* (2<sup>nd</sup> Edition). Washington DC, US: AASHTO.

Aschauer, David (1990). *Why is Infrastructure Important*. Retrieved from the Federal Reserve Bank of Boston: <https://www.bostonfed.org/-/media/Documents/conference/34/conf34b.pdf>

ASCE (2013). *Report Card for America's Infrastructure*. Retrieved from the American Society of Civil Engineers: <http://www.infrastructurereportcard.org/>

ASCE (2010). *Minimum Design Loads for Buildings and Other Structures*. Reston, VA: American Society of Civil Engineers.

American Institute of Steel Construction (2011). *Steel Construction Manual* (14<sup>th</sup> Edition). United States: AISC.

Billah, K.Y., Scanlan, R. (1991). *Resonance, Tacoma Narrows Bridge Failure, and Undergraduate Physics Textbooks*. American Association of Physics Teachers.

Cardin, M., Griesing, K. (2010). *Design and Construction of the Pont Bacalan-Bastide Vertical Lift Bridge*. Heavy Movable Structures, Inc. 13<sup>th</sup> Biannual Symposium.

Catbas, F.N., Gul, M., Zaurin, R., Gokce, B., Terrell, T., Dumplupinar, T., Maier, D. (2010). *Long Term Bridge Maintenance Monitoring Demonstration on a Movable Bridge Frame*. Florida Department of Transportation.

Catbas, F.N., Malekzadeh, M., Khuc, T. (2013). *Movable Bridge Maintenance Monitoring*. Retrieved from the Florida Department of Transportation: [http://www.fdot.gov/structures/structuresresearchcenter/Final%20Reports/2013/BDK78-977-10\\_rpt.pdf](http://www.fdot.gov/structures/structuresresearchcenter/Final%20Reports/2013/BDK78-977-10_rpt.pdf)

Chopra, Anil K. (2012). *Dynamic of Structures – Theory and Applications to Earthquake Engineering* (4<sup>th</sup> Edition). New Jersey, US: Prentice Hall.

Cole, Jim (Photographer). (2010). *Memorial Bridge Truss Degradation*. Retrieved from: <http://bangordailynews.com/2010/12/20/business/mainenh-bridge-reopens-ahead-of-schedule/>

Conner, Jerome J. (2002). *Introduction to Structural Motion Control*. New Jersey, US: Prentice Hall.

Crown (2011). Highway Structures, Approval Procedures, and General Design. *Design Manual for Roads and Bridges BD 49/01*. Norwich, UK: The Stationary Office.

Crown (2011). Loads for Highway Bridges. *Design Manual for Roads and Bridges BD 37/01*. Norwich, UK: The Stationary Office.

Davenport, A.G. (1961). The Spectrum of Horizontal Gustiness Near the Ground in High Winds. *Quarterly Journal of the Royal Meteorological Society, Volume 87* (Issue 372), pp. 194 – 211.

Energy Division of the American Society of Civil Engineers (2011). *Wind Loads for Petrochemical and Other Industrial Facilities*. Reston, VA: ASCE.

European Committee for Standardization (2005). *British Standard Eurocode 3*. London, UK: British Standards Institution.

FHWA (2011). *Bridge Preservation Guide* (Report No. FHWA-HIF-11042). Retrieved from the Federal Highway Administration: <http://www.fhwa.dot.gov/bridge/preservation/guide/guide.pdf>

Koglin, Terry L. (2003). *Movable Bridge Engineering*. Hoboken, NJ: John Wiley & Sons, Inc.

London Tower Bridge. Retrieved from: <http://www.towerbridge.org.uk/lift-times/>

Memorial Bridge Project (2015). *Memorial Bridge Project*. Retrieved from: <http://memorialbridgeproject.com/>

Mohammadi, M.S., Mukherjee, R. (2013). *Wind Loads on Bridges: Analysis of a Three Span Bridge Based on Theoretical Methods and Eurocode 1* (Master's Thesis). ISSN 1103-4297.

National Economic Council and the President's Council of Economic Advisors (2014). *An Economic Analysis of Transportation Infrastructure Investment*. Retrieved from the White House: [https://www.whitehouse.gov/sites/default/files/docs/economic\\_analysis\\_of\\_transportation\\_investments.pdf](https://www.whitehouse.gov/sites/default/files/docs/economic_analysis_of_transportation_investments.pdf)

NOAA (1996). *Portsmouth NH, Engineering Weather Data*. Retrieved from the National Centers for Environmental Information: [https://www1.ncdc.noaa.gov/pub/data/EngineeringWeatherData\\_CDROM/engwx/pease\\_nh.pdf](https://www1.ncdc.noaa.gov/pub/data/EngineeringWeatherData_CDROM/engwx/pease_nh.pdf)



Reij, A.W.F. (1991). *Wind Loads on Movable Bridge*. International Association for Bridge and Structural Engineering (IABSE) – Reports. Zurich, Switzerland: IABSE.

State of New Hampshire Division of Ports and Harbors (2003). *Portsmouth Terminal Information*. Retrieved from the NH Division of Ports and Harbors:  
<http://www.portofnh.org/terminal.html>

Taly, N. (2014). *Highway Bridge Superstructure Engineering: LRFD Approaches to Design and Analysis*. Boca Raton, Florida: CRC Press, LLC.

Torregrossa, Mark (July 18<sup>th</sup>, 2013). Semi-truck Blown Over on Mackinac Bridge: Is that the beginning of our severe weather. *Michigan Live*. Retrieved from:  
[http://www.mlive.com/weather/index.ssf/2013/07/semi-truck\\_blow\\_n\\_on\\_macki.html](http://www.mlive.com/weather/index.ssf/2013/07/semi-truck_blow_n_on_macki.html)

US Census Bureau (2015). *Portsmouth NH, Demographics*. Retrieved from the US Census Bureau: <http://www.census.gov/quickfacts/table/PST045215/3362900>

## **APPENDICES**

## APPENDIX A

### WIND LOADS BY CODE

#### AASHTO

##### ***Aero-Elastic Check***

“Aero-elastic force shall be taken into account in the design of bridges and structural components apt to be wind-sensitive. For the purpose of this Article, all bridges with a span to depth ratio, and structural components thereof with a length to width ratio, exceeding 30.0 shall be deemed to be wind-sensitive.” (AASHTO 3.8.3.1 – General)

- $\frac{\text{span}}{\text{depth}} = \frac{300}{22} = 13.6 \ll 30.0 \quad \text{CHECKS}$

“... [30.0 is] a somewhat arbitrary value helpful only in identifying likely wind-sensitive cases.” (AASHTO 3.8.3.1 Revision)

##### ***Sample Wind Load Calculation***

- $P_D = P_B \left( \frac{V_{DZ}^2}{10,000} \right) = (0.050) \left( \frac{138^2}{10000} \right) = 0.095 < \boxed{0.30klf}$
- $P_B = 0.050ksf$
- $V_{DZ} = 2.5V_0 \left( \frac{V_{30}}{V_B} \right) \ln \left( \frac{Z}{Z_0} \right) = 2.5(8.2) \left( \frac{100}{100} \right) \ln \left( \frac{192}{0.23} \right) = 138mph$ 
  - $V_0 = 8.20mph$  [AASHTO Table 3.8.1.1-1]
  - $V_{30} = 100mph$  [AASHTO Equation 3.8.1.1-1]
    - 100mph speed noted beneath Table 3.8.1.1-1
  - $V_B = 100mph$  [AASHTO Equation 3.8.1.1-1]
  - $Z = 192ft$
  - $Z_0 = 0.23ft$  [AASHTO Table 3.8.1.1-1]

## Excel Calculations

Table 11 - Bridge member areas and lengths

Total Member Areas		
Lift Span	2165	sf
South Span	3310	sf
Total Member Lengths		
Lift Span	1072	ft
South Span	1625	ft

Table 12 - AASHTO total wind pressure calculations in Excel

Total Wind Pressure Skew Angle = 0°		
<b>P_D,windward</b>	<b>0.095</b>	<b>ksf</b>
P_B	0.050	ksf
V_DZ	138	mph
V_B	100	mph
<b>V_DZ</b>	<b>138</b>	<b>mph</b>
V_0	8.20	mph
V_30	100	mph
V_B	100	mph
Z	192	ft
Z_0	0.23	ft
<b>P_D,leeward</b>	<b>0.048</b>	<b>ksf</b>
P_B	0.025	ksf
V_DZ	138	mph
V_B	100	mph
<b>V_DZ</b>	<b>138</b>	<b>mph</b>
V_0	8.20	mph
V_30	100	mph
V_B	100	mph
Z	192	ft
Z_0	0.23	ft

Table 13 - Final AASHTO wind loads from Excel

Uniform Wind Load (AASHTO-1) Unreduced loads			Uniform Wind Load (AASHTO-1) 60% reduction		
<b>Windward</b>			<b>Windward</b>		
<i>Lift Span</i>	<i>0.300</i>	<i>klf</i>	Lift Span	0.180	klf
<i>South Span</i>	<i>0.300</i>	<i>klf</i>	South Span	0.180	klf
<b>Leeward</b>			<b>Leeward</b>		
<i>Lift Span</i>	<i>0.150</i>	<i>klf</i>	Lift Span	0.090	klf
<i>South Span</i>	<i>0.150</i>	<i>klf</i>	South Span	0.090	klf

## EUROCODE

### Sample Wind Load Calculation

$$\bullet \quad F_w = \frac{\frac{1}{2}\rho v_b^2 C A_{ref,x}}{L_{total}} = \frac{0.5(1.269)(44.7)^2(5.07)(201.1)}{326.8} = \frac{1292607.6}{326.8} = 3954.8 \frac{kg}{m} = \boxed{0.152klf}$$

$$\bullet \quad \rho_{5^\circ C} = 1.269 \frac{kg}{m^3}$$

$$\bullet \quad v_b = 75mph = 33.5mps$$

$$\bullet \quad C = c_{f,x} c_e = 5.07$$

- According to Eurocode 8.3.1,  $c_{f,x}$  may be taken as equal to 1.3 for normal bridges since a bridge usually has no free-end flow because the flow is “deviated only along two sides (over and under the bridge deck).”

$$\bullet \quad c_{f,x} = 1.3$$

- $c_e = 3.9$  (Error! Reference source not found., Category 0)

Figure 28 - Eurocode  $c(e)$  factor

$$\bullet \quad A_{ref,x} = 2165sf = 201.1m^2$$



Figure 29 - Lift span area as calculated in AutoCAD

- $L_{total}$  is the total member exposed perpendicular to the wind per truss system as established from the model of the Memorial Bridge generated in AutoCAD

## Excel Calculations

Table 14 - Tabulation of wind loads developed by Eurocode

Temperature (C) -20			Temperature (C) 15			Temperature (C) 40		
<b>Lift Span (Up Position)</b>								
A_ref,x	201.1	m <sup>2</sup>	A_ref,x	201.1	m <sup>2</sup>	A_ref,x	201.1	m <sup>2</sup>
d_tot	7.91	m	d_tot	7.91	m	d_tot	7.91	m
C	5.07	-	C	5.07	-	C	5.07	-
b/d_tot	1.91	-	b/d_tot	1.91	-	b/d_tot	1.91	-
q_b	1394	-	q_b	1224	-	q_b	1126	-
L_tot	326.8	m	L_tot	326.8	m	L_tot	326.8	m
<b>F_w</b>	<b>0.298</b>	<b>klf</b>	<b>F_w</b>	<b>0.262</b>	<b>klf</b>	<b>F_w</b>	<b>0.241</b>	<b>klf</b>
<b>Lift Span (Down Position)</b>								
A_ref,x	201.1	m <sup>2</sup>	A_ref,x	201.1	m <sup>2</sup>	A_ref,x	201.1	m <sup>2</sup>
d_tot	7.91	m	d_tot	7.91	m	d_tot	7.91	m
C	2.90	-	C	2.90	-	C	2.90	-
b/d_tot	1.91	-	b/d_tot	1.91	-	b/d_tot	1.91	-
L_mem,tot	326.8	m	L_mem,to	326.8	m	L_mem,to	326.8	m
<b>F_w</b>	<b>0.170</b>	<b>klf</b>	<b>F_w</b>	<b>0.150</b>	<b>klf</b>	<b>F_w</b>	<b>0.138</b>	<b>klf</b>
<b>South Span</b>								
A_ref,x	227.6	m <sup>2</sup>	A_ref,x	227.6	m <sup>2</sup>	A_ref,x	227.6	m <sup>2</sup>
d_tot	8.67	m	d_tot	8.67	m	d_tot	8.67	m
C	2.90	-	C	2.90	-	C	2.90	-
b/d_tot	1.74	-	b/d_tot	1.74	-	b/d_tot	1.74	-
L_mem,tot	495.3	m	L_mem,to	495.3	m	L_mem,to	495.3	m
<b>F_w</b>	<b>0.127</b>	<b>klf</b>	<b>F_w</b>	<b>0.112</b>	<b>klf</b>	<b>F_w</b>	<b>0.103</b>	<b>klf</b>
<b>Tower</b>								
A_ref,x	68.1	m <sup>2</sup>	A_ref,x	68.1	m <sup>2</sup>	A_ref,x	68.1	m <sup>2</sup>
d_tot	50.88	m	d_tot	50.88	m	d_tot	50.88	m
C	3.60	-	C	3.60	-	C	3.60	-
b/d_tot	0.30	-	b/d_tot	0.30	-	b/d_tot	0.30	-
L_mem,tot	130.5	m	L_mem,to	130.5	m	L_mem,to	130.5	m
<b>F_w</b>	<b>0.179</b>	<b>klf</b>	<b>F_w</b>	<b>0.158</b>	<b>klf</b>	<b>F_w</b>	<b>0.145</b>	<b>klf</b>

Table 15 - Reference air density for VLOOKUP in Excel

Temperature	Density	Specific Weight	
(°F)	(slugs/ft <sup>3</sup> ) × 10 <sup>-3</sup>	(lb/ft <sup>3</sup> ) × 10 <sup>-2</sup>	(lb/ft <sup>3</sup> )
-40	2.939	9.46	0.0946
-20	2.805	9.03	0.0903
0	2.683	8.63	0.0863
10	2.626	8.45	0.0845
20	2.571	8.27	0.0827
30	2.519	8.10	0.0810
40	2.469	7.94	0.0794
50	2.420	7.79	0.0779
60	2.373	7.64	0.0764
70	2.329	7.49	0.0749
80	2.286	7.35	0.0735
90	2.244	7.22	0.0722
100	2.204	7.09	0.0709
120	2.128	6.85	0.0685
(°C)	(kg/m <sup>3</sup> )	(N/m <sup>3</sup> )	(lb/ft <sup>3</sup> )
-40	1.514	14.85	0.0945
-20	1.395	13.68	0.0871
0	1.293	12.67	0.0807
5	1.269	12.45	0.0792
10	1.247	12.23	0.0778
15	1.225	12.01	0.0765
20	1.204	11.81	0.0752
25	1.184	11.61	0.0739
30	1.165	11.43	0.0727
40	1.127	11.05	0.0704
50	1.109	10.88	0.0692



## ASCE 7-10 AND HYBRID LOADING

Calculations below establish the wind pressure as a function of height through  $K_z$ :

- $F = q_z G C_f$ 
  - $q_z = 0.00256 K_z K_{zt} K_d V^2$ 
    - $K_z$  variable by height
    - $K_{zt} = 1.0$
    - $K_d = 0.95$  (trussed tower)
    - $V = 100 \text{mph}$
  - $G = 0.85$  (natural frequency less than 1 Hertz)
  - $C_f = 4.0\varepsilon^2 - 5.9\varepsilon + 4.0 = 4.0(0.32)^2 - 5.9(0.32) + 4.0 = 2.52$ 
    - $\varepsilon = 0.32$  as established from AutoCAD model

Using Excel to establish a polynomial function for pressure as a function of height allows for the input of member elevation data, outlined in Table 16 below, to find the maximum pressure experienced on a per-member basis. Dividing this pressure by the member length establishes the pressure in terms of kips per linear foot.

## Excel Calculations

Table 16 - Excel member elevation and geometry data for ASCE analysis

Member Elevation + Geometry Data									
Down Position				Up Position				Geometry Data	
South Span	Max	Min	Units	South Span	Max	Min	Units	Area (sf)	Length (ft)
Bot Chord	28.88	25.55	ft	Bot Chord	28.88	25.55	ft	1044.6	300.0
Top Chord	50.22	47.88	ft	Top Chord	50.22	47.88	ft	682.3	264.0
W14's	48.99	27.28	ft	W14's	48.99	27.28	ft	32.6	27.3
Lift Span	Max	Min	Units	Lift Span	Max	Min	Units	Area	Length (ft)
Bot Chord	28.88	25.59	ft	Bot Chord	157.31	154.02	ft	964.1	300.0
Top Chord	51.33	49.09	ft	Top Chord	179.81	176.48	ft	605.3	264.0
W14's	50.19	27.28	ft	W14's	177.52	157.31	ft	33.4	28.2
South Tower	Max	Min	Units	South Span	Max	Min	Units	Width	Length (ft)
<b>A-A (listed from bottom of tower to top)</b>									
A-A 1	88.44	49.58	ft	A-A 1	88.44	49.58	ft	2.17	38.9
A-A 2	127.81	88.44	ft	A-A 2	127.81	88.44	ft	2.17	39.3
A-A 3	167.11	127.81	ft	A-A 3	167.11	127.81	ft	2.17	39.4
A-A 4	185.22	167.11	ft	A-A 4	185.22	167.11	ft	2.17	18.1
<b>B-B (listed from bottom of tower to top)</b>									
B-B 1	35.28	25.55	ft	B-B 1	35.28	25.55	ft	2.31	9.7
B-B 2	125.55	75.55	ft	B-B 2	125.55	75.55	ft	2.31	50.0
B-B 3	175.55	125.55	ft	B-B 3	175.55	125.55	ft	2.31	50.0
B-B 4	185.22	175.55	ft	B-B 4	185.22	175.55	ft	2.31	9.7
<b>W14's (listed from bottom of tower to top)</b>									
1	72.48	49.58	ft	1	72.48	49.58	ft	1.19	28.5
2	88.44	72.48	ft	2	88.44	72.48	ft	1.19	22.6
3	111.22	88.44	ft	3	111.22	88.44	ft	1.19	27.8
4	127.76	111.22	ft	4	127.76	111.22	ft	1.19	22.3
5	150.55	127.76	ft	5	150.55	127.76	ft	1.19	27.3
6	167.11	150.55	ft	6	167.11	150.55	ft	1.19	21.7
7	185.22	167.11	ft	7	185.22	167.11	ft	1.19	22.9

Table 17 - Basic pressure profile and polynomial function in Excel

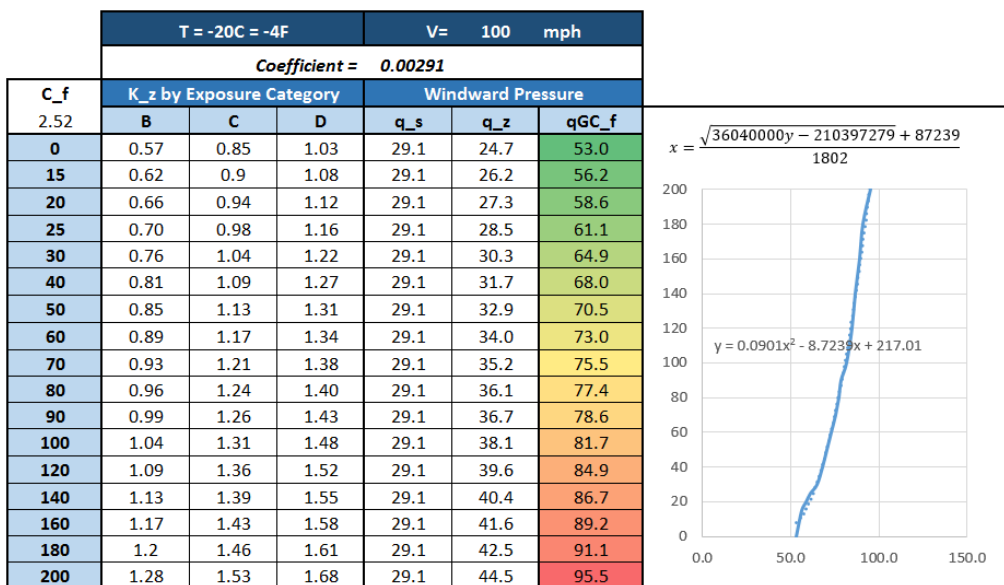


Table 18 - Example ASCE wind loads at 100mph and variable temperature

100 mph	T = -20C = -4F		T = 15C = 59F		T = 40C = 104F		
	W (ksf)	W (klf)	W (ksf)	W (klf)	W (ksf)	W (klf)	
<b>DOWN - 100 mph</b>	<b>South Span</b>						
	Bot Chord	0.0644	0.224	0.0565	0.197	0.0520	0.181
	Top Chord	0.0706	0.182	0.0620	0.160	0.0570	0.147
	W14's	0.0703	0.084	0.0617	0.074	0.0568	0.068
	<b>Lift Span</b>						
	Bot Chord	0.0644	0.207	0.0565	0.182	0.0520	0.167
	Top Chord	0.0709	0.163	0.0622	0.143	0.0572	0.131
	W14's	0.0706	0.083	0.0619	0.073	0.0570	0.067
	<b>South Tower</b>						
	<b>A-A (listed from bottom of tower to top)</b>						
	A-A 1	0.0787	0.170	0.0691	0.150	0.0635	0.138
	A-A 2	0.0852	0.185	0.0748	0.162	0.0688	0.149
	A-A 3	0.0907	0.197	0.0796	0.173	0.0733	0.159
	A-A 4	0.0930	0.202	0.0817	0.177	0.0751	0.163
	<b>B-B (listed from bottom of tower to top)</b>						
	B-B 1	0.0665	0.154	0.0583	0.135	0.0537	0.124
	B-B 2	0.0849	0.196	0.0745	0.172	0.0685	0.158
	B-B 3	0.0918	0.212	0.0806	0.186	0.0741	0.171
	B-B 4	0.0930	0.215	0.0817	0.189	0.0751	0.174
	<b>W14's (listed from bottom of tower to top)</b>						
	1	0.0756	0.090	0.0663	0.079	0.0610	0.073
	2	0.0787	0.094	0.0691	0.082	0.0635	0.076
	3	0.0826	0.099	0.0725	0.087	0.0667	0.080
	4	0.0852	0.102	0.0748	0.089	0.0688	0.082
	5	0.0885	0.106	0.0777	0.093	0.0715	0.085
	6	0.0907	0.108	0.0796	0.095	0.0733	0.087
	7	0.0930	0.111	0.0817	0.097	0.0751	0.090

Table 19 - Eurocode minimum wind loads by temperature

DOWN 50 - Eurocode Maximums								
W(klf) when T = -20C = -4F			W (klf) when T = 15C = 59F			W (klf) when T = 40C = 104F		
SS	LS	TWR	SS	LS	TWR	SS	LS	TWR
0.032	0.043	0.045	0.028	0.037	0.039	0.026	0.034	0.036
UP 50 - Eurocode Maximums								
W(klf) when T = -20C = -4F			W (klf) when T = 15C = 59F			W (klf) when T = 40C = 104F		
SS	LS	TWR	SS	LS	TWR	SS	LS	TWR
0.032	0.074	0.045	0.028	0.065	0.039	0.026	0.060	0.036
DOWN 135 - Eurocode Maximums								
W(klf) when T = -20C = -4F			W (klf) when T = 15C = 59F			W (klf) when T = 40C = 104F		
SS	LS	TWR	SS	LS	TWR	SS	LS	TWR
0.127	0.170	0.179	0.112	0.150	0.158	0.103	0.138	0.145
UP 135 - Eurocode Maximums								
W(klf) when T = -20C = -4F			W (klf) when T = 15C = 59F			W (klf) when T = 40C = 104F		
SS	LS	TWR	SS	LS	TWR	SS	LS	TWR
0.127	0.298	0.179	0.112	0.262	0.158	0.103	0.241	0.145

Table 20 - Final hybrid wind loads after application of Eurocode minimums for 100mph wind

100 mph	DOWN - 100 mph			100 mph	UP - 100 mph		
	-20	15	40		-20	15	40
<b>South Span</b>				<b>South Span</b>			
Bot Chord	0.224	0.197	0.181	Bot Chord	0.224	0.197	0.181
Top Chord	0.182	0.160	0.147	Top Chord	0.182	0.160	0.147
W14's	0.127	0.112	0.103	W14's	0.127	0.112	0.103
<b>Lift Span</b>				<b>Lift Span</b>			
Bot Chord	0.207	0.182	0.167	Bot Chord	0.298	0.262	0.241
Top Chord	0.170	0.150	0.138	Top Chord	0.298	0.262	0.241
W14's	0.170	0.150	0.138	W14's	0.298	0.262	0.241
<b>South Tower</b>				<b>South Tower</b>			
<b>A-A</b>				<b>A-A</b>			
A-A 1	0.179	0.158	0.145	A-A 1	0.179	0.158	0.145
A-A 2	0.185	0.162	0.149	A-A 2	0.185	0.162	0.149
A-A 3	0.197	0.173	0.159	A-A 3	0.197	0.173	0.159
A-A 4	0.202	0.177	0.163	A-A 4	0.202	0.177	0.163
<b>B-B</b>				<b>B-B</b>			
B-B 1	0.179	0.158	0.145	B-B 1	0.179	0.158	0.145
B-B 2	0.196	0.172	0.158	B-B 2	0.196	0.172	0.158
B-B 3	0.212	0.186	0.171	B-B 3	0.212	0.186	0.171
B-B 4	0.215	0.189	0.174	B-B 4	0.215	0.189	0.174
<b>W14's</b>				<b>W14's</b>			
1	0.179	0.158	0.145	1	0.179	0.158	0.145
2	0.179	0.158	0.145	2	0.179	0.158	0.145
3	0.179	0.158	0.145	3	0.179	0.158	0.145
4	0.179	0.158	0.145	4	0.179	0.158	0.145
5	0.179	0.158	0.145	5	0.179	0.158	0.145
6	0.179	0.158	0.145	6	0.179	0.158	0.145
7	0.179	0.158	0.145	7	0.179	0.158	0.145

Table 21 - Final hybrid wind loads after application of Eurocode minimums for 50mph wind

50mph	DOWN - 50 mph			50mph	UP - 50 mph		
	-20	15	40		-20	15	40
<b>South Span</b>				<b>South Span</b>			
Bot Chord	0.056	0.049	0.045	Bot Chord	0.056	0.049	0.049
Top Chord	0.046	0.040	0.037	Top Chord	0.046	0.040	0.040
W14's	0.032	0.028	0.026	W14's	0.032	0.028	0.026
<b>Lift Span</b>				<b>Lift Span</b>			
Bot Chord	0.052	0.045	0.042	Bot Chord	0.074	0.065	0.060
Top Chord	0.043	0.037	0.034	Top Chord	0.074	0.065	0.060
W14's	0.043	0.037	0.034	W14's	0.074	0.065	0.060
<b>South Tower</b>				<b>South Tower</b>			
<b>A-A</b>				<b>A-A (listed from bottom of tower to top)</b>			
A-A 1	0.045	0.039	0.036	A-A 1	0.045	0.039	0.036
A-A 2	0.046	0.041	0.037	A-A 2	0.046	0.041	0.037
A-A 3	0.049	0.043	0.040	A-A 3	0.049	0.043	0.040
A-A 4	0.050	0.044	0.041	A-A 4	0.050	0.044	0.041
<b>B-B</b>				<b>B-B (listed from bottom of tower to top)</b>			
B-B 1	0.045	0.039	0.036	B-B 1	0.045	0.039	0.036
B-B 2	0.049	0.043	0.040	B-B 2	0.049	0.043	0.040
B-B 3	0.053	0.047	0.043	B-B 3	0.053	0.047	0.043
B-B 4	0.054	0.047	0.043	B-B 4	0.054	0.047	0.043
<b>W14's</b>				<b>W14's (listed from bottom of tower to top)</b>			
1	0.045	0.039	0.036	1	0.045	0.039	0.036
2	0.045	0.039	0.036	2	0.045	0.039	0.036
3	0.045	0.039	0.036	3	0.045	0.039	0.036
4	0.045	0.039	0.036	4	0.045	0.039	0.036
5	0.045	0.039	0.036	5	0.045	0.039	0.036
6	0.045	0.039	0.036	6	0.045	0.039	0.036
7	0.045	0.039	0.036	7	0.045	0.039	0.036

## DESIGN MANUAL FOR ROADS AND BRIDGES (DMRB)

### Solidity Ratio

$$\phi = \frac{A_{windward}}{A_{net}} = \frac{6296ft^2}{5110ft^2} = 0.19 < 0.5, \text{ therefore stable in regards to vortex shedding}$$

The figures below show the net projected area of the lift span and front face area of the windward truss of the lift span. These models, developed in AutoCAD, allowed the calculation of the solidity ratio, shown above, of the lift span and south span systems.



Figure 30 - Net Projected area of lift span ( $A_{net}$ )

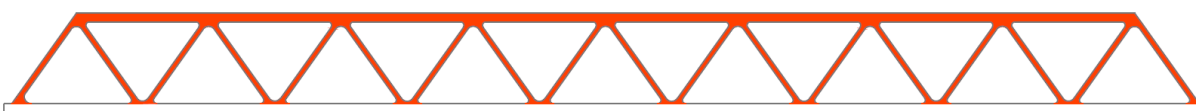


Figure 31 - Front face of windward truss ( $A_{windward}$ )

### DMRB 2.1.1.3c – Limiting Criteria

“In addition, truss girder bridges shall be considered stable with regard to vortex excited vibrations provided  $\phi < 0.5$ , where  $\phi$  is the solidity ratio of the front face of the windward truss, defined as the ratio of the net total projected area of the truss components to the projected area encompassed by the outer boundaries of the truss (i.e. excluding the depth of the deck). For trusses with  $\phi \geq 0.5$ , refer to 2.1.1.2.”

### Mean Hourly Wind Speed Calculation

- $V_{r,up} = S_m V_s = (S_c T_c S'_h)(V_b S_p S_a S_d) = ((S'_c K_F) T_c S'_h)(V_b S_p S_a S_d)$ 
  - $V_b$  is the basic hourly mean wind speed for a 50 year return period in flat, open country at 10m above sea level



- $S_p$  may be taken as 1.05 for highway, railway, foot, and cycle bridges
  - $S_a$  may be taken as  $1+0.001\Delta$ 
    - $\Delta$  is the altitude in meters above mean sea level of base topographic features
  - $S'_c$  is shown in Figure 32, below
  - $K_F$  is shown in Figure 33, below
  - $T_c$  is taken as 1.0 for town reduction
  - $S'_h$  is taken as 1.0 for flat terrain
  - $S_d$  is 1.0 when wind direction is ignored
- $V_{r,up} = ((1.17)(0.96)(1.0)(1.0)) \left( (44.7)(1.05)(1 + 0.001(0))(1.0) \right) = \boxed{52.7\text{m/s}}$
  - $V_{r,down} = ((1.47)(1.0)(1.0)(1.0)) \left( (44.7)(1.05)(1 + 0.001(0))(1.0) \right) = \boxed{69.0\text{m/s}}$

Height above ground (m)	Terrain and Bridge Factor $S_b'$						Hourly Speed Factor $S_c'$
	LOADED LENGTH (m)						
	20	40	60	100	200	400	
5	1.56	1.51	1.48	1.44	1.39	1.34	1.02
10	1.68	1.64	1.61	1.57	1.52	1.47	1.17
15	1.76	1.71	1.68	1.64	1.60	1.55	1.25
20	1.81	1.76	1.73	1.69	1.65	1.60	1.31
30	1.88	1.83	1.80	1.76	1.71	1.66	1.39
40	1.92	1.87	1.85	1.81	1.76	1.71	1.43
50	1.96	1.91	1.88	1.84	1.80	1.75	1.47
60	1.98	1.94	1.91	1.87	1.83	1.78	1.50
80	2.02	1.98	1.95	1.92	1.87	1.82	1.55
100	2.05	2.01	1.98	1.95	1.90	1.86	1.59
150	2.11	2.06	2.04	2.01	1.97	1.92	1.67
200	2.15	2.11	2.08	2.05	2.01	1.97	1.73

Figure 32 - DMRB terrain and bridge factor

Height above ground (m)	Fetch Correction Factor, $K_f$					
	UPWIND DISTANCE OF SITE FROM SEA (km)					
	≤0.3	1	3	10	30	≥100
5	1.00	0.96	0.94	0.91	0.90	0.85
10	1.00	0.99	0.96	0.94	0.92	0.88
15	1.00	0.99	0.98	0.96	0.94	0.89
20	1.00	1.00	0.99	0.97	0.95	0.90
30	1.00	1.00	0.99	0.98	0.96	0.92
40	1.00	1.00	1.00	0.99	0.98	0.93
50	1.00	1.00	1.00	0.99	0.98	0.93
60	1.00	1.00	1.00	0.99	0.99	0.94
80	1.00	1.00	1.00	1.00	0.99	0.95
100	1.00	1.00	1.00	1.00	0.99	0.95
150	1.00	1.00	1.00	1.00	1.00	0.96
200	1.00	1.00	1.00	1.00	1.00	0.97

Figure 33 - DMRB fetch correction factor

**Excel Calculations**

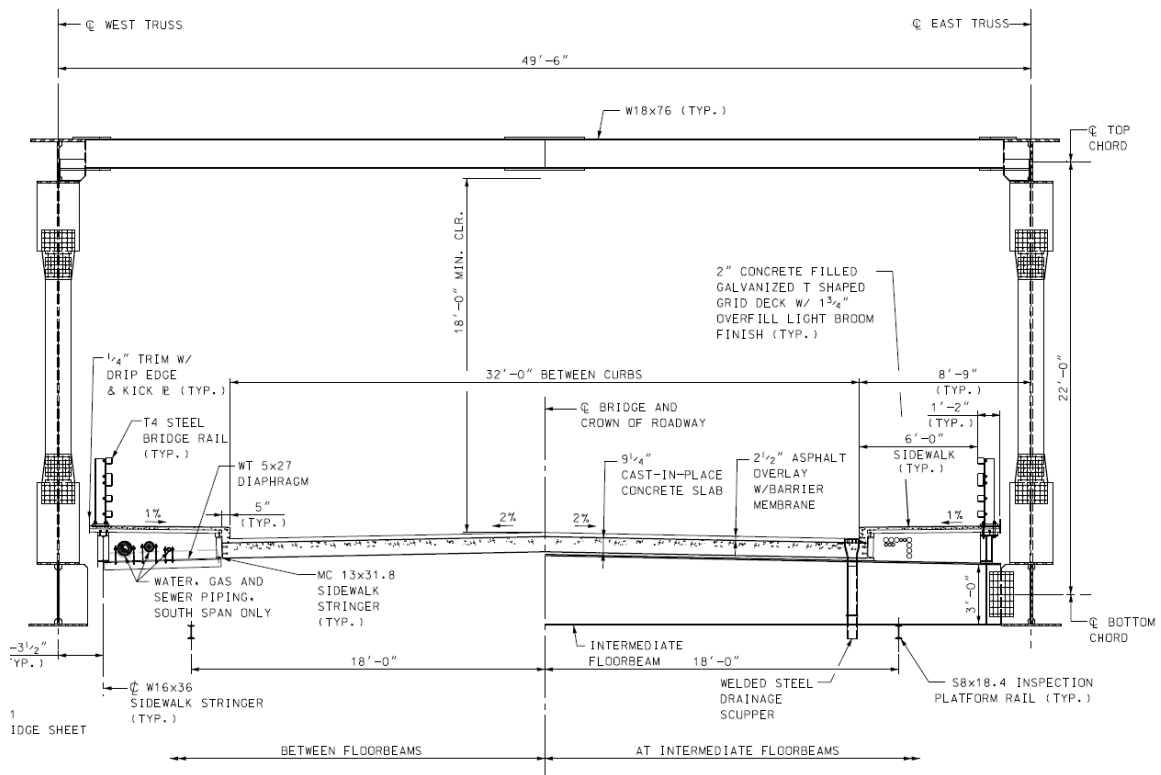


Figure 34 - Memorial Bridge typical fixed-span cross section

Table 22 - DMRB susceptibility recommendation and input

<b>P<sub>b</sub> = 0.362</b>		<b>1.0 &gt; P<sub>b</sub> &gt; 0.04</b>	<b>WARNING: Bridge may be subject to some aerodynamic excitation.</b>
Where...	$P_b = \left(\frac{\rho b^2}{m}\right) \left(\frac{16V_r^2}{bLf_b^2}\right)$		
rho (kg/m <sup>3</sup> )	1.395	Denser air increases susceptibility	
b (m)	15.10	Wider bridge significantly increases wind effects	
m (kg/m)	11848	Heavier bridge decreases effect of wind	
V <sub>r</sub> (m/s)	52.7	Higher wind speeds increase bridge susceptibility	
	(mph) 117.9		
L (m)	91.5		
T (s)	0.65	Lower period = higher frequency = more stability	
Bridge Type	5		

Table 23 - DMRB susceptibility warnings by temperature, wind speed, and lift state

Temperature (C)	Lift Position	V_r	P_b	
-20	Down	52.7	0.362	WARNING: Bridge may be subject to some aerodynamic excitation.
15	Down	52.7	0.318	WARNING: Bridge may be subject to some aerodynamic excitation.
40	Down	52.7	0.293	WARNING: Bridge may be subject to some aerodynamic excitation.
-20	Up	69.0	0.621	WARNING: Bridge may be subject to some aerodynamic excitation.
15	Up	69.0	0.546	WARNING: Bridge may be subject to some aerodynamic excitation.
40	Up	69.0	0.502	WARNING: Bridge may be subject to some aerodynamic excitation.

Table 24 - DMRB calculated variables

m_span	1,084,080	kg	NOTE: m_span is the total mass of lift span
	2,390,000	lb	
f_b	1.544	Hz	WARNING: Bridge stability from vortex excitation requires investigation
f_b, est, min	0.983	Hz	
f_b, est, max	1.966	Hz	
b*/d_4	0.424	-	
b*	49.5	ft	NOTE: b* is the effective bridge width (underside of deck)
	15.1	m	
d_4	22.0	ft	NOTE: d_4 is the bridge depth (the average value along the middle third of the longest span)
	6.7	m	
φ	0.19	-	NOTE: Solidity ratio is the ratio of the net total area presented to the wind to the total area encompassed by the outer boundaries of the deck for trusses
V_cr	67.3	m/s	NOTE: V_cr is the critical wind speed for vortex excitation for both bending and torsion
CHECK: V_vs	52.7	m/s	NOTE: Given V_vs, bridge is stable in regards to vortext shedding
CHECK: φ > 0.5	0.19	-	NOTE: Given the solidity ratio < 0.5, the bridge can be considered stable in regards to vortext shedding

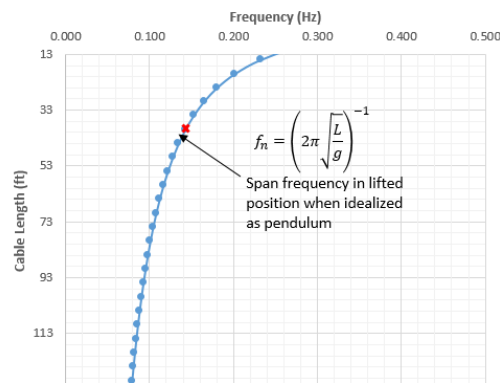
## APPENDIX B DYNAMICS

### COUNTERWEIGHT TUNED MASS DAMPER CALCULATIONS

Span Down - Weight Up		
z_sheave	192.25	ft
z_bracket	178.35	ft
L_cable	13.9	ft
g	32.2	ft/s <sup>2</sup>
T_n_weight	4.13	s
f_n_weight	0.242	Hz

Span Up - Weight Down		
z_sheave	192.25	ft
z_bracket	60.59	ft
L_cable	131.66	ft
g	32.2	ft/s <sup>2</sup>
T_n_weight	12.70	s
f_n_weight	0.079	Hz

Span Up - Weight Down		
z_sheave	192.25	ft
z_drum	152.49	ft
L_cable	39.76	ft
g	32.2	ft/s <sup>2</sup>
T_n_span	6.98	s
f_n_span	0.143	Hz



NOTE: Above figure shows the change of natural frequency of the counterweight (modeled as a simple pendulum) at varying lift heights. Cable length increases as the lift span is raised

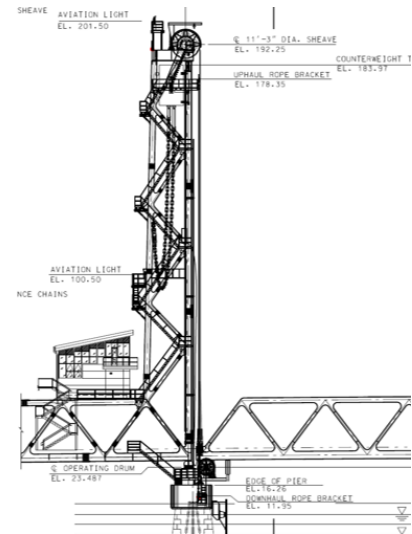


Figure 35 - Excel sample showing natural frequencies as a function of counterweight elevation

The calculation values shown above in Figure 35 yielded critical information about the frequencies of the counterweight system and allowed for their comparison to the natural frequency of the system as a whole (established from analyses in SAP2000®) to determine rho. Using Excel, an input table was created (Table 25, below) so dynamic values for the Memorial Bridge system could be entered and manipulated. These input values were run through an extensive set of calculations to develop Figure 7 and Figure 24 in the above sections.

Table 25 - Input table for amplification factor calculations

ξ <sub>1</sub>	1
ξ <sub>0</sub>	0
ξ <sub>mid</sub>	0.03
f	1.0
m <sub>bar</sub>	0.01
f <sub>spn</sub>	1.16
f <sub>cw</sub>	0.24
rho	4.79
m <sub>bar,b</sub>	0.38

Table 26 - Sample tabulation of H2 factor data for typical TMD system

Check for aplification from counterweight...								D_2			H_2		
$\rho$	$1 - \rho^2$	$f^2 - \rho^2$	$mp^2f^2$	$2(\xi_1)_{pf}$	$2(\xi_0)_{pf}$	$2(\xi_{mid})_{pf}$	$1 + m$	D_2,1	D_2,0	D_2,mid	H_2,1	H_2,0	H_2,mid
0.025	0.999	0.999	2.35E-04	0.05	0.00	0.001	1.38	1.001	0.999	0.999	1.38	1.38	1.38
0.050	0.998	0.998	9.42E-04	0.10	0.00	0.003	1.38	1.004	0.994	0.994	1.38	1.38	1.38
0.075	0.994	0.994	2.12E-03	0.15	0.00	0.004	1.38	1.008	0.987	0.987	1.38	1.39	1.39
0.100	0.990	0.990	3.77E-03	0.20	0.00	0.005	1.38	1.014	0.976	0.976	1.38	1.40	1.40
0.125	0.984	0.984	5.89E-03	0.25	0.00	0.007	1.38	1.021	0.963	0.963	1.38	1.41	1.41
0.150	0.978	0.978	8.48E-03	0.30	0.00	0.008	1.38	1.029	0.947	0.947	1.38	1.43	1.43
0.175	0.969	0.969	1.15E-02	0.35	0.00	0.009	1.38	1.039	0.928	0.928	1.38	1.45	1.45
0.200	0.960	0.960	1.51E-02	0.40	0.00	0.011	1.38	1.049	0.907	0.907	1.38	1.47	1.47
0.225	0.949	0.949	1.91E-02	0.45	0.00	0.012	1.38	1.060	0.882	0.882	1.38	1.50	1.50
0.250	0.938	0.938	2.35E-02	0.50	0.00	0.014	1.38	1.071	0.855	0.856	1.38	1.54	1.54
0.275	0.924	0.924	2.85E-02	0.55	0.00	0.015	1.38	1.083	0.826	0.826	1.39	1.58	1.57
0.300	0.910	0.910	3.39E-02	0.60	0.00	0.016	1.38	1.094	0.794	0.794	1.40	1.62	1.62
0.325	0.894	0.894	3.98E-02	0.65	0.00	0.018	1.38	1.104	0.760	0.760	1.41	1.67	1.67
0.350	0.878	0.878	4.61E-02	0.70	0.00	0.019	1.38	1.113	0.724	0.724	1.42	1.73	1.73
0.375	0.859	0.859	5.30E-02	0.75	0.00	0.020	1.38	1.121	0.686	0.686	1.44	1.80	1.80
0.400	0.840	0.840	6.03E-02	0.80	0.00	0.022	1.38	1.128	0.645	0.646	1.45	1.89	1.88
0.425	0.819	0.819	6.80E-02	0.85	0.00	0.023	1.38	1.133	0.603	0.604	1.48	1.98	1.98
0.450	0.798	0.798	7.63E-02	0.90	0.00	0.024	1.38	1.136	0.560	0.560	1.50	2.10	2.10
0.475	0.774	0.774	8.50E-02	0.95	0.00	0.026	1.38	1.136	0.515	0.515	1.53	2.24	2.23
0.500	0.750	0.750	9.42E-02	1.00	0.00	0.027	1.38	1.134	0.468	0.469	1.57	2.41	2.40
0.525	0.724	0.724	1.04E-01	1.05	0.00	0.028	1.38	1.129	0.421	0.422	1.61	2.62	2.61
0.550	0.698	0.698	1.14E-01	1.10	0.00	0.030	1.38	1.120	0.373	0.374	1.66	2.88	2.88
0.575	0.669	0.669	1.25E-01	1.15	0.00	0.031	1.38	1.108	0.324	0.325	1.71	3.23	3.22
0.600	0.640	0.640	1.36E-01	1.20	0.00	0.032	1.38	1.092	0.274	0.275	1.78	3.71	3.69
0.625	0.609	0.609	1.47E-01	1.25	0.00	0.034	1.38	1.072	0.224	0.226	1.85	4.40	4.37
0.650	0.578	0.578	1.59E-01	1.30	0.00	0.035	1.38	1.048	0.174	0.177	1.93	5.47	5.41
0.675	0.544	0.544	1.72E-01	1.35	0.00	0.036	1.38	1.019	0.125	0.128	2.03	7.38	7.22
0.700	0.510	0.510	1.85E-01	1.40	0.00	0.038	1.38	0.986	0.076	0.080	2.15	11.74	11.09
0.725	0.474	0.474	1.98E-01	1.45	0.00	0.039	1.38	0.947	0.027	0.037	2.29	31.47	22.91
0.750	0.438	0.438	2.12E-01	1.50	0.00	0.041	1.38	0.904	0.020	0.032	2.46	39.78	25.63
0.775	0.399	0.399	2.26E-01	1.55	0.00	0.042	1.38	0.855	0.067	0.071	2.66	11.63	11.02
0.800	0.360	0.360	2.41E-01	1.60	0.00	0.043	1.38	0.801	0.111	0.114	2.90	6.61	6.51
0.825	0.319	0.319	2.56E-01	1.65	0.00	0.045	1.38	0.742	0.154	0.156	3.20	4.51	4.49
0.850	0.278	0.278	2.72E-01	1.70	0.00	0.046	1.38	0.678	0.195	0.196	3.58	3.35	3.35
0.850	0.278	0.278	7.23E-03	1.70	0.00	0.046	1.01	0.482	0.070	0.071	3.62	4.12	4.10
0.875	0.234	0.234	7.66E-03	1.75	0.00	0.047	1.01	0.417	0.047	0.049	4.28	5.17	5.13
0.900	0.190	0.190	8.10E-03	1.80	0.00	0.049	1.01	0.347	0.028	0.030	5.28	7.14	6.98
0.925	0.144	0.144	8.56E-03	1.85	0.00	0.050	1.01	0.270	0.012	0.014	6.94	12.56	11.37
0.950	0.098	0.098	9.03E-03	1.90	0.00	0.051	1.01	0.187	0.000	0.005	10.27	223.38	23.52
0.975	0.049	0.049	9.51E-03	1.95	0.00	0.053	1.01	0.098	0.007	0.008	20.21	8.40	10.57
1.000	0.000	0.000	1.00E-02	2.00	0.00	0.054	1.01	0.010	0.010	0.010	202.00	1.00	5.54
1.025	-0.051	-0.051	1.05E-02	2.05	0.00	0.055	1.01	0.105	0.008	0.008	19.70	5.11	8.20
1.050	-0.103	-0.103	1.10E-02	2.10	0.00	0.057	1.01	0.217	0.001	0.006	9.77	178.31	18.46
1.075	-0.156	-0.156	1.16E-02	2.15	0.00	0.058	1.01	0.338	0.013	0.016	6.44	11.50	10.06
1.100	-0.210	-0.210	1.21E-02	2.20	0.00	0.059	1.01	0.468	0.032	0.034	4.77	6.25	6.07
1.125	-0.266	-0.266	1.27E-02	2.25	0.00	0.061	1.01	0.606	0.058	0.060	3.77	4.41	4.37
1.150	-0.323	-0.323	1.32E-02	2.30	0.00	0.062	1.01	0.755	0.091	0.093	3.11	3.44	3.43
1.175	-0.381	-0.381	1.38E-02	2.35	0.00	0.063	1.01	0.913	0.131	0.133	2.63	2.83	2.82
1.200	-0.440	-0.440	1.44E-02	2.40	0.00	0.065	1.01	1.082	0.179	0.181	2.28	2.40	2.40
1.225	-0.501	-0.501	1.50E-02	2.45	0.00	0.066	1.01	1.261	0.236	0.238	2.00	2.08	2.08
1.250	-0.563	-0.563	1.56E-02	2.50	0.00	0.068	1.01	1.452	0.301	0.303	1.78	1.84	1.84
1.275	-0.626	-0.626	1.63E-02	2.55	0.00	0.069	1.01	1.654	0.375	0.378	1.60	1.64	1.64
1.300	-0.690	-0.690	1.69E-02	2.60	0.00	0.070	1.01	1.869	0.459	0.462	1.45	1.48	1.48
1.325	-0.756	-0.756	1.76E-02	2.65	0.00	0.072	1.01	2.097	0.553	0.556	1.33	1.35	1.35
1.350	-0.823	-0.823	1.82E-02	2.70	0.00	0.073	1.01	2.338	0.658	0.661	1.22	1.23	1.23
1.375	-0.891	-0.891	1.89E-02	2.75	0.00	0.074	1.01	2.592	0.774	0.777	1.12	1.14	1.14
1.400	-0.960	-0.960	1.96E-02	2.80	0.00	0.076	1.01	2.861	0.902	0.905	1.04	1.05	1.05
1.425	-1.031	-1.031	2.03E-02	2.85	0.00	0.077	1.01	3.144	1.042	1.045	0.97	0.98	0.98
1.450	-1.103	-1.103	2.10E-02	2.90	0.00	0.078	1.01	3.443	1.194	1.198	0.91	0.91	0.91
1.475	-1.176	-1.176	2.18E-02	2.95	0.00	0.080	1.01	3.758	1.360	1.364	0.85	0.86	0.86
1.500	-1.250	-1.250	2.25E-02	3.00	0.00	0.081	1.01	4.089	1.540	1.543	0.80	0.81	0.81

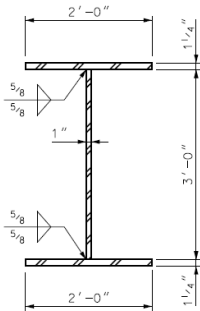
1.500	-1.250	-1.250	2.25E-02	3.00	0.00	0.081	1.01	4.089	1.540	1.543	0.80	0.81	0.81
1.525	-1.326	-1.326	2.33E-02	3.05	0.00	0.082	1.01	4.437	1.734	1.738	0.76	0.76	0.76
1.550	-1.403	-1.403	2.40E-02	3.10	0.00	0.084	1.01	4.802	1.943	1.947	0.71	0.72	0.72
1.575	-1.481	-1.481	2.48E-02	3.15	0.00	0.085	1.01	5.185	2.167	2.171	0.68	0.68	0.68
1.600	-1.560	-1.560	2.56E-02	3.20	0.00	0.086	1.01	5.587	2.408	2.412	0.64	0.64	0.64
1.625	-1.641	-1.641	2.64E-02	3.25	0.00	0.088	1.01	6.009	2.665	2.669	0.61	0.61	0.61
1.650	-1.723	-1.723	2.72E-02	3.30	0.00	0.089	1.01	6.450	2.940	2.944	0.58	0.58	0.58
1.675	-1.806	-1.806	2.81E-02	3.35	0.00	0.090	1.01	6.912	3.232	3.236	0.55	0.56	0.56
1.700	-1.890	-1.890	2.89E-02	3.40	0.00	0.092	1.01	7.394	3.543	3.548	0.53	0.53	0.53
1.725	-1.976	-1.976	2.98E-02	3.45	0.00	0.093	1.01	7.899	3.873	3.878	0.51	0.51	0.51
1.750	-2.063	-2.063	3.06E-02	3.50	0.00	0.095	1.01	8.426	4.223	4.228	0.49	0.49	0.49
1.775	-2.151	-2.151	3.15E-02	3.55	0.00	0.096	1.01	8.976	4.594	4.598	0.47	0.47	0.47
1.800	-2.240	-2.240	3.24E-02	3.60	0.00	0.097	1.01	9.549	4.985	4.990	0.45	0.45	0.45
1.825	-2.331	-2.331	3.33E-02	3.65	0.00	0.099	1.01	10.147	5.399	5.403	0.43	0.43	0.43
1.850	-2.423	-2.423	3.42E-02	3.70	0.00	0.100	1.01	10.770	5.834	5.839	0.41	0.41	0.41
1.875	-2.516	-2.516	3.52E-02	3.75	0.00	0.101	1.01	11.419	6.293	6.298	0.40	0.40	0.40
1.900	-2.610	-2.610	3.61E-02	3.80	0.00	0.103	1.01	12.094	6.776	6.781	0.38	0.38	0.38
1.925	-2.706	-2.706	3.71E-02	3.85	0.00	0.104	1.01	12.796	7.283	7.289	0.37	0.37	0.37
1.950	-2.803	-2.803	3.80E-02	3.90	0.00	0.105	1.01	13.526	7.816	7.822	0.36	0.36	0.36
1.975	-2.901	-2.901	3.90E-02	3.95	0.00	0.107	1.01	14.284	8.375	8.380	0.34	0.35	0.35
2.000	-3.000	-3.000	4.00E-02	4.00	0.00	0.108	1.01	15.072	8.960	8.966	0.33	0.33	0.33
2.025	-3.101	-3.101	4.10E-02	4.05	0.00	0.109	1.01	15.890	9.573	9.579	0.32	0.32	0.32
2.050	-3.203	-3.203	4.20E-02	4.10	0.00	0.111	1.01	16.739	10.214	10.220	0.31	0.31	0.31
2.075	-3.306	-3.306	4.31E-02	4.15	0.00	0.112	1.01	17.619	10.884	10.891	0.30	0.30	0.30
2.100	-3.410	-3.410	4.41E-02	4.20	0.00	0.113	1.01	18.532	11.584	11.591	0.29	0.29	0.29

2.100	-3.410	-3.410	4.41E-02	4.20	0.00	0.113	1.01	18.532	11.584	11.591	0.29	0.29	0.29
2.125	-3.516	-3.516	4.52E-02	4.25	0.00	0.115	1.01	19.478	12.314	12.321	0.28	0.28	0.28
2.150	-3.623	-3.623	4.62E-02	4.30	0.00	0.116	1.01	20.457	13.076	13.083	0.28	0.28	0.28
2.175	-3.731	-3.731	4.73E-02	4.35	0.00	0.117	1.01	21.472	13.870	13.877	0.27	0.27	0.27
2.200	-3.840	-3.840	4.84E-02	4.40	0.00	0.119	1.01	22.522	14.697	14.704	0.26	0.26	0.26
2.225	-3.951	-3.951	4.95E-02	4.45	0.00	0.120	1.01	23.608	15.558	15.565	0.25	0.25	0.25
2.250	-4.063	-4.063	5.06E-02	4.50	0.00	0.122	1.01	24.731	16.453	16.461	0.25	0.25	0.25
2.275	-4.176	-4.176	5.18E-02	4.55	0.00	0.123	1.01	25.893	17.384	17.392	0.24	0.24	0.24
2.300	-4.290	-4.290	5.29E-02	4.60	0.00	0.124	1.01	27.093	18.351	18.359	0.23	0.23	0.23
2.325	-4.406	-4.406	5.41E-02	4.65	0.00	0.126	1.01	28.333	19.355	19.364	0.23	0.23	0.23
2.350	-4.523	-4.523	5.52E-02	4.70	0.00	0.127	1.01	29.613	20.398	20.406	0.22	0.22	0.22
2.375	-4.641	-4.641	5.64E-02	4.75	0.00	0.128	1.01	30.936	21.479	21.487	0.22	0.22	0.22
2.400	-4.760	-4.760	5.76E-02	4.80	0.00	0.130	1.01	32.300	22.600	22.609	0.21	0.21	0.21
2.425	-4.881	-4.881	5.88E-02	4.85	0.00	0.131	1.01	33.708	23.762	23.770	0.20	0.20	0.20
2.450	-5.003	-5.003	6.00E-02	4.90	0.00	0.132	1.01	35.159	24.965	24.974	0.20	0.20	0.20
2.475	-5.126	-5.126	6.13E-02	4.95	0.00	0.134	1.01	36.656	26.211	26.220	0.20	0.20	0.20
2.500	-5.250	-5.250	6.25E-02	5.00	0.00	0.135	1.01	38.199	27.500	27.509	0.19	0.19	0.19

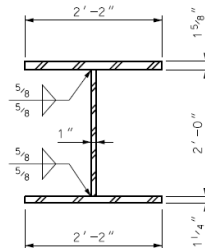
## APPENDIX C MEMORIAL BRIDGE GEOMETRY AND SITE DATA

### CUSTOM BRIDGE SECTIONS

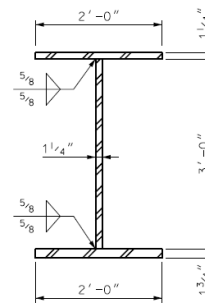
#### Lift Span



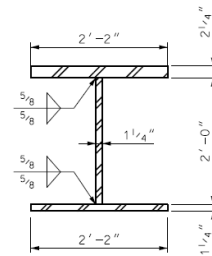
SECTION A-A  
3/4" = 1'-0"



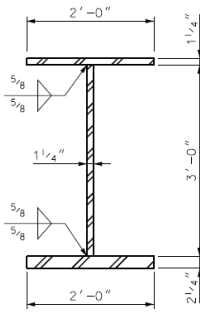
SECTION B-B  
3/4" = 1'-0"



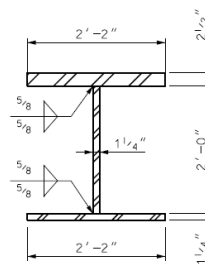
SECTION C-C  
3/4" = 1'-0"



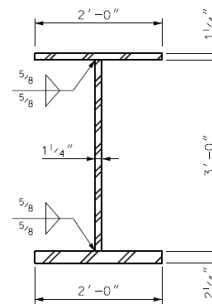
SECTION D-D  
3/4" = 1'-0"



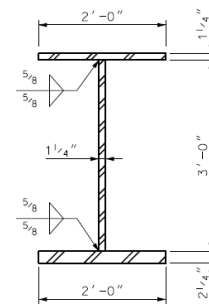
SECTION G-G  
3/4" = 1'-0"



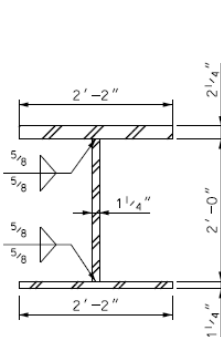
SECTION H-H  
3/4" = 1'-0"



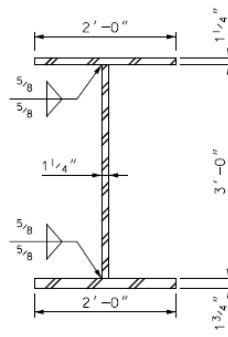
SECTION I-I  
3/4" = 1'-0"



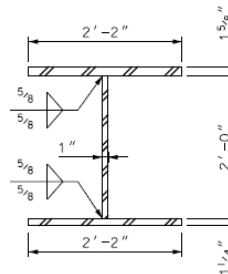
SECTION J-J  
3/4" = 1'-0"



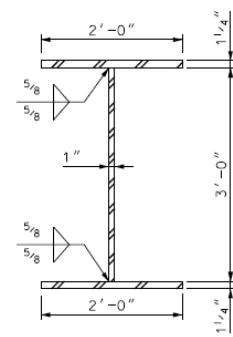
SECTION K-K  
3/4" = 1'-0"



SECTION L-L  
3/4" = 1'-0"



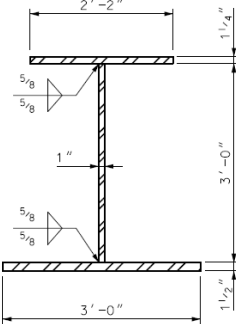
SECTION M-M  
3/4" = 1'-0"



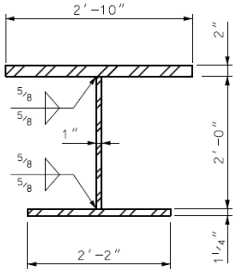
SECTION N-N  
3/4" = 1'-0"



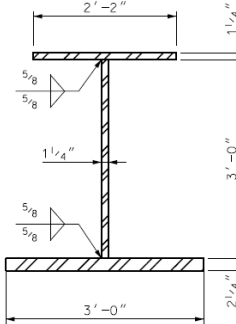
South Span



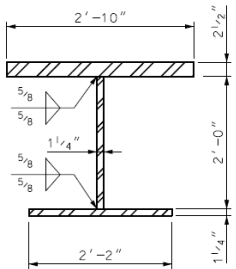
SECTION A-A  
3/4" = 1'-0"



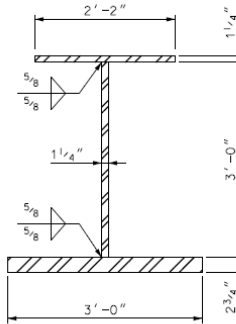
SECTION B-B  
3/4" = 1'-0"



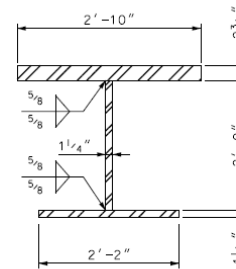
SECTION C-C  
3/4" = 1'-0"



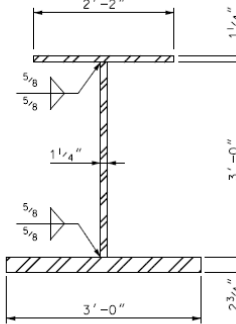
SECTION D-D  
3/4" = 1'-0"



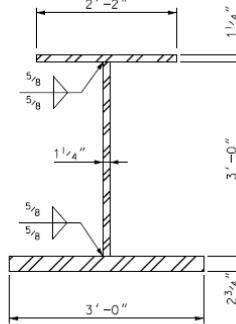
SECTION F-F  
3/4" = 1'-0"



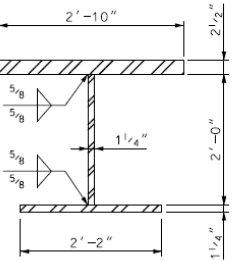
SECTION G-G  
3/4" = 1'-0"



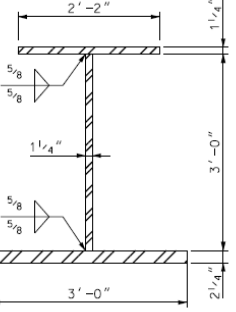
SECTION H-H  
3/4" = 1'-0"



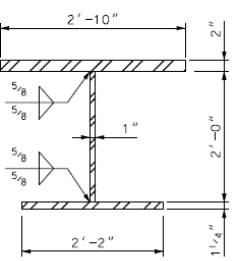
SECTION I-I  
3/4" = 1'-0"



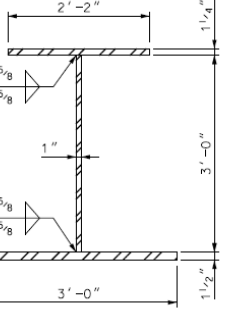
SECTION J-J  
3/4" = 1'-0"



SECTION K-K  
3/4" = 1'-0"

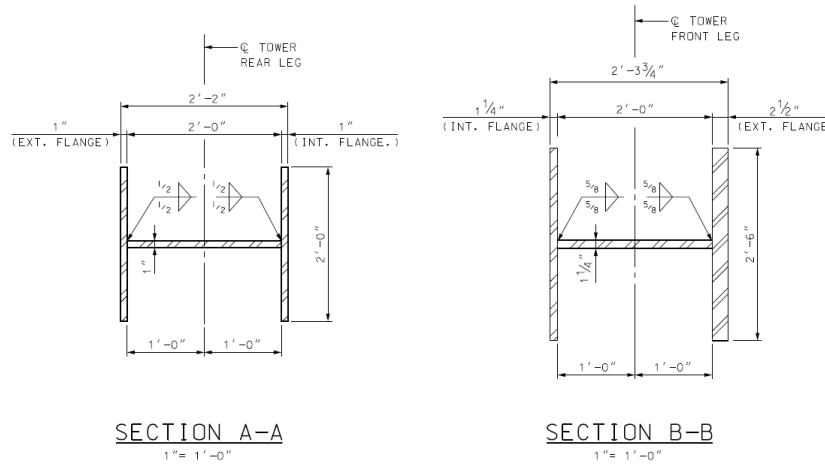


SECTION L-L  
3/4" = 1'-0"



SECTION M-M  
3/4" = 1'-0"

## South Tower



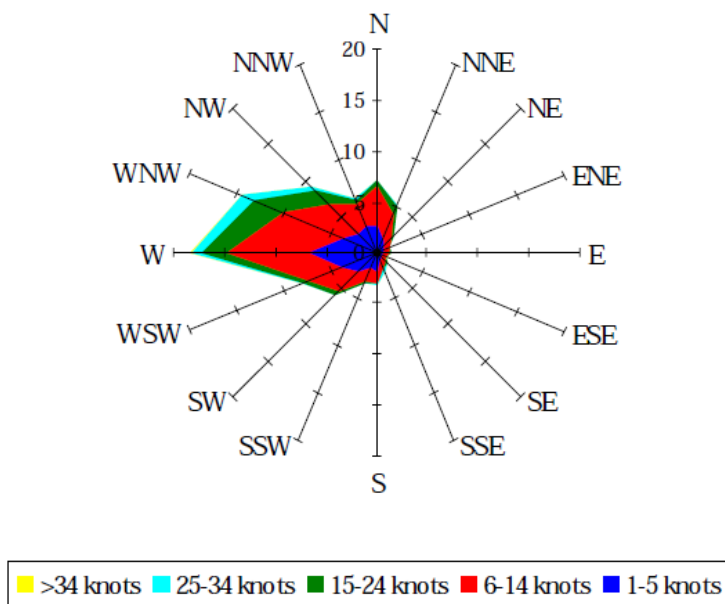
## Tabulation of Critical Moment Capacities

Table 27 - Critical lift and south span member moment capacities

	Model Member ID	Name	Type	Location	S_minor (in <sup>3</sup> )	Z_minor (in <sup>3</sup> )	S_major (in <sup>3</sup> )	Z_major (in <sup>3</sup> )	F_y (ksi)	M_minor Capacity (k-ft)	M_major Capacity (k-ft)
Lift Span Model	1	AA	Bottom chord	Windward	240.3	369.0	1283.6	1441.5	50	1538	5348
	4	II	Bottom chord	Windward	336.5	517.7	1404.3	1817.1	50	2157	5851
	21	II	Bottom chord	Leeward	336.5	517.7	1404.3	1817.1	50	2157	5851
	187	HH	Top chord	Windward	394.6	601.0	978.4	1238.1	50	2504	4077
	192	HH	Top chord	Leeward	394.6	601.0	978.4	1238.1	50	2504	4077
	185	BB	Top chord	Windward	324.1	491.9	899.2	1071.9	50	2049	3747
	190	BB	Top chord	Leeward	324.1	491.9	899.2	1071.9	50	2049	3747
	256	Portal	Portal	South	356.0	511.3	346.6	414.9	50	2131	1444
	260	Portal	Portal	North	356.0	511.3	346.6	414.9	50	2131	1444
	32	FB	Floor beam	Bottom	81.0	123.5	686.5	764.4	50	515	2861
South Span Model	15	BC2.75	Bottom chord	Windward	696.0	1116.3	1633.7	2133.2	50	4651	6807
	13	BC2.75	Bottom chord	Leeward	696.0	1116.3	1633.7	2133.2	50	4651	6807
	31	TC2.75	Top chord	Windward	637.8	1015.4	1013.3	1281.8	50	4231	4222
	29	TC2.75	Top chord	Leeward	637.8	1015.4	1013.3	1281.8	50	4231	4222
	315	TOC	BB	Windward	562.8	853.1	1108.4	1377.1	50	3555	4618
	296	TOC	BB	Leeward	562.8	853.1	1108.4	1377.1	50	3555	4618
	307	TIC	AA	Windward	192.2	294.0	665.8	744.0	50	1225	2774
	288	TIC	AA	Leeward	192.2	294.0	665.8	744.0	50	1225	2774
	34	TC2.00	Top chord	Windward	493.1	795.3	941.0	1155.3	50	3314	3921
	36	TC2.00	Top chord	Leeward	493.1	795.3	941.0	1155.3	50	3314	3921

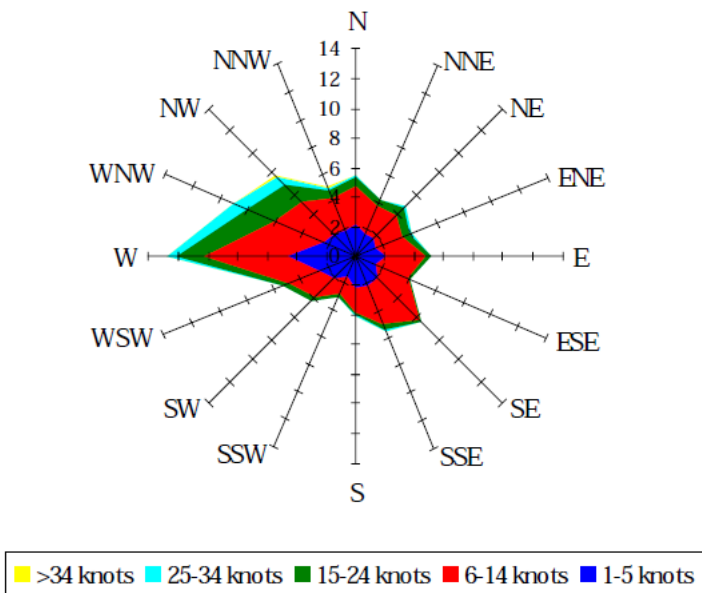
**SITE ANNUAL WIND DATA FROM NOAA**

**Wind Summary - December, January, and February**  
**Labels of Percent Frequency on North Axis**



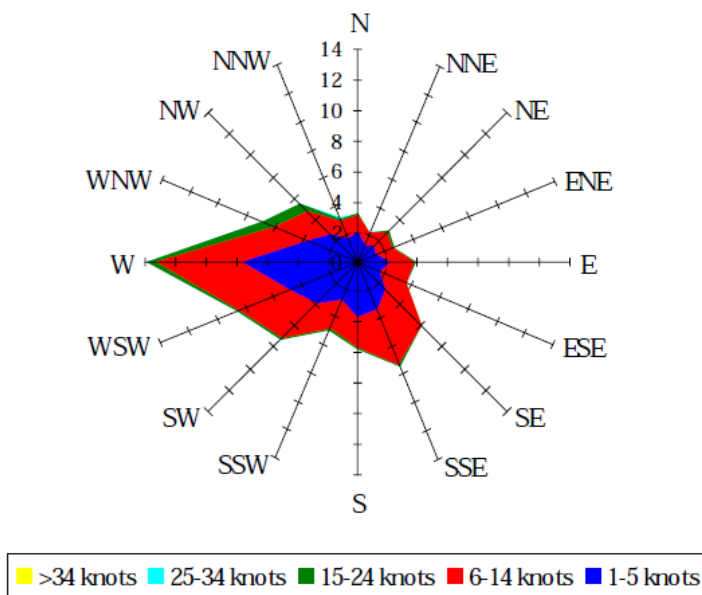
Percent Calm = 11.51

**Wind Summary - March, April, and May**  
**Labels of Percent Frequency on North Axis**



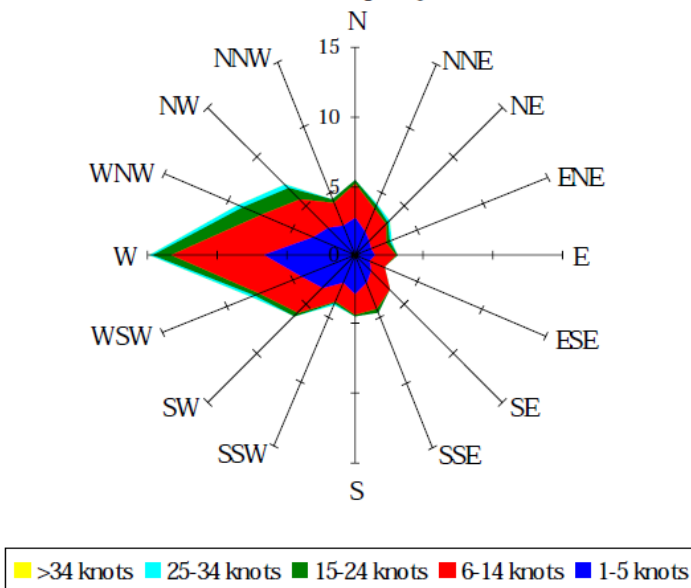
Percent Calm = 10.91

### Wind Summary - June, July, and August Labels of Percent Frequency on North Axis



Percent Calm = 13.54

### Wind Summary - September, October, and November Labels of Percent Frequency on North Axis



Percent Calm = 13.98

## APPENDIX D

### TIDAL TURBINE DEPLOYMENT PLATFORM (TDP)

#### MODELING IN SAP2000® AND AUTOCAD

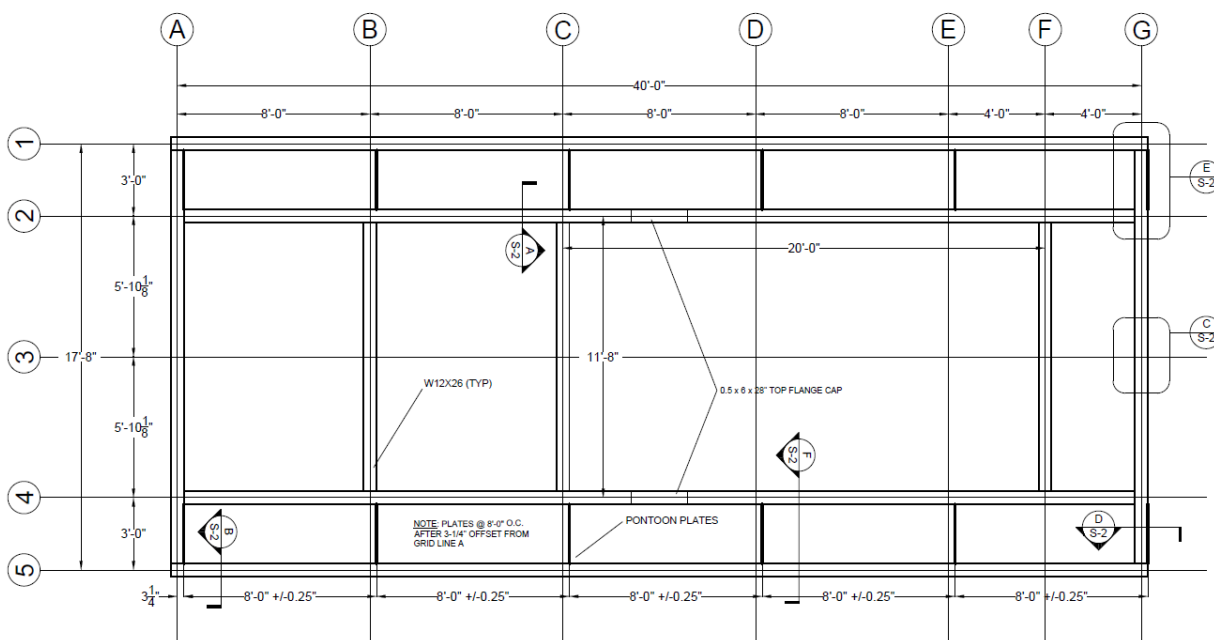


Figure 36 - Plan view of turbine deployment platform

#### Member Capacity

Minor Moment with 0.5 x 6 x 28" Flange Cap:

- $\Omega M_p = \frac{F_y Z_{tot}}{1.67} = \frac{(50)(12.65)}{1.67} = 31.6 \text{ kip} - \text{ft}$
- $Z_{tot} = \sum \frac{bh^2}{4} = \left( \frac{0.38(6.49)^2}{4} \right) + \left( \frac{0.38(6.49)^2}{4} \right) + \left( \frac{(12.2 - 2(0.38))(0.23)^2}{4} \right) + \left( \frac{0.5(6)^2}{4} \right) = 12.65 \text{ in}^3$

#### Load Combination Development

The table below describes the loads considered for LC1 and LC2. In essence, the only difference between both cases is the wave loading. In LC1, only perpendicular wave loads are considered

while, in LC2, only parallel are considered. The live load was developed with 40psf distributed across the walkable area of the platform.

Table 28 - Loading for TDP

Load Type	Load (English, SI)
<b>Dead</b>	0.0483 klf, 0.705kN/m
<b>Live</b>	0.0692 klf, 1.01kN/m
<b>Drag</b>	
Point (turbine support)	5.23 kip, 23.3kN
Point (18ft length)	0.35 kip, 1.56kN
Moment (turbine support)	4.0 kip-ft, 58.37kN-m
<b>Wind</b>	0.0283 klf, 0.41kN/m
<b>Parallel Wave</b>	
Point (turbine support)	12.2 kips, 54.3kN
Distributed (18ft length)	0.20 klf, 2.92kN/m
<b>Perpendicular Wave</b>	
Point	12.2 kips, 54.3kN
Distributed	0.20 klf, 2.92kN/m

## STEEL CONNECTION DESINGS

### *Pinned and Moment Connection Calculations*

The pinned connection for the turbine platform uses the same plate and bolt arrangement as the moment connection but has no welds. Full penetration welds supply the majority of moment capacity for the moment connection.

#### ASSUMPTIONS:

1. All calculations in accordance to AISC 14<sup>th</sup> Edition and ASD
2. A992 steel plates
3. A325 bolts (3/4" unless otherwise noted)
4. Slip critical bolts

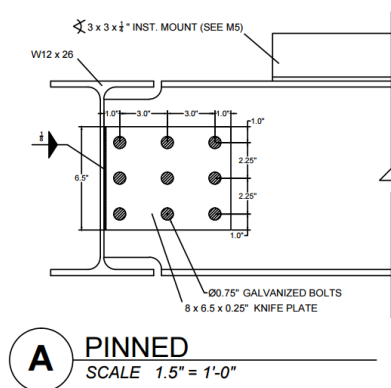


Figure 37 - Pinned connection detail

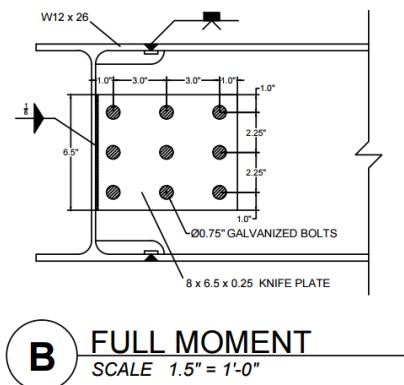


Figure 38 - Full moment connection detail

Table 29 - Summary of pinned and moment connection capacities

Moment Connection Required Capacities			Moment Connection Calculated Capacities			CHECK
M_max	48.7	kip-ft	M_max	45.3	kip-ft	FAIL
V_max	3.0	kips	V_max	19.0	kips	PASS
P_max	17.7	kips	P_max	36.8	kips	PASS
Pinned Connection Required Capacities			Pinned Connection Calculated Capacities			CHECK
M_max	1.9	kip-ft	M_max	7.1	kip-ft	PASS
V_max	0.7	kips	V_max	19.0	kips	PASS
P_max	5.5	kips	P_max	17.1	kips	PASS

Note: The major moment D/C ratio of the full-moment connection is equal to 1.08. While the welds of the moment connections are substantial, the base metal controls the strength of the connection – putting its capacity 8% below demand. However, owing to the extremely conservative nature of the DNVGL calculations compounded with the conservative nature of ASD, it was determined that the connection being 8% under demanded capacity is not a concern.

Table 30 - Available slip critical shear

Available Shear (Slip Critical)			
Group	A	-	AISC 14 Table 7-3
$\mu$	0.3	-	AISC 14 / J3.8c
d_b	0.75	in	
Hole type	STD	-	AISC 14 Table 7-3
Loading	S	-	AISC 14 Table 7-3
R_n,bolt	6.33	kips	AISC 14 Table 7-3
R_n,tot	<b>18.99</b>	<b>kips</b>	



Table 31 - Shear and tension check of coped web

Shear and Tension Check for Coped Web of W12x26			
<b>T_coped</b>	7.125	in	Total height of web with coping
<b>d_cope</b>	1.5	in	Depth of coping
<b>A_g</b>	1.64	in <sup>2</sup>	$T_{coped} * t_w$
<b>A_n</b>	1.04	in <sup>2</sup>	$A_g - 3(t_w * d_{bh})$
<b>t_w</b>	0.23	in	AISC 14 / Table 1-1
<b>F_y * A_g</b>	<b>81.9</b>	<b>kips</b>	
<b>F_y</b>	50	ksi	
<b>F_u * A_n</b>	<b>67.3</b>	<b>kips</b>	
<b>F_u</b>	65	ksi	

Table 32 - Available bearing shear

Available Bearing on Plate at Bolt Holes			
<b>d_b</b>	0.75	in	Bolt diameter
<b>d_blt,edge</b>	1	in	Min spacing by AISC 14 (p.16.1-122)
<b>CHECK</b>	PASS	-	$d_{blt,edge} < 1in$
<b>d_blt,blt</b>	2.25	in	Min bolt-edge by AISC 14 (p.16.1-122)
<b>CHECK</b>	PASS	-	$d_{blt,blt} > 3d_b$
<b>L_c</b>	0.625	in	Clear between bolt edges
<b>d_bh</b>	0.875	in	Bolt hole diameter
<b>t</b>	0.23	in	Connected material thickness = $t_w$
<b>F_u</b>	65	ksi	Min tensile strength
<b>Ω</b>	2.0	-	AISC 14 / J3.10
<b>R_n,bolt</b>	5.6	kips	AISC 14 / J3-6a
	5.6	kips	AISC 14 / J3-6a
	13.5	kips	AISC 14 / J3-6a
<b>R_n,tot</b>	<b>50.5</b>	<b>kips</b>	

Table 33 - Available bevel weld strength

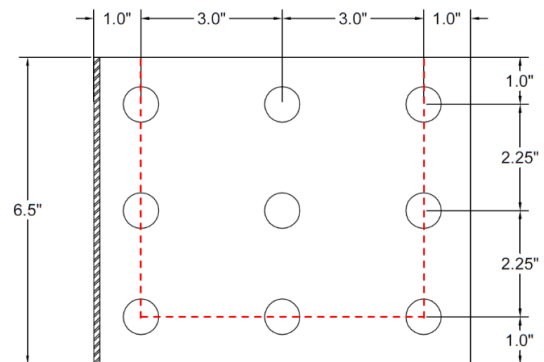
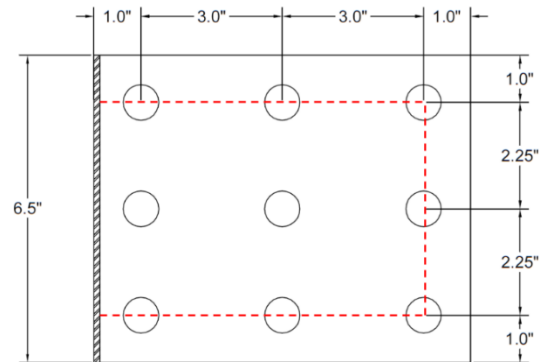
Available Bevel Weld Strength			
<b>Weld</b>	<b>54.4</b>	<b>kips</b>	AISC 14 (Table J2.5)
$\Omega$	1.88	-	
<b>0.6*F<sub>exx</sub></b>	42	ksi	
<b>A<sub>we</sub></b>	2.43	in <sup>2</sup>	
<b>Base Metal</b>	<b>37.5</b>	<b>kips</b>	
$\Omega$	2	-	
<b>F<sub>nBM</sub></b>	50	ksi	
<b>A<sub>BM</sub></b>	1.5	in <sup>2</sup>	

Table 34 - Available fillet weld strength

Available Fillet Weld Strength			
<b>Weld - 1/8" F</b>	<b>17.1</b>	<b>kips</b>	AISC 14 (Table J2.5)
$\Omega$	2	-	
<b>0.6*F<sub>exx</sub></b>	42	ksi	
<b>A<sub>we</sub></b>	0.813	in <sup>2</sup>	
<b>Base Metal</b>	<b>37.4</b>	<b>kips</b>	
$\Omega$	2	-	
<b>F<sub>nBM</sub></b>	50	ksi	
<b>A<sub>BM</sub></b>	1.495	in <sup>2</sup>	

Table 35 - Block shear check in axial and shear directions

Block Shear - Axial Direction (Bolts Only)			
$F_u$	65	ksi	AISC 14 (Table J4-5)
$t_w$	0.23	in	
$A_{gv}$	3.22	in <sup>2</sup>	
$A_{gt}$	1.035	in <sup>2</sup>	
$A_{nv}$	1.540	in <sup>2</sup>	
$A_{nt}$	0.633	in <sup>2</sup>	
$F_u \cdot A_{nt}$	41.11	kips	
$0.6 \cdot F_u \cdot A_{nv}$	60.1	kips	
$U_{bs}$	1.0	-	
$\Omega$	2	-	
$R_n$	101.2	kips	
$R_n/\Omega$	<b>50.6</b>	<b>kips</b>	
Block Shear - Shear Direction (Bolts Only)			
$F_u$	65	ksi	AISC 14 (Table J4-5)
$t_w$	0.23	in	
$A_{gv}$	1.265	in <sup>2</sup>	
$A_{gt}$	1.38	in <sup>2</sup>	
$A_{nv}$	0.259	in <sup>2</sup>	
$A_{nt}$	0.978	in <sup>2</sup>	
$F_u \cdot A_{nt}$	63.5	kips	
$0.6 \cdot F_u \cdot A_{nv}$	10.1	kips	
$U_{bs}$	1.0	-	
$\Omega$	2	-	
$R_n$	73.6	kips	
$R_n/\Omega$	<b>36.8</b>	<b>kips</b>	



*Table 36 - Summary of contributing moment capacities*

<b>Moment Connection Capacity</b>		
<b>Weld</b>	38.2	kip-ft
<b>Bolts</b>	7.12	kip-ft
<b>Total</b>	<b>45.3</b>	<b>kip-ft</b>
CHECK	FAIL	See note above

### Splice Connection Calculations

Splices were designed for the maximum moment experienced by the members at the locations shown below. The controlling load case was  $M_p$  of the DNVGL calculations. Splicing was necessary for the galvanization of the TDP.

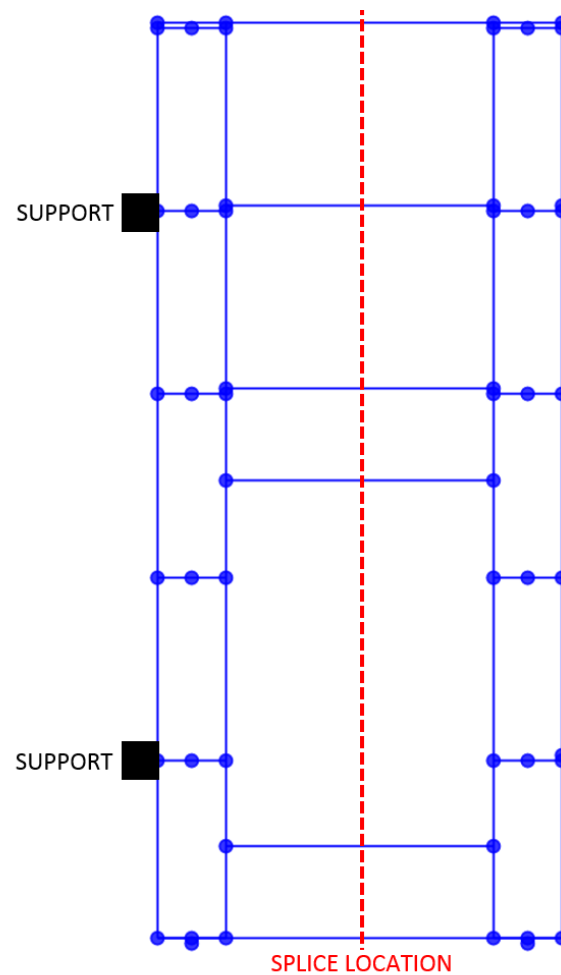


Figure 39 - TDP splice location diagram

#### ASSUMPTIONS

1. All calculations in accordance to AISC 14<sup>th</sup> Edition and ASD
2. A992 steel plates
3. A325 bolts (7/8" unless otherwise noted)
4. Slip critical bolts

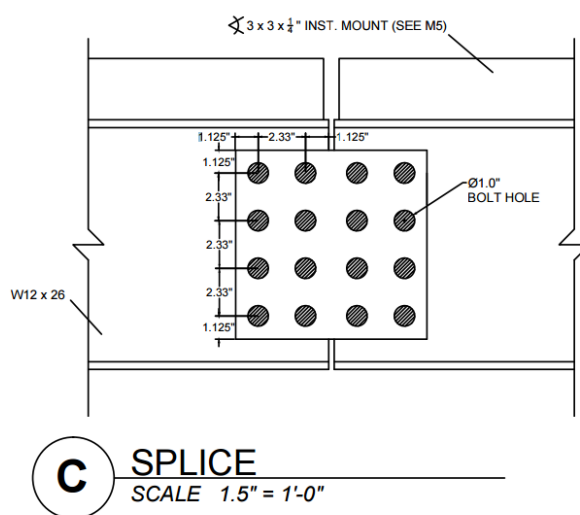


Figure 40 - Splice connection detail

Table 37 - Splice connection capacity summary

Splice Connection Required Capacities			Splice Connection Calculated Capacities			CHECK
<b>M<sub>max</sub></b>	13.1	kip-ft	<b>M<sub>max</sub></b>	20.6	kip-ft	PASS
<b>V<sub>max</sub></b>	1.44	kips	<b>V<sub>max</sub></b>	35.2	kips	PASS
<b>P<sub>max</sub></b>	0.20	kips	<b>P<sub>max</sub></b>	69.5	kips	PASS

Table 38 - Available slip critical shear

Available Shear (Slip Critical)			
<b>Group</b>	A	-	AISC 14 Table 7-3
<b>μ</b>	0.3	-	AISC 14 / J3.8c
<b>d<sub>b</sub></b>	0.875	in	
<b>Hole type</b>	STD	-	AISC 14 Table 7-3
<b>Loading</b>	S	-	AISC 14 Table 7-3
<b>R<sub>n,bolt</sub></b>	8.81	kips	AISC 14 Table 7-3
<b>R<sub>n,tot</sub></b>	<b>35.24</b>	<b>kips</b>	

Table 39 - Block shear check in axial and shear directions

Block Shear - Axial Direction (Bolts Only)			
F <sub>u</sub>	65	ksi	AISC 14 (Table J4-5)
t <sub>w</sub>	0.23	in	
A <sub>gv</sub>	1.59	in <sup>2</sup>	
A <sub>gt</sub>	1.61	in <sup>2</sup>	
A <sub>nv</sub>	1.24	in <sup>2</sup>	
A <sub>nt</sub>	1.00	in <sup>2</sup>	
F <sub>u</sub> *A <sub>nt</sub>	65.3	kips	
0.6*F <sub>u</sub> *A <sub>nv</sub>	48.5	kips	
U <sub>bs</sub>	1.0	-	
Ω	2	-	
R <sub>n</sub>	113.8	kips	
R <sub>n</sub> /Ω	<b>56.9</b>	<b>kips</b>	
Block Shear - Shear Direction (Bolts Only)			
F <sub>u</sub>	65	ksi	AISC 14 (Table J4-5)
t <sub>w</sub>	0.23	in	
A <sub>gv</sub>	1.87	in <sup>2</sup>	
A <sub>gt</sub>	3.18	in <sup>2</sup>	
A <sub>nv</sub>	1.18	in <sup>2</sup>	
A <sub>nt</sub>	2.49	in <sup>2</sup>	
F <sub>u</sub> *A <sub>nt</sub>	161.8	kips	
0.6*F <sub>u</sub> *A <sub>nv</sub>	45.9	kips	
U <sub>bs</sub>	1.0	-	
Ω	2	-	
R <sub>n</sub>	207.6	kips	
R <sub>n</sub> /Ω	<b>103.8</b>	<b>kips</b>	

Table 40 - Shear and tension checks for web of splice connection

Shear and Tension for Web of Splice Connection			
<b>A<sub>g</sub></b>	2.33	in <sup>2</sup>	$T_{coped} * t_w$
<b>A<sub>n</sub></b>	1.41	in <sup>2</sup>	$A_g - 3(t_w * d_{bh})$
<b>t<sub>w</sub></b>	0.23	in	AISC 14 / Table 1-1
<b>F<sub>y</sub>*A<sub>g</sub></b>	<b>116.4</b>	<b>kips</b>	
<b>F<sub>y</sub></b>	50	ksi	
<b>F<sub>u</sub>*A<sub>n</sub></b>	<b>91.6</b>	<b>kips</b>	
<b>F<sub>u</sub></b>	65	ksi	

Table 41 - Available plate bearing

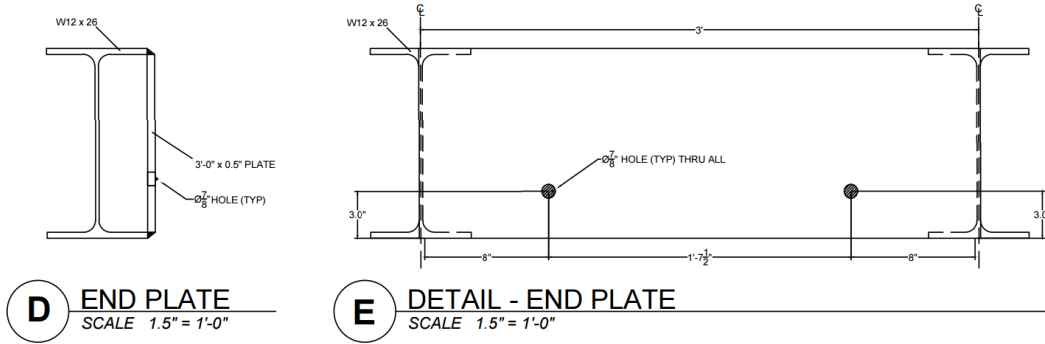
Available Bearing on Plate at Bolt Holes			
<b>d<sub>b</sub></b>	0.875	in	Bolt diameter
<b>d<sub>blt,edge</sub></b>	1.125	in	Min spacing by AISC 14 (p.16.1-122)
<b>CHECK</b>	PASS	-	$d_{blt,edge} < 1.125in$
<b>d<sub>blt,blt</sub></b>	2.33	in	Min bolt-edge by AISC 14 (p.16.1-122)
<b>CHECK</b>	PASS	-	$d_{blt,blt} < 2.67d_b$
<b>L<sub>c</sub></b>	0.63	in	Clear between bolt edges
<b>d<sub>bh</sub></b>	1.0	in	Bolt hole diameter
<b>t</b>	0.23	in	Connected material thickness = t <sub>w</sub>
<b>F<sub>u</sub></b>	65	ksi	Min tensile strength
<b>Ω</b>	2.0	-	AISC 14 / J3.10
<b>R<sub>n,bolt</sub></b>	5.6	kips	AISC 14 / J3-6a
	5.6	kips	AISC 14 / J3-6a
	15.7	kips	AISC 14 / J3-6a
<b>R<sub>n,tot</sub></b>	<b>89.7</b>	<b>kips</b>	



Table 42 - Splice connection moment capacity calculation

Moment Capacity of Splice Connection					
Dist. (in)	Dist. (ft)	R <sub>n</sub> (kip)	M per blt (kip-ft)	M <sub>tot</sub> (kip-ft)	Capacity
2.33	0.19	8.81	1.71	6.85	<b>20.55 kip-ft</b>
1.17	0.10	8.81	0.86	3.43	
0.00	0.00	8.81	0.00	0.00	
1.17	0.10	8.81	0.86	3.43	
2.33	0.19	8.81	1.71	6.85	

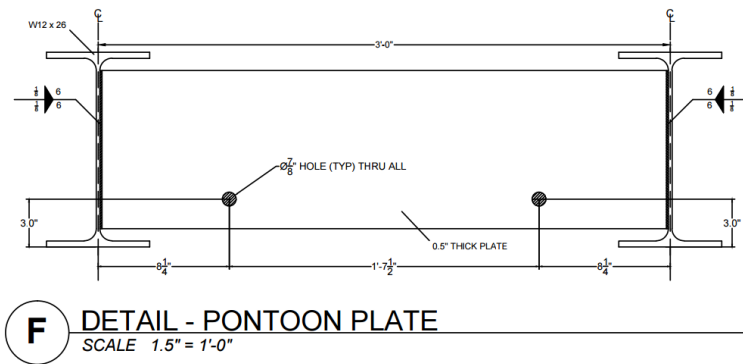
### Welded Mounting and End Plate Connections



**D** END PLATE  
SCALE 1.5" = 1'-0"

**E** DETAIL - END PLATE  
SCALE 1.5" = 1'-0"

Figure 41 - End plate details



**F** DETAIL - PONTOON PLATE  
SCALE 1.5" = 1'-0"

Figure 42 - Pontoon plate detail

Table 43 - Fillet weld strength check for pontoon plate

Available Fillet Weld Strength - Mounting			
Weld	56.5	kips	AISC 14 (Table J2.5)
$\Omega$	1.88	-	
$0.6 \cdot F_{exx}$	42	ksi	
$A_{we}$	1.27	in <sup>2</sup>	
Base Metal	58.2	kips	
$\Omega$	2	-	
$F_{nBM}$	50	ksi	
$A_{BM}$	2.33	in <sup>2</sup>	

Table 44 - Fillet weld strength check for end plate

Available Fillet Weld Strength - End			
<b>Weld</b>	<b>201.1</b>	<b>kips</b>	AISC 14 (Table J2.5)
$\Omega$	1.88	-	
<b>0.6*F<sub>exx</sub></b>	42	ksi	
<b>A<sub>we</sub></b>	4.50	in <sup>2</sup>	
<b>Base Metal</b>	<b>207.0</b>	<b>kips</b>	
$\Omega$	2	-	
<b>F<sub>nBM</sub></b>	50	ksi	
<b>A<sub>BM</sub></b>	8.28	in <sup>2</sup>	